ABSTRACT

Title of Dissertation: SUSTAINED DELIVERY AND PHARMACODYNAMICS OF AN INTEGRIN ANTAGONIST FOR OCULAR ANGIOGENESIS

Yingli Fu, Doctor of Philosophy, 2007

Directed By: Professor Nam Sun Wang
Department of Chemical and Biomolecular Engineering
the Fischell Department of Bioengineering

Ocular angiogenesis, or the formation of new blood vessels in the eye, is the leading cause of blindness in a variety of clinical conditions. Success in elucidation of several key steps in angiogenesis cascade has opened a door for anti-angiogenesis therapies. Development of novel therapeutic agents provides effective treatment for ocular disorders. However, treatment of many posterior segment diseases like age-related macular degeneration (AMD) and diabetic retinopathy (DRP) is far from satisfactory due to the limited availability of novel therapeutic drugs and the low efficiency of traditional drug delivery methods. In the present study, we investigated the anti-angiogenic properties of a novel small integrin antagonist, EMD478761, and developed sustained release systems to locally and continuously deliver this compound.

In part I, sustained delivery implants were designed and investigation of their anti-angiogenic efficacy, including inhibition and regression, was performed using *in vivo* chick chorioallantoic membrane (CAM) assay. In part II, laser-induced choroidal neovascularization (CNV) rat model was employed to further examine the angiogenic inhibitory effect of EMD478761 from a sustained release microimplant. And in part III, the pharmacodynamics of EMD478761 was studied to reveal the mechanisms by which EMD478761 inhibited angiogenesis.

Results from *in vivo* CAM assay and CNV rat model demonstrated that EMD478761 inhibited and regressed basic fibroblast growth factor (bFGF)-induced angiogenesis, and suppressed laser-induced CNV via sustained release implants. The pharmacodynamics of this drug was studied to better understand the mechanisms of the drug's action mode in preventing neovascularization. *In vitro*, EMD478761 inhibited human umbilical vein endothelial cell (HUVEC) proliferation, caused HUVEC detachment in vitronectin-coated surfaces in a time- and dose-dependent manner, and disrupted endothelial cell tube formation on Matrigel. In addition, EMD478761 induced HUVEC apoptosis on vitronectin via caspase-3 activation pathway. *In vivo*, EMD478761 induced endothelial cell apoptosis within CNV lesions as demonstrated by terminal deoxynucleotidyl transferase dUTP nick-end labeling (TUNEL) assay. In addition, EMD478761 increased the integrin $\alpha_v\beta_3$ internalization in HUVECs, while it did not affect integrin $\alpha_v\beta_3$ expression levels after 12 hours treatment. Taken together, these findings demonstrate that sustained delivery of EMD478761 may provide an effective antiangiogenic approach for the treatment of ocular angiogenesis.

SUSTAINED DELIVERY AND PHARMACODYNAMICS OF AN INTEGRIN ANTAGONIST FOR OCULAR ANGIOGENESIS

By

Yingli Fu

Dissertation submitted to the Faculty of the Graduate School of the
University of Maryland, College Park, in partial fulfillment
of the requirements for the degree of
Doctor of Philosophy
2007

Advisory Committee:
Professor Nam Sun Wang, Chair
Professor Karl G. Csaky
Professor Mohammad Al-sheikhly
Professor William E. Bentley
Professor Adam Hsieh
Professor Y. Martin Lo, Dean's Representative

Dedication

To my family

Acknowledgements

I am pleased and honored to have worked with so many great people, who helped me in every aspect of my life during the past few years. I am greatly indebted to my advisor, the chair of this committee, Dr. Nam Sun Wang for his strong support, stimulating encouragement to take on challenges, and guidance to go through all the frustrations.

My special thanks go to Dr. Karl G. Csaky at the National Eye Institute/ National Institutes of Health (now at Duke University), who closely advised me through the entire project. Without his help, encouragement and support, it is impossible for me to accomplish this project.

I would like to thank my other committee members, Dr. Mohammad Al-shiekhly, Dr. William E. Bentley, Dr. Adam Hsieh and Dr. Y. Martin Lo for their insightful comments on my proposal and their input to this research work.

I am much obligated to Dr. M. Lourdes Ponce, who not only cordially helped me with my experiment, edited my papers and dissertation, but also provided tremendous help in my daily life. I would like to thank Dr. Michael R. Robinson for introducing me to ocular drug delivery field, Dr. Hyuncheol Kim for help in implant designs, Dr. Peng Yuan at the NIH Clinical Center for taking time to assay the release rates of my implants, they always came out perfectly.

Thank you to my other lab members at the National Eye Institute, Dr. Michelle Thill and Dr. Connie Zhang, for their help in animal experiment and their

expert advice in cell and molecular biology. Many thanks also go to all of the lab members at the University of Maryland for their assistance, support and feedback.

I would also like to thank Dr. Sheldon Miller, Dr. Ian MacDonald and Dr. Sarah Sohraby at the NEI for discussing with me about this project and going over my presentation, Dr. Mathias Wiesner at Merck KGaA (Germany) for synthesizing EMD478761 compound.

And finally, to my family for always being there for me.

Table of Contents

Page

List of Tables

Page

List of Figures

Page

Chapter 1: Introduction

1.1 Background and Motivations

1.1.1 Ocular Angiogenesis

Angiogenesis-related ocular diseases such as age-related macular degeneration (AMD) and diabetic retinopathy (DRP) are the leading cause of legal blindness in the developed countries (1, 2). Retinal neovascularization often occurs in young people with DPR. Choroidal neovascularization (CNV), as seen in AMD, mainly affects aged individuals. Around 9 million US citizens are suffering from AMD and the number of people affected by AMD is expected to double by 2020, according to estimates by the Foundation Fight Blindness (3). The threat of a rapidly aging population provides the impetus for aggressive efforts to control the prevalence and progression of this disease.

There are two forms of AMD (Fig. 1-1): the dry form, characterized by drusen formation and photoreceptor degeneration, and the wet form (exudative form), characterized by choroidal neovascularization and fluid accumulation under the retina (4). Dry form AMD accounts for 90% of cases, and it progresses slowly. However, there is no efficient treatment available yet. CNV only accounts for 10% of the patients diagnosed with AMD, but it is responsible for 90% of vision loss caused by AMD.

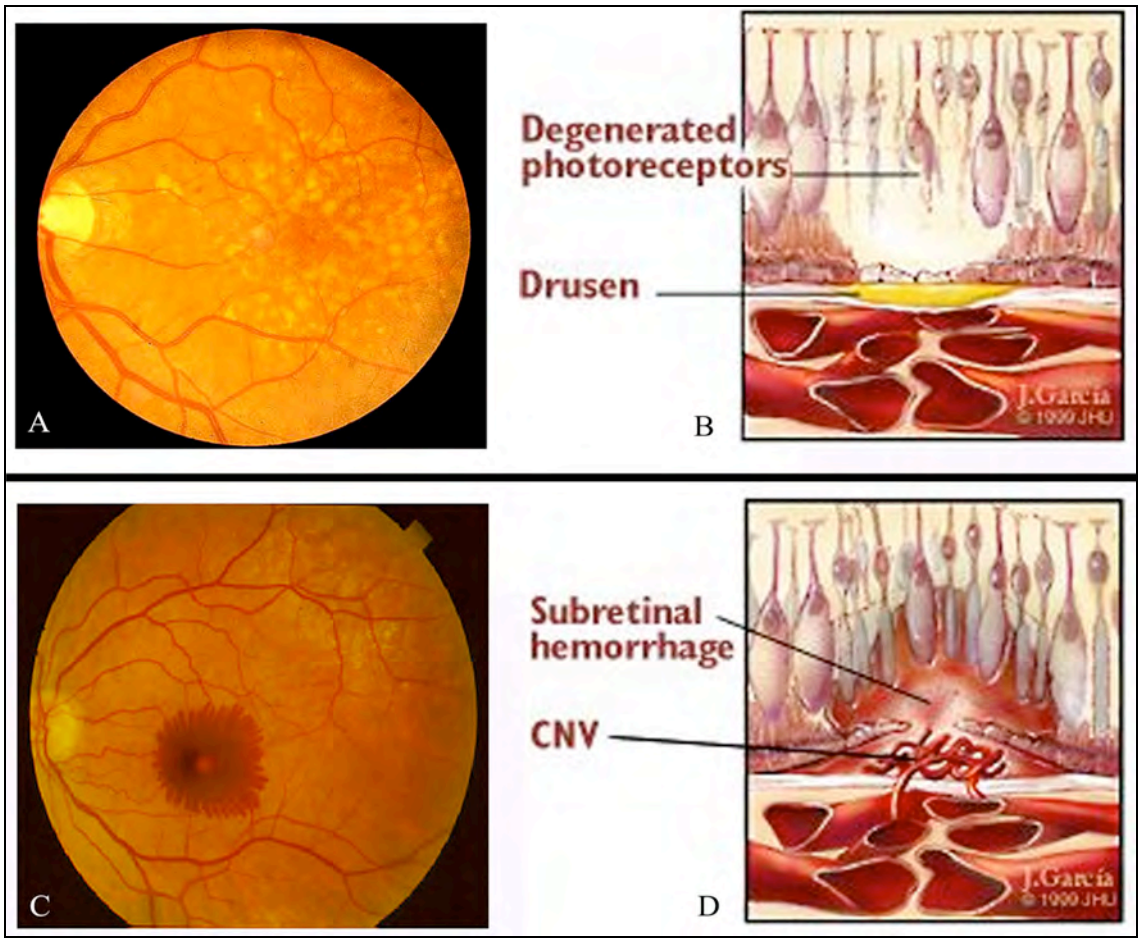

Figure 1-1. Fundus photograph of patients with age-related macular degeneration (AMD). (http://nei.nih.gov, http://dermatlas.jhmi.edu) A) Dry form AMD with drusen deposition; B) Schematic diagram of dry form AMD; C) Wet (Neovascular) AMD; D) Schematic diagram of wet form AMD

Moreover, patients with dry form are often at the risk of developing into wet form. Although significant progress has been made in identifying factors that promote or inhibit angiogenesis, current treatments for CNV, including laser panretinal photocoagulation (PRP) intervention either directly or in tandem with the photosensitizing porphyrin

Visudyne® as a photodynamic therapy, and macular translocation, are not optimal for majority of the affected individuals (5-7). Patients under these treatments often suffer significant recurrence.

The importance of ocular angiogenesis has stimulated the search for novel therapeutic agents and efficient delivery methods that either directly target the new vessel formation or potentially facilitate the prevention of neovascularization. The roles of anti-angiogenic agents are important when considering therapeutic strategies for neovascular diseases. These agents can affect various aspects of the angiogenic process, including endothelial cell migration and proliferation, and the three-dimensional restructuring of blood vessels. Our understanding of the molecular events involved in the angiogenic process has advanced significantly since the purification of the first angiogenic molecules nearly two decades ago (8). These advances have led to the development of several compounds that are currently approved for the treatment of ocular angiogenesis, others that are in various phases of clinical trials, and several factors with promising pre-clinical data that suggest their potential therapeutic use as anti-angiogenic compounds or targets. Among those compounds, the anti- vascular endothelial growth factor (VEGF) drugs represent a breakthrough in ocular pharmaceuticals. Nevertheless, they are often large, complex molecules that are difficult to pass through the ocular barriers, and are routinely delivered by the invasive intravitreal administration.

Given the short half life of most drugs injected into the vitreous (9, 10) and the recurrence of neovascularization, repeated intravitreal injections may be required to maintain drug concentrations within their therapeutic windows. However, multiple intraocular injections to patients that may need months or years of treatment have been

associated with cataract formation, retinal detachment and endophthalmitis (11-13). To improve the treatment for CNV, other alternative therapeutic modalities including novel antiangiogenic compounds and delivery methods need to be explored.

A better understanding of the mechanism of CNV will provide a basis for alternative treatments. CNV is the result of pathological angiogenesis which is a multistage, complex process involving a series of biochemical signals and receptors working together to create the "angiogenesis cascade" (Fig. 1-2). This process is delicately regulated and balanced by angiogenesis activators and inhibitors in the normal adult. However, it may be turned on by specific angiogenic molecules, such as basic and acidic fibroblast growth factor (FGF) (14), VEGF (15), transforming growth factor (16). tumor necrosis factor α (17), and platelet derived growth factor (18, 19). The central mechanism of angiogenesis requires proteolysis of the extracellular matrix, proliferation, migration of endothelial cells, and synthesis of new matrix components. Once the endothelial tube is formed from the existing vasculature, maturation starts with recruitment of mural cell precursors and formation of a new basement membrane.

During angiogenesis, endothelial cells response to the extracellular matrix (ECM) is partially mediated by integrins, a superfamily of transmembrane glycoprotein receptors that participate in cell-to-cell and cell-to-substrate interactions (20). In ocular angiogenesis, some integrins, growth factors, and proteinases have been found up-regulated (13, 21-26), which results in endothelial cell activation, proliferation and migration. Thus far, VEGF and proteolytic enzymes such as matrix metalloproteinases (MMPs) have become the primary treatment targets (27-30). A number of studies have demonstrated the efficacy of certain anti-VEGF compounds including

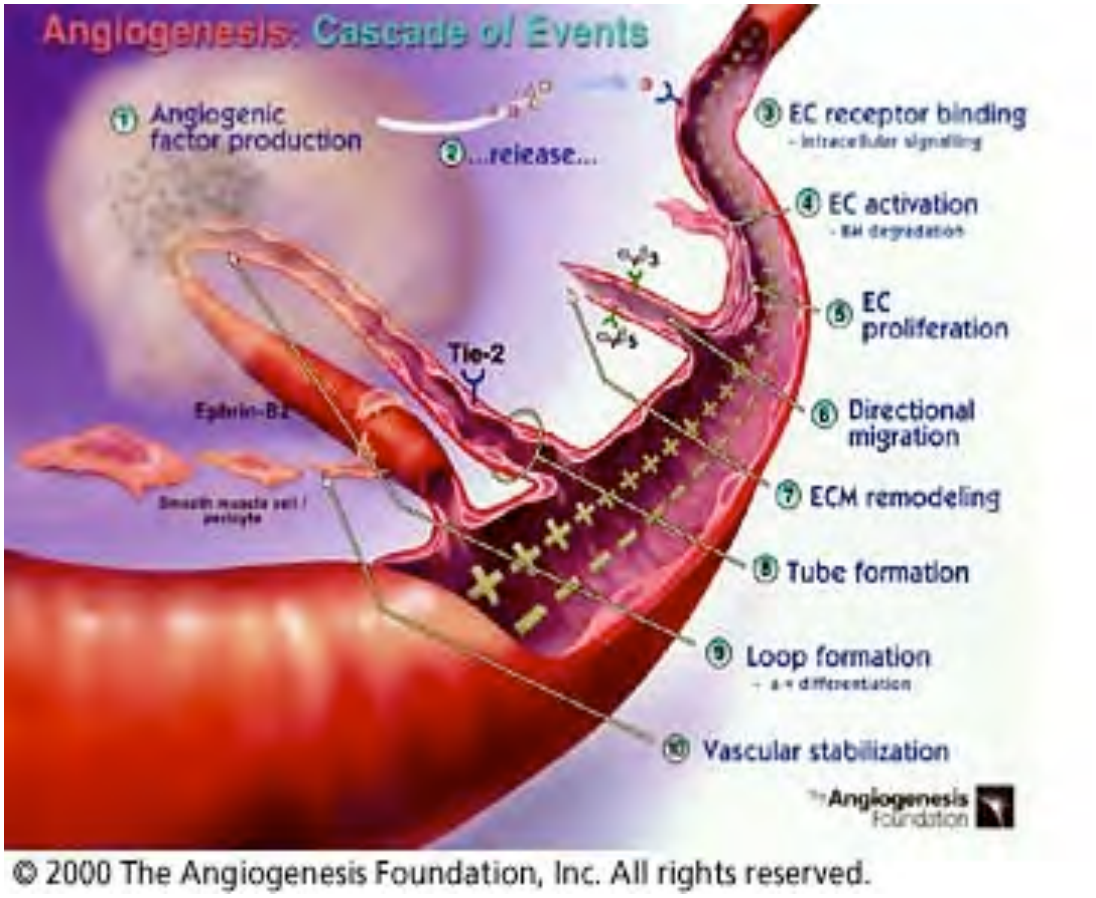

Figure 1-2. Angiogenesis cascade. (http://www.angio.org/understanding/understanding.html). (1) Angiogenic growth factors released from diseased or injured tissues, (2) binding to their receptors on endothelial cells, (3) activating signal transduction pathways and (4) stimulating endothelial proliferation, (5) migration, and (6) vessel formation. (7) Bone marrow derived endothelial stem cells are mobilized and become incorporated into new blood vessels. (8) Stabilization of the vasculature occurs through the recruitment of smooth muscle cells and pericytes.

administration of VEGF-neutralizing antibodies, the use of soluble VEGF receptor chimeric proteins or VEGF receptor suppressing small interfering RNA (siRNA), and the inhibition of VEGF signaling using specific kinase inhibitors (31-34). However, only two anti-VEGF therapies, Macugen™ (pegaptanib sodium) and Lucentis™ (ranibizumab), have been approved by the FDA for the treatment of advanced AMD at this point. A third anti-VEGF therapy, Avastin™ (bevacizumab), a humanized full-length antibody against VEGF formulated as an intravenous drug, has been approved for treating colorectal cancer, but not specifically for ophthalmic use. However, Avastin™ has been widely used off-label to treat advanced CNV (35-38). Despite all the excitement that these agents have generated, the long-term effects of any of these anti-VEGF agents are still unclear (39).

On the other hand, targeting VEGF might be problematic as a therapy for ocular neovascularization. VEGF is a multifunctional factor that is constitutively produced by the retinal pigmented epithelium (RPE) of the normal eye. One of the functions of VEGF is to serve as a survival factor for retinal vessels (40). In addition, the chronic nature of CNV and the intrinsic risk of repeated intraocular injections might necessitate a prolonged systemic administration of VEGF antagonists, which could adversely affect other ocular tissues or organ systems. Accordingly, there continues to be an unmet medical need to search for new and safe therapeutic agents and novel delivery methods.

Alternative drugs that block other key components of angiogenesis cascade have been developed. Some of these compounds, such as anecortave acetate, pigment epithelium-derived factor (PEDF) and μPA/μPAR inhibitor Å6, have entered clinical trials for choroidal neovascularization management. Anecortave acetate, an analog of

cortisol acetate that decreases extracellular protease expression and inhibits endothelial cell migration (41), was administrated through posterior juxtascleral injection with a specially designed cannula after a small incision was made in the conjunctiva and Tenon's capsule. Six and twelve months after treatment, the visual acuity of those patients with 15 mg anecortave acetate injection was better than the placebo (42, 43). In addition, this dose of the drug prevented severe vision loss without causing clinical side effects. PEDF, which is present in the corneal and the vitreous, has been found to be the most potent natural inhibitor in cell migration assay. PEDF has been in clinical trial using an adenoviral gene delivery system (GeneVec) for patients with severe CNV, who are not eligible for laser or PDT treatment (44). Å6, an inhibitor of the urokinase/urokinase receptor, is in phase I clinical trial, and its safety and tolerability is being investigated in CNV patients (Angstron Pharmaceiticals) (45). Despite all the progress that has been made, all of these treatments, while successful in halting vision deterioration in the majority of patients, are only effective in improving vision in 6-33% of patients (46-49). To improve the treatment for CNV, alternative therapeutic modalities including novel antiangiogenic compounds and delivery methods are being explored.

Although the exact cause of CNV is poorly understood, increasing evidence has shown that angiogenesis is partially regulated by integrin molecules (24, 25), a superfamily of transmembrane glycoprotein receptors that are involved in signal transductions (20). Integrins are heterodimeric cell adhesion molecules consisting of noncovalently associated α and β subunits. The α subunit is relatively long, consisting of around 1000-1200 amino acids and some contain an insert domain (I domain) near the amino terminal end; while the β subunit is relatively shorter with about 750 amino acids.

Integrins are not only the main receptors for ECM proteins, such as fibronectin vitronectin , collagens and laminin (50), but also provide anchor points for the cytoskeleton and mediate signaling events through a complex of associated adaptor proteins and kinases (51). To date, 24 integrins, with different combinations of the α and β chains, have been reported in mammalian cells (Fig. 1-3) (52).

Integrin-mediated signaling events are crucial for cell proliferation, migration, survival and differentiation (53). Integrins signaling can be directly activated by ligand binding, or indirectly stimulated by growth factors or cytokines. Depending on the composition of the ECM, integrins can activate one or more intra-cellular signaling pathways. This is called "outside-in signaling", which typically involves phosphorylation of focal adhesion kinase (FAK), recruitment of adaptor proteins, activation of small GTPases and subsequent activation of downstream effector molecules (54). On the other hand, integrins also respond to intracellular cues and alter the way in which they interact with the ECM. This is so called "inside-out signaling", which regulates integrin adhesiveness by modulating the affinity and avidity of integrins to their ECM ligands, therefore controlling cell adhesion, migration and proliferation (54) . Many studies indicate that integrins are important modulators of postnatal angiogenesis (55). Integrin $\alpha_v\beta_3$ is highly expressed in angiogenic endothelial cells in wound granulation tissue and in malignant tumors (24, 56). In ocular angiogenesis, $\alpha_v\beta_3$ has been found selectively expressed on the CNV membrane, while both of $\alpha_v\beta_3$ and $\alpha_v\beta_5$ are present in diabetic retinopathy tissue (25). The fact that anti- $\alpha_v\beta_3$ antibodies and some other integrin antagonists to $\alpha_v\beta_3$/ $\alpha_v\beta_5$ specifically and potentially block cytokine- and tumor-mediated

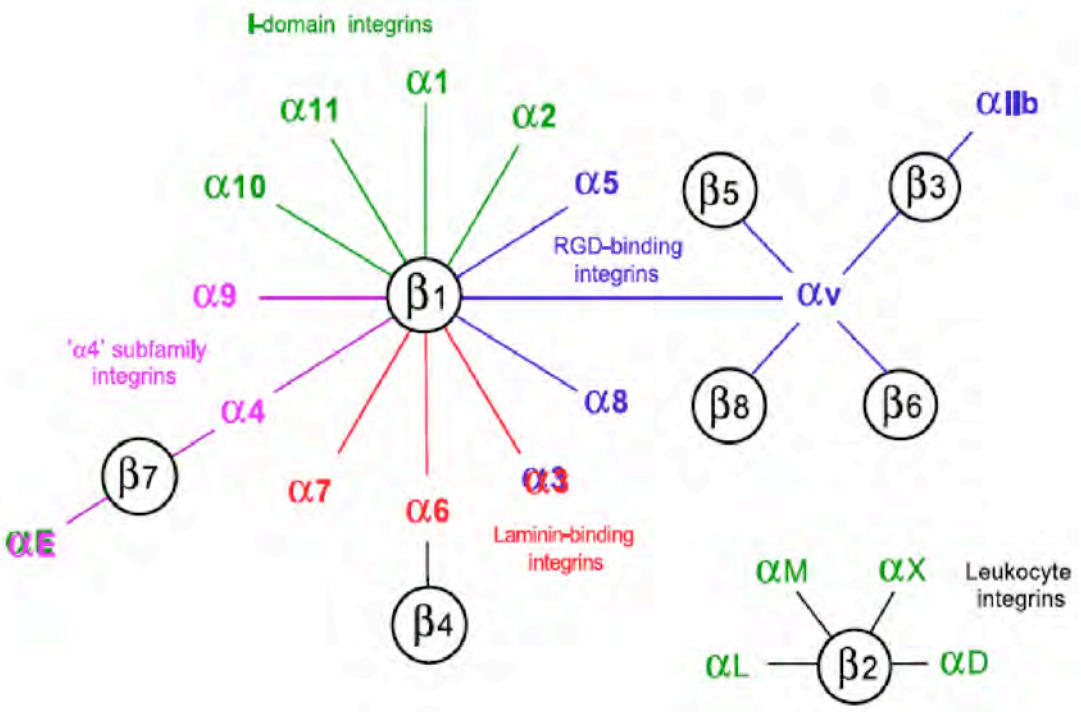

Figure 1-3. Integrin heterodimers and their subfamilies (52). The integrin family can be classified into the following subfamilies: the RGD-binding integrins (blue), the I-domain containing integrins (green), the laminin-binding integrins (red), the leukocyte integrins (black) and the α4-subfamily integrins (purple).

angiogenesis in several animal models (24, 25, 57, 58), suggests that $\alpha_v\beta_3$ and $\alpha_v\beta_5$ might be good targets for ocular angiogenesis treatment. Most of these integrin antagonists are peptides that are delivered by either systemic administration or intravitreal injection. Repeated ocular drug applications are often required to achieve efficacy while frequently cause discomfort to the patient and side effects in other tissues. In this study, we selected a small molecule integrin antagonist, EMD478761, with dual antagonism to integrin

$\alpha_v\beta_3/\alpha_v\beta_5$ and investigated its anti-angiogenic properties from a sustained delivery implant.

1.1.2 Eye Anatomy and Ocular Barriers

The eye is a very delicate sense organ and presents several anatomic and physiologic barriers that pose a major challenge for ocular drug delivery (Fig. 1-4). It has three layers: the outer fibrous layer of connective tissue forms the cornea and sclera, the middle vascular layer is composed of iris, ciliary body and choroid, and the inner nervous layer is the retina. These layers form three compartments: anterior chamber, posterior chamber and vitreous chamber. Among the eye structures are three intraocular fluids: aqueous humor, vitreous humor and blood.

Clinically, the eye can be considered to be composed of an anterior segment and a posterior segment and each segment forms its unique barriers. In the anterior segment, the cornea and lens are highly resistant to drug penetration. The cornea is a nonvascular optically transparent tissue. The central part of the cornea is about 0.5 mm thick and it is composed of 5 layers: epithelium and its basement membrane, Bowman's layer, stroma, Descemet's membrane and endothelium. The epithelium is a hydrophobic layer with many tight junctions which impede drug penetration into the eye. Bowman's layer lies between the epithelium and the stroma, the major tissue of the cornea. In contrast to the epithelium, the stroma is highly hydrophilic consisting of 85% of water. The endothelium layer contacts with the aqueous humor. It is the unique structure of the cornea that confers high resistance to both hydrophilic and lipophilic drug delivery.

Indeed, less than 5% of drug can penetrate into the vitreous through topical eye drop application (59).

The posterior segment of the eye consists of three layers, the sclera, choroid, and retina that surround the vitreous cavity. The sclera is a tough opaque fibrous layer, mainly composed of water and connective tissue. The choroid is a highly vascular and pigmented tissue that lines the inner surface of the sclera. It carries the largest blood flow per unit tissue in the body, brings in the nutrients for the outer layers of the retina and absorbs energy as light strikes the retinal pigment epithelium (60). The retina is a multi-cellular membrane occupying the internal space of the posterior portion of the eyeball. The retina is composed of neural retina and retinal pigment epithelium (RPE). The detailed retinal structure is shown in Figure 1-4C. The inner border of neural retina faces vitreous and the outer border is next to RPE. Neural retina is composed of nine layers whereas RPE is a monolayer of polarized cells. Bruch's membrane provides a basal lamina for the RPE cells, and it is located between RPE and choroid capillaris. The blood supply to the inner two thirds of the retina comes from the retinal vessels. The choroidal circulation nourishes the outer one third of the neural retina and RPE. The retinal endothelial cells have basal lamina that are surrounded by pericytes. The blood–retinal barrier (BRB), which has been shown to have similar features to the blood–brain barrier, restricts the movements of substances following systemic and periocular administration to the retina. The blood–retinal barrier is composed of two parts: the outer part is formed by RPE and the inner part by the endothelial cells of the retinal vessels. In the RPE and retinal endothelium, the cells are connected to each other by tight junctions which form

the permeation barrier to hydrophilic substances, thereby limiting the transfer of compounds both to inward (blood to vitreous) and outward (vitreous to blood) directions.

The blood ocular barriers, consisting of the blood-aqueous and blood-retinal barriers, are the main obstacles for the effective treatment of most intraocular diseases by systemic drug delivery (61). The blood-aqueous barrier is composed of ciliary non-pigmented epithelium and iridal vascular endothelium. This barrier limits the access of hydrophilic drugs from plasma into the aqueous humor (61, 62). The inner and outer blood-retinal barriers are formed by retinal pigment epithelium and retinal vascular endothelium, respectively. The inner limiting membrane on the vitreoretinal interface imposes a formidable barrier to macromolecules such as antibodies.

In summary, the eye represents many barriers that hinder drug delivery into the back of the eye. Efficient drug delivery systems for posterior segment ocular diseases need to overcome those barriers to achieve therapeutic drug concentrations while minimizing other side effects.

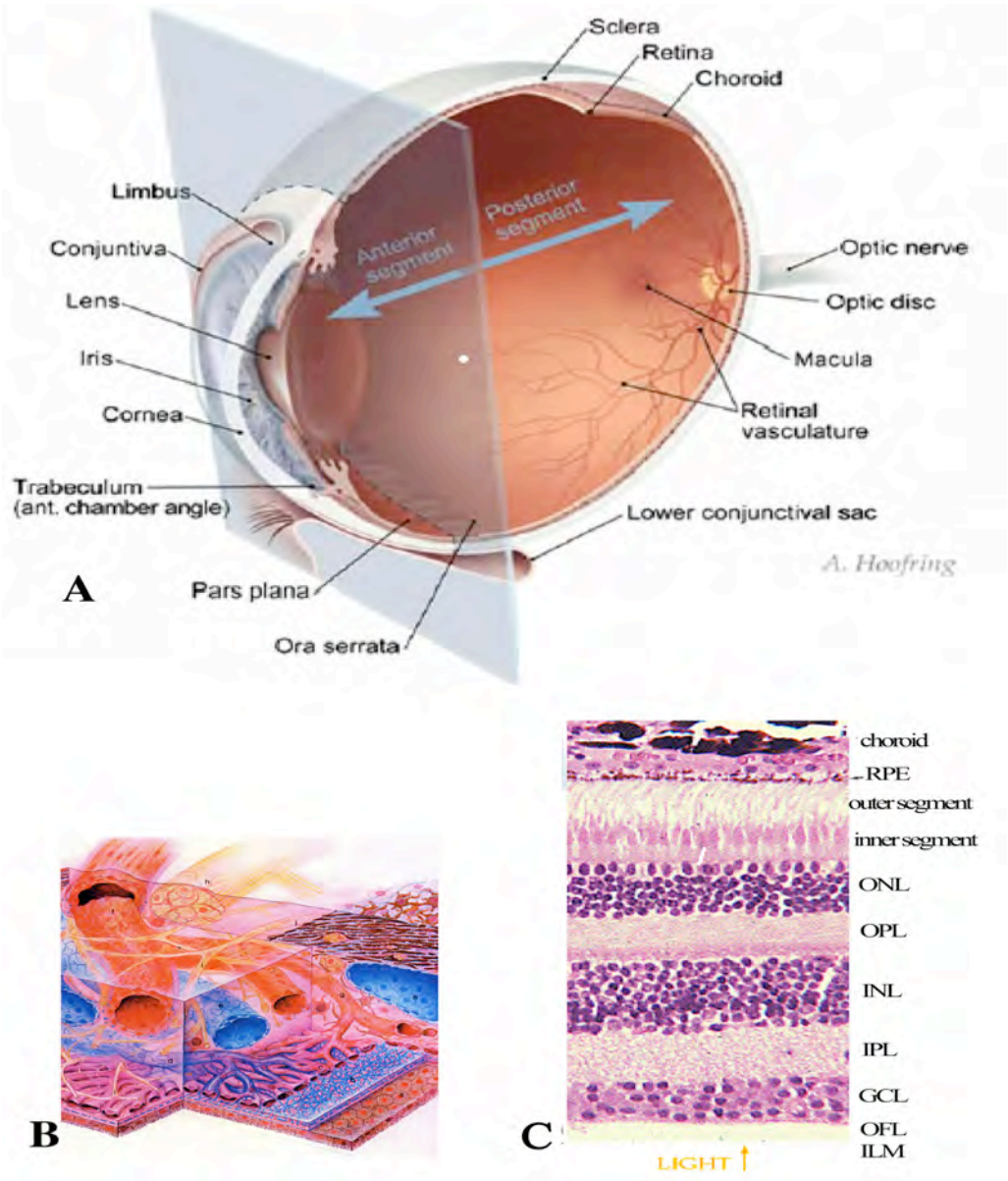

Figure 1-4. Human eye anatomy and main barriers to ocular drug delivery. A) Human eye anatomy; B) Schematic illustration of choroidal vasculature; C) Structure of the retina (http://thalamus.wustl.edu/course/eyeret.html). RPE: retinal pigment epithelium; ONL: outer nuclear layer; OPL: outer plexiform layer; INL: inner nuclear layer; IPL: inner plexiform layer; GCL: ganglion cell layer; OFL: optic fiber layer; ILM: inner limiting membrane. The main barriers are cornea, sclera, ILM, RPE, blood-aqueous and blood-retina barriers.

1.1.3 Ocular Drug Delivery Methods

The unique anatomy of the eye allows not only for systemic ophthalmic drug delivery, but also local, topical and very targeted drug delivery. As mentioned before, systemic administration is subject to blood-aqueous and blood-retinal barriers. Thus, repeated drug application and high dosage are often required for refractory vitreoretinal diseases such as choroidal neovascularization. Other principal methods of ocular therapeutic agent delivery, including topical eye drops, intravitreal or suprascleral injection, and controlled release implants (scleral plug, intravitreal implant, subconjunctival implant, transscleral implant and suprachoroidal implant) (Fig.1-5) (63), have been investigated to tackle the sight-threatening diseases. Among those, topical ophthalmic drops are the most common formulations used. However, it has been found that less than 5% of applied drug reaches the intraocular tissue because of the formidable cornea and scleral barriers and the continuous turnover of tears (59).

Intraocular injection through pars plana has been widely used in the clinic to deliver high concentration of drugs to the posterior tissues. However, drugs injected inside the vitreous are often rapidly cleared by the aqueous humor, the fast choroidal blood flow, or by enzymatic degradation. Consequently, frequent treatments are often necessary to maintain drug concentrations within therapeutic windows.

An ideal pharmaceutical approach for patients with ocular angiogenesis would be to incorporate a system that maintains the therapeutic drug levels in the targeted disease site for extended periods without causing local or systemic side effects.

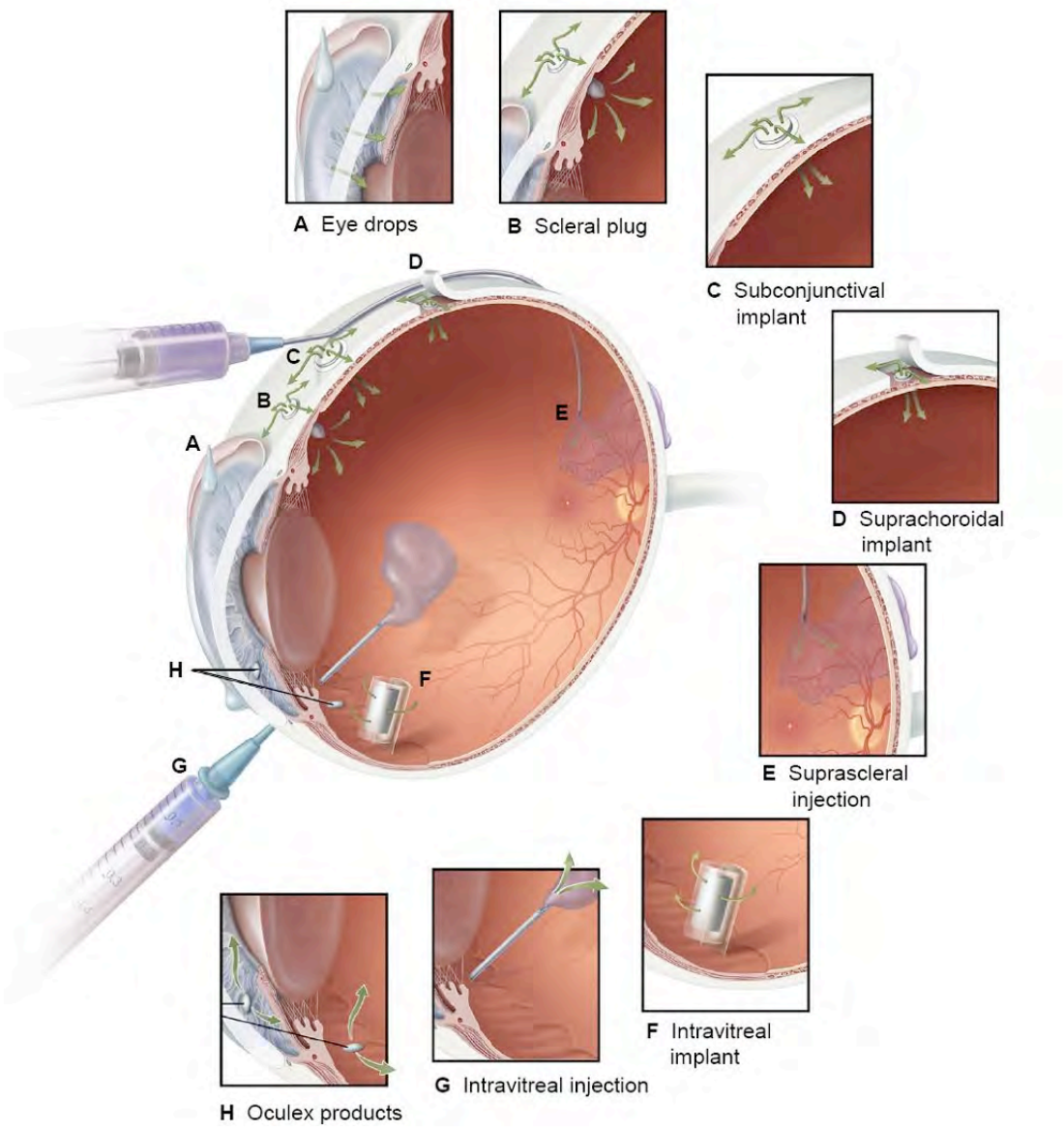

Figure 1-5. Principal ocular drug delivery methods (63).

Sustained delivery devices may offer an excellent alternative to multiple intravitreous injections. These controlled release devices can deliver drugs at predictable and constant release rates for an extended period of time, thus avoiding the frequency of repeated injections. Microsphere and nanoparticle formulations have gained popularity in the past few decades for controlled drug delivery, especially for proteins and peptides. One of the main advantages of these particle formulations is to provide stability for labile compounds that are often rapidly degraded or cleared out *in vivo*. Macrophages or enzymes such as proteases in the surrounding tissues would not be in contact with the encapsulated drug until it is released from the matrix. Moreover, microspheres or nanoparticles are readily injected intravitreally, subcutaneously or into other target sites without surgery. Microparticles diffuse poorly in the vitreous gel, thus act like reservoir after intravitreal injection. Poly (lactic acid) (PLA) microspheres remain in the vitreous of the normal rabbit eye for as long as 1.5 months (64). In contrast, nanoparticles diffuse rapidly and can be easily internalized into ocular tissues and cells (65, 66). The residence time of these particles depends not only on their sizes, but also on the physiological conditions of the eyes where the particles are injected. For example, the clearance of liposomes from vitreous in infected eyes is found to be much faster than those in the normal eye. This might be a result of increase rate of diffusion through the liquified vitreous, or an elevated uptake by recruited macrophages, or by a breakdown of the blood-retinal barrier in infected eyes (67). However, PLA or poly (lactic-co-glycolic) acid (PLGA) containing particles have been found to induce inflammatory reactions in the eye (66). Nevertheless, albumin nanoparticles have shown excellent intraocular tolerance (68, 69), and they might serve as a better carriers for ocular drug delivery.

Despite of the advantages that these micro-or nanoparticles offer, delivery of a large amount of drug for an extended period of time is still challenging. To overcome this problem, several implants have been developed and investigated. Drugs are usually encapsulated (reservoir implant) (70) or blended (matrix implant) (71) within a particular matrix, or conjugated to polymer carriers (72). The advantage of these implants is that release rates are determined by the matrix employed and the properties of the drugs incorporated. The release rates can be typically controlled well below toxic levels, and at the same time, higher drug concentrations can be intraocularly delivered without causing systemic side effects. According to the properties of the polymer used, these devices are either biostable (e.g. silicone) or biodegradable (e.g. PLA, PLGA, poly vinyl alcohol (PVA), liposome, gelatin, albumin etc). For posterior segment diseases, an intravitreal implant is often used to avoid the major ocular barriers. Cylindrical PLGA implant loaded with 1 mg fluorouracil allowed drug release for nearly 3 weeks in vitreous cavity of rabbits and reduced the incidence of tractional retinal detachment (73). However, the implant itself caused trauma to the retina. Vitrasert™ (Bausch and Lomb, Rochester, NY) is one of the first FDA approved reservoir type implants for the treatment of cytomegalovirus (CMV) retinitis in patients with acquired immunodeficiency. It is capable of releasing drug for about 8 months with *in vivo* release rates between 0.5 and 2.88 μg/h and has been shown to be therapeutically effective in human CMV retinitis (74). Other implants that have been developed include scleral plugs and rod-shaped devices. These implants have shown favorable results compared to systemic administrations (75-77).

In summary, various ocular implants have been engineered to avoid or minimize the ocular barriers that often impede the delivery of drug via traditional methods.

1.2 Objectives and Approaches

The research objective of this dissertation was to develop a sustained delivery system for a small integrin antagonist, EMD478761, and to determine its efficacy via a sustained delivery method for preventing and/or reversing ocular angiogenesis, and finally, to investigate the mechanisms under which this compound acts.

To this end, we explored the integration of a potential therapeutic compound with sustained release systems as a route to provide a useful modality for CNV treatment. We focused on systems where the drug targets a specific angiogenesis marker and the carriers allow for a continuous long time release of this drug to the posterior segment of the eye. The following studies have been done:

1. Reservoir type sustained delivery implants releasing EMD478761 have been designed. *In vitro* release rates of these implants were measured, and parameters influencing their release rates were evaluated and optimized.

2. The effect of EMD478761 on angiogenesis inhibition or regression using *in vitro* and *in vivo* angiogenesis assays has been studied, and the differences between bolus dosing and sustained implant delivery methods were compared.

3. The mechanisms of the drug's effect on angiogenesis inhibition have been investigated. In particular, integrin expression, internalization and endothelial cell apoptosis were studied.

1.3 Significance

The studies described in this dissertation are potentially significant from several different standpoints: (a) they offer a feasible therapeutic approach for fast growing ocular angiogenesis management by expanding the availability of therapeutic agents and prolonging the delivery time period; (b) they provide fundamental insight into the action model of this drug that could be important for the development and utilization of a new therapeutic agent and controlled drug delivery methods in clinical applications.

Chapter 2: *In vivo* Angiogenesis Inhibition in Chick Chorioallantoic Membrane (CAM) Assay from a Sustained Release EMD478761 Implant

Part of results in this chapter was published in the following journal article:

Y. Fu, M. L. Ponce, M. Thill, P. Yuan, N.S. Wang and K.G. Csaky. 2007. Angiogenesis Inhibition and Choroidal Neovascularization Suppression by Sustained Delivery of an Integrin Antagonist EMD478761. *Invest Ophthalmol Vis Sci* 48(11):5184-5190

2.1 Purpose

Most studies of angiogenesis inducers and inhibitors rely on various *in vitro* and *in vivo* models as indicators of efficacy. In this chapter, we have designed sustained release implants for a small molecular integrin antagonist, EMD478761, and we employ a modified *in vivo* chick chorioallantoic membrane (CAM) assay to investigate the anti-angiogenic efficacy of EMD478761 from sustained release implants.

2.2 Introduction

The field of angiogenesis has become active since neovascularization has been found to be involved in the progression of many diseases, such as tumor growth and metastasis,

choroidal neovascularization and diabetic retinopathy (78). The molecular basis is being studied in many branches of biology. Angiogenesis is a multi-stage, complex process that involves an appropriate environment of growth factors, extracellular matrix proteins, proteases, as well as cell surface integrins to be present so that cellular events of proliferation, proteolysis, invasion and migration can take place (79). Identification and assessment of new substances with the ability to inhibit angiogenesis highly relies on *in vitro* and *in vivo* assays. The chick chorioallantoic membrane (CAM) assay is frequently used for anti-angiogenic drug screening, due to its advantages of economy, high capacity and ease of manipulation (80, 81).

The chorioallantoic membrane (Fig. 2-1) is an extraembryonic membrane which serves as a gas exchange surface and its respiratory function is provided by an extensive capillary network (82). Its development starts at embryonal day 4 and the chorionic and the allantoic epithelia together with the vascularized stroma participate in its formation. Undifferentiated blood vessels, scattered in the mesoderm, grow very rapidly until day 8, forming a network of capillaries that migrate to occupy an area at the base of the chorion and mediate gas exchange with the outer environment. Rapid capillary proliferation goes on until day 10; thereafter, the endothelial mitotic index declines rapidly, and the vascular system attains its final arrangement on day 18, just before hatching. Because of its extensive vascularization, the CAM has been utilized as an *in vivo* model for the evaluation of angiogenic and anti-angiogenic molecules.

The development of the vascular system of the CAM is a complex, highly regulated process that depends on genetic and epigenetic factors expressed by endothelial and non-endothelial cells. In light of the evidence that several growth factors are

angiogenic in the CAM assay (57), we used basic fibroblast growth factor (bFGF) as an angiogenic stimulus to investigate the anti-angiogenesis efficacy of EMD478761 from a sustained release implant.

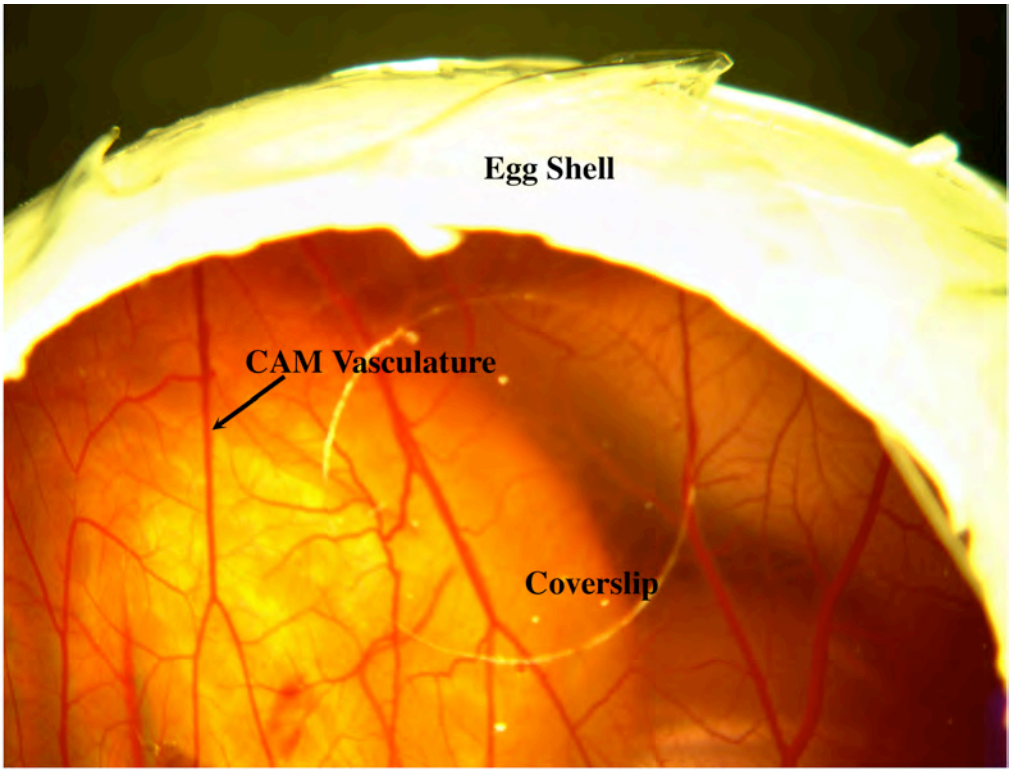

Figure 2-1. Normal chick chorioallantoic membrane (CAM).

2.3 Materials and Methods

2.3.1 Implant Design

Circular EMD478761 containing reservoir implants were designed (Fig. 2-2) using the following procedure: a 10%-20% (w/v) polyvinyl alcohol (PVA) solution was formulated by placing 3-6 g of PVA (Airvol® 125) in 30 ml of molecular biology grade water (Eppendorf Scientific, Inc, Westbury, NY) in a closed vial, and placed in a water bath at 100°C until completely dissolved. The freshly made PVA solution was poured onto a glass plate forming a thin film. Compressed pellets, containing either 2mg (1.5 mm), 4 mg (2 mm) or 10 mg (4 mm) of EMD478761 were embedded within this film during its wet phase. After allowing the film to dry at room temperature, sections of the film with the drug core centered within the section were cut with a biopsy puncher (Acu Punch® 2 mm, 2.5 mm or 4.5 mm, Acuderm, USA). Each section represented a reservoir implant.

The PVA polymer used this study is made by complete hydrolysis of polyvinyl acetate to remove acetate groups, rather than by polymerization of the corresponding vinyl alcohol monomer. At room temperature, its solubility is very low (~ 4%), therefore, it is necessary to heat and stir to make PVA solutions. Once PVA film is formed, it is pretty stable within a long period of time at physiological temperature.

To determine the influence of formulation parameters on release rates of the implants, the implants were made with different matrix concentrations, compressed pellet sizes, and curing temperatures. Sham implants were made in a similar fashion except that

no drug was incorporated. All implants were sterilized (3×10^4 grays, gamma radiation) before use.

2.3.2 In Vitro Release Rates

In vitro release rates on representative implants of each design were measured daily with an HPLC. Five implants from each design were randomly selected and placed in a closed vial with a constant volume of phosphate buffered saline (PBS, pH 7.4) at 37°C. PBS was replaced every 24 hours. The drug assays were performed with an Agilent HP1100 HPLC system (Agilent Technologies, Palo Alto, CA) equipped with a G1329A autosampler, a G1315A diode array detector, a G1312A binary pump, and a Dell workstation that controlled the operation of HPLC and analyzed the data. A Beckman Ultrasphere C-18 column (5 μm; 4.6 × 250 mm) (Beckman Coulter, Inc., Fullerton, CA) was used for separation, and detection was set at 280 nm. The flow rate used was 1.0 mL/min with a mobile phase of 20% of acetonitrile, 40% of water, and 40% of methanol by volume. The retention time was 5.0 minutes, and the detection limit was 10 ng/mL. The release rates were determined by calculating the amount of drug released in a given volume over time and recorded for each implant design in μg/day (± 1 standard deviation (SD)). The cumulative drug released was calculated based on daily release rates and recorded separately for each implant design.

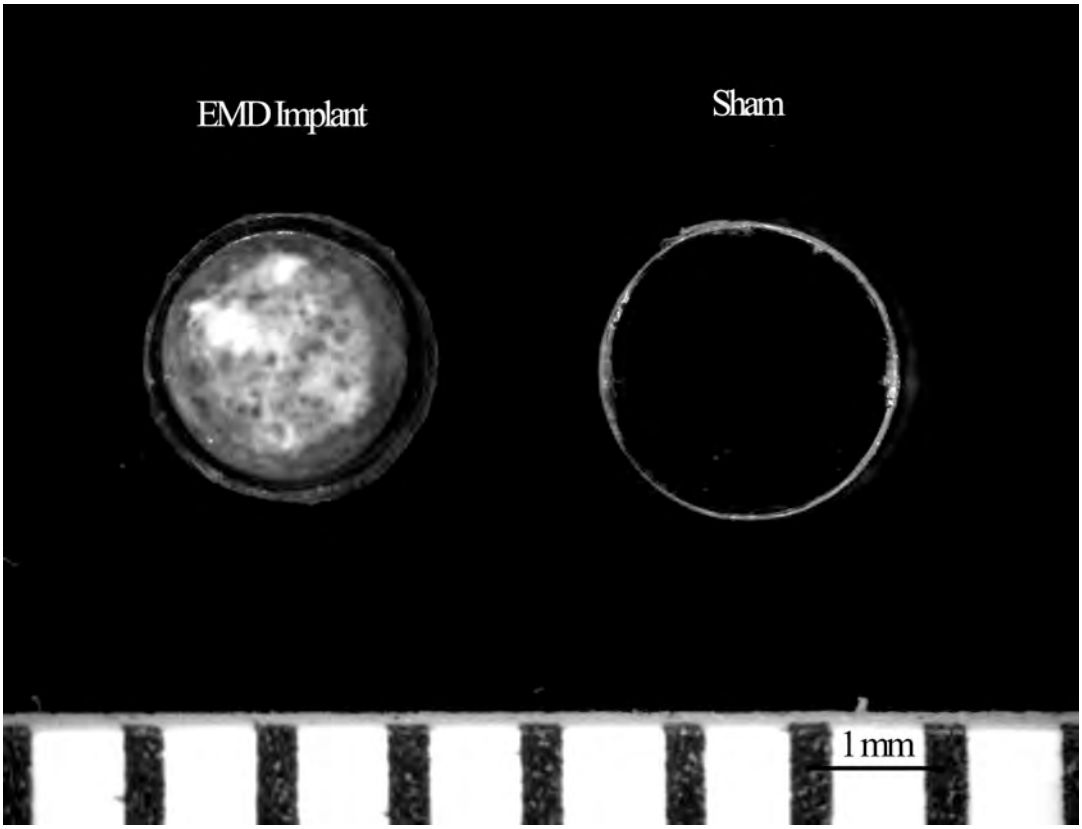

Figure 2-2. Representative image of circular implants. The 2-mm diameter implants made with 15% PVA were shown. Sham implant was made without EMD478761.

2.3.3 CAM

The CAM assay was performed using 10-day-old embryonated eggs (CBT, Charlestown, MD) as described previously with slight modification (83). A doughnut glass coverslip was constructed by creating a 2.5 mm hole in an 8 mm glass coverslip. On embryonal day 3, 3 ml of ovalbumin was removed from each egg. After opening windows on embryonal day 10, the angiogenic stimulus (100 ng bFGF), previously dried on the precut

doughnut glass coverslips, was applied to the CAM. Implant A was placed centrally in the pre-cut circular hole in the coverslip to locally deliver the drug. The eggs were photographed 3 days after the stimulus was added and the angiogenesis response was examined. The neovascularization area was quantified with a modular imaging software (Openlab, ver 3.1.5, Improvision Inc., Lexington, MA).

To determine the ability of sustained delivery of EMD478761 to regress neovascularization, an EMD478761 implant with 2 mm diameter and 15% PVA was added to the pre-cut circular hole in the coverslip 3 days after bFGF applied to the CAM. Neovascularization responses were examined 2 or 4 days after implantation and the angiogenesis area was quantified from captured images.

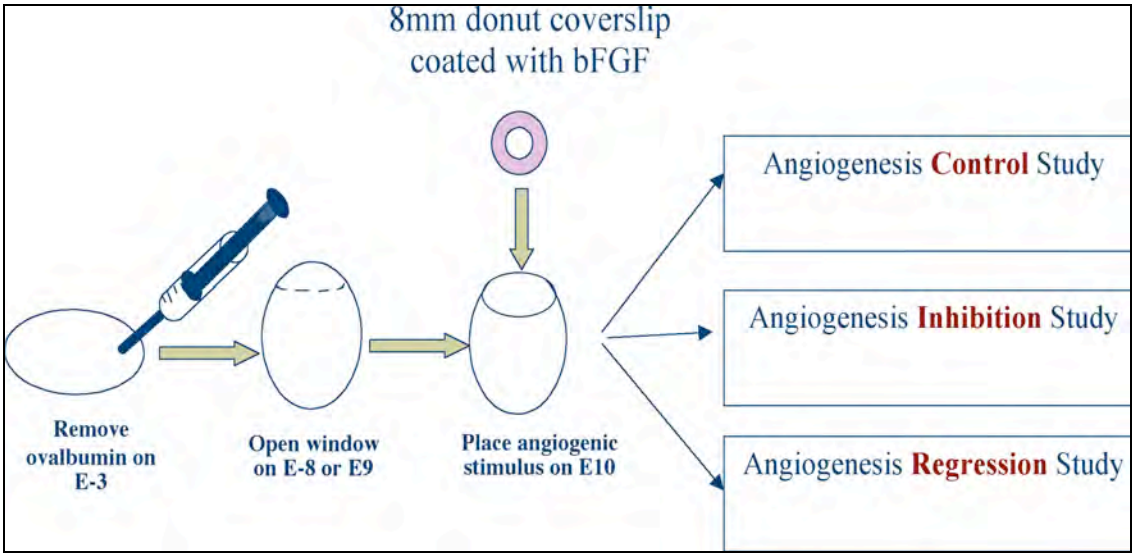

Figure 2-3. CAM assay procedure. E3: embryonal day 3.

2.4 Results

2.4.1 In vitro Release Rates of EMD478761 Implant

To optimize the release rates of the implants, we investigated the parameters that may influence the release kinetics of the implants, including PVA concentration, implant size, curing temperature and initial drug encapsulation amount.

Figure 2-4 shows the *in vitro* release profiles of various circular implants with diameter sizes of 2.0, 2.5 and 4.5 mm. The initial mean drug loading amounts are 2, 4 and 10 mg, respectively. As shown in Figure 2-4A, the circular implants delivered an initial bolus of drug on the first day followed by a steady-state release of drug throughout the assay period. The size of the implants greatly influenced *in vitro* mean release rate. Over the assay period, the mean release rates of the implants increased with the increase of the implant sizes. The steady-state cumulative release after day 1, estimated from the mean release rates, followed a zero order release kinetics (Fig 2-4), which is typical for diffusion controlled reservoir implants (84). The steady-state release rate for 2.0 mm implant was 119 ± 30 μg/day. By day 17, drug was completely released from 2.0 mm implant, while about 91.2% and 80.9% of drug was released from 2.5 and 4.5 mm implant, respectively.

We next examined the effect of curing temperature on *in vitro* release rates of the implants. For this experiment, the 2.0 mm implants were further incubated at 110°C or 150 °C for 3 hours. Figure 2-5A demonstrates that the *in vitro* release rate of the implants decreased as the curing temperature increased. Indeed, as shown in Figure 2-

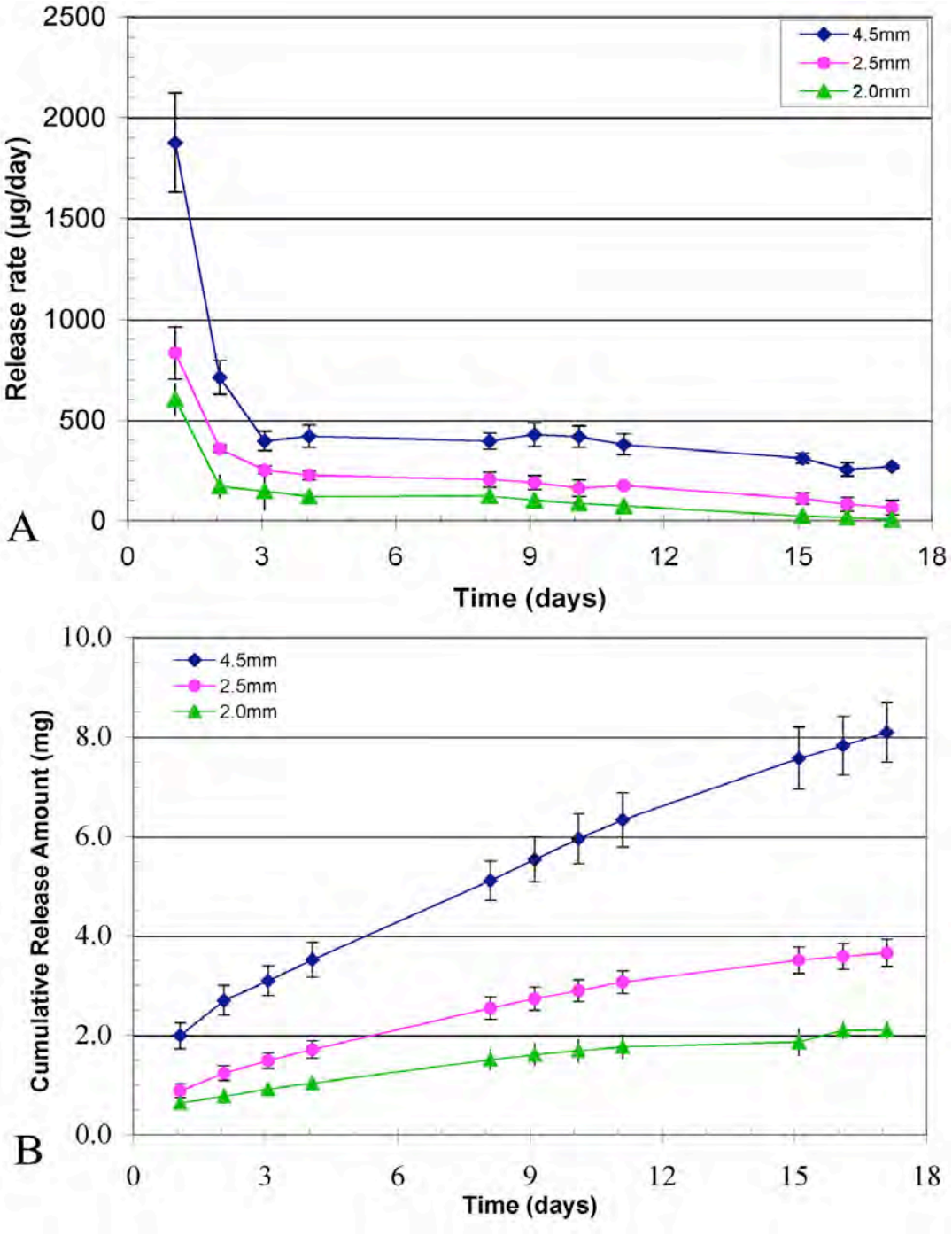

Figure 2-4. *In vitro* mean release rates (A) and cumulative release amount (B) of circular implants (n=5) with different diameters at 37°C. The implants were made with 15% PVA. Initial average drug loading amounts were 10, 4 and 2 mg for 4.5, 2.5 and 2 mm diameter implants, respectively.

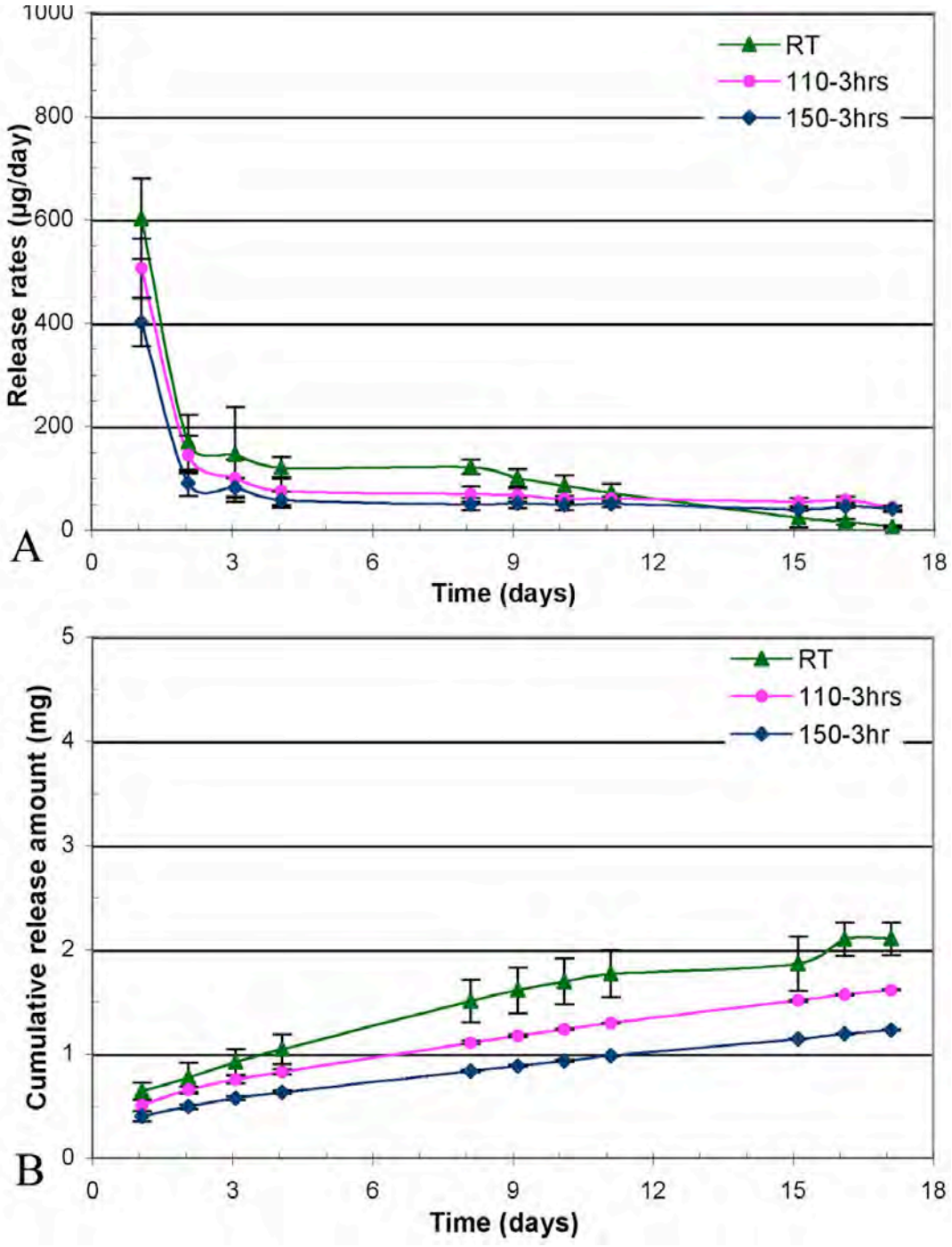

Figure 2-5. Effect of curing temperature on *in vitro* release rates (A) and cumulative release amount (B) of the implants (n=5). Implants were 2.0 mm in diameter and were made with 15% PVA. RT: room temperature; 110-3hrs: heated at 110°C for 3 hours; 150-3hrs: heated at 150°C for 3 hours

5B, the mean cumulative release amount by day 4 decreased 20.5% and 39.3% for implants heated at 110°C and 150°C, respectively, as compared to controls. The effect of PVA concentrations on *in vitro* release rates was also investigated with 2.0 mm implants. As shown in Figure 2-6, the *in vitro* release rates of EMD478761 implants were inversely proportional to the concentrations of PVA.

These results suggest that the release rates of EMD478761 reservoir implants can be finely tuned, by adjusting the size of the implant, the curing temperature or the PVA concentration, to deliver constant drug levels over a long period of time. In the following *in vivo* CAM assay, a doughnut glass coverslip with a 2.5 mm hole was constructed. Therefore, a 2.0 mm EMD478761 implant was used. The implant was made with 15% PVA at room temperature.

2.4.2 Sustained Delivery of EMD478761 Inhibits Angiogenesis in the CAM

To evaluate the inhibitory effect of EMD478761 implant on blocking bFGF-induced angiogenesis in an *in vivo* animal model, we used a modified CAM assay. To induce angiogenesis, a modified doughnut shaped coverslip with a 2.5 mm hole at its center was constructed. The angiogenesis stimulus, bFGF, was dried on the coverslip and placed on the CAM. An EMD478761 implant or sham was placed at the center of the doughnut glass coverslip. Results showed that the EMD478761 implant (Fig. 2-7C) significantly inhibited bFGF-induced neovascularization, relative to controls (Fig. 2-7), by 93%. No statistically significant difference was noted between sham-treated CAMs (Fig. 2-7B) and

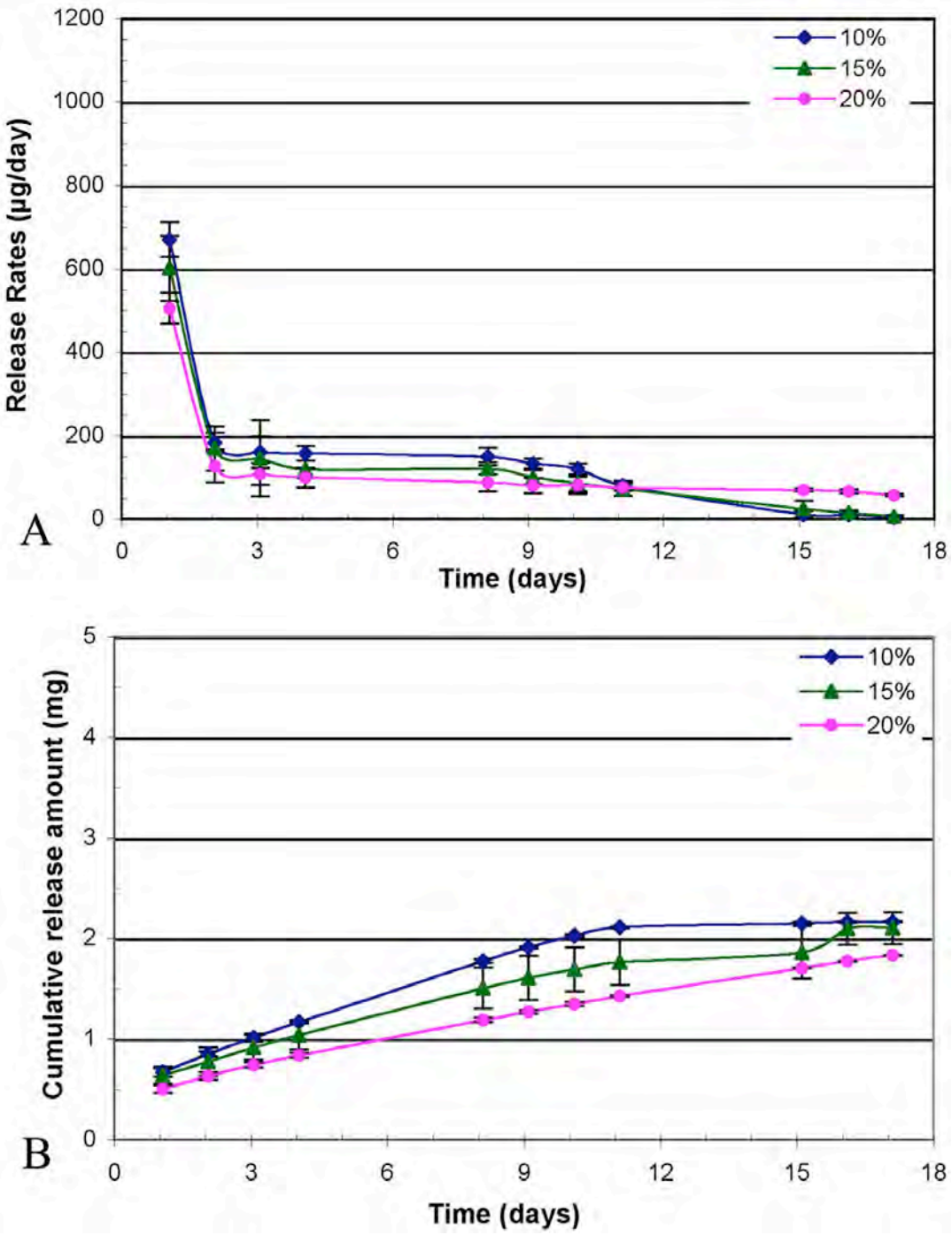

Figure 2-6. Effect of PVA concentrations on *in vitro* release rates (A) and cumulative release amount (B) of the implants (n=5). The implants were 2.0 mm in diameter.

controls (Fig. 2-7A). The mean neovascularization area induced by bFGF alone was 6.8 mm^2 (Fig. 2-8B) and the neovascular response was 83% positive (Fig. 2-8A). Vehicle (sham) treated CAMs did not have an effect on inhibiting bFGF-induced vessel formation and followed a similar response in which the neovascularization area was unchanged. On the other hand, in the presence of EMD478761 implant, only 19% of the bFGF-induced CAMs were weakly angiogenic, and the angiogenesis area was dramatically reduced to an average of 0.47 mm^2, which is significantly different from those treated with bFGF only ($P = 0.0008$) or with sham ($P = 0.0001$). In addition, there were no signs of local drug toxicity and no effect on the normal CAM vasculature was observed (Fig. 2-7B, C).

2.4.3 EMD478761 Implant Reverses Angiogenesis in the CAM

Since we observed the significant inhibitory effect of sustained delivery of EMD478761 on an *in vivo* CAM assay, we decided to examine whether EMD478761 delivered by this method could reverse angiogenesis, a process which is more relevant to neovascularization-related diseases, using the same model system. To this end, angiogenesis on the CAM was induced by bFGF on 10-day old embryos and EMD478761 implant was placed 3 days after bFGF was applied. CAMs were examined 2 or 4 days after implantation. Figure 2-9 showed that bFGF-induced angiogenesis was remarkably abrogated 2 days after EMD478761 implant treatment. The mean neovascularization area decreased from 6.7 mm^2 to 1.3 mm^2 (Fig. 2-10, $P < 0.001$), yet no significant change was observed for sham implant-treated CAMs (Fig. 2-9 E, F).

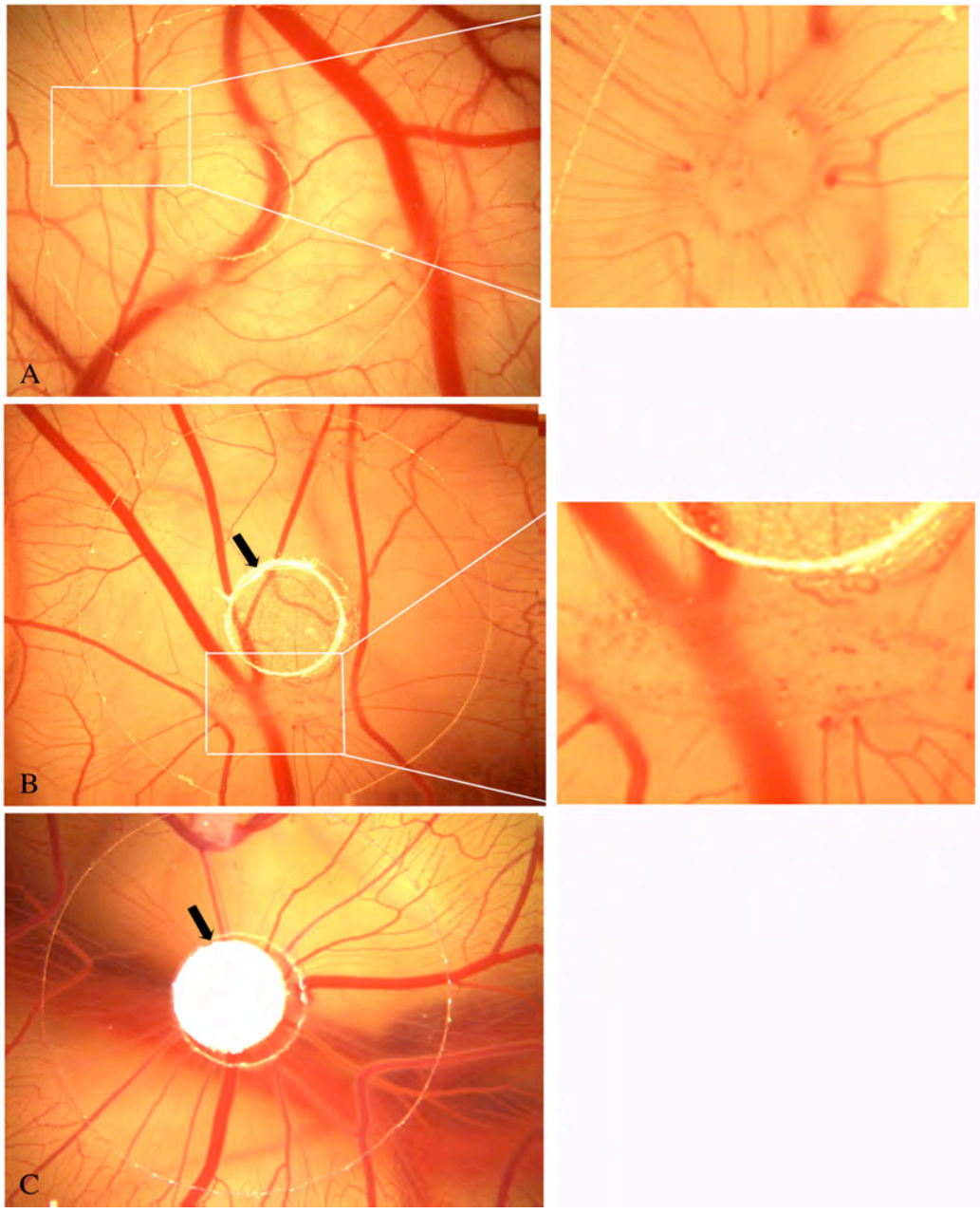

Figure 2-7. Effect of EMD478761 implant on angiogenesis inhibition in the chick CAM assay. A). bFGF only; B). bFGF with sham placed at the center of the coverslip; C). bFGF with an EMD478761 implant. The right panels are the corresponding magnified images showing the neovasculature. Arrows indicate the position of the implant used per condition. Minimum of 8 eggs per treatment were used and the experiment was repeated 3 times.

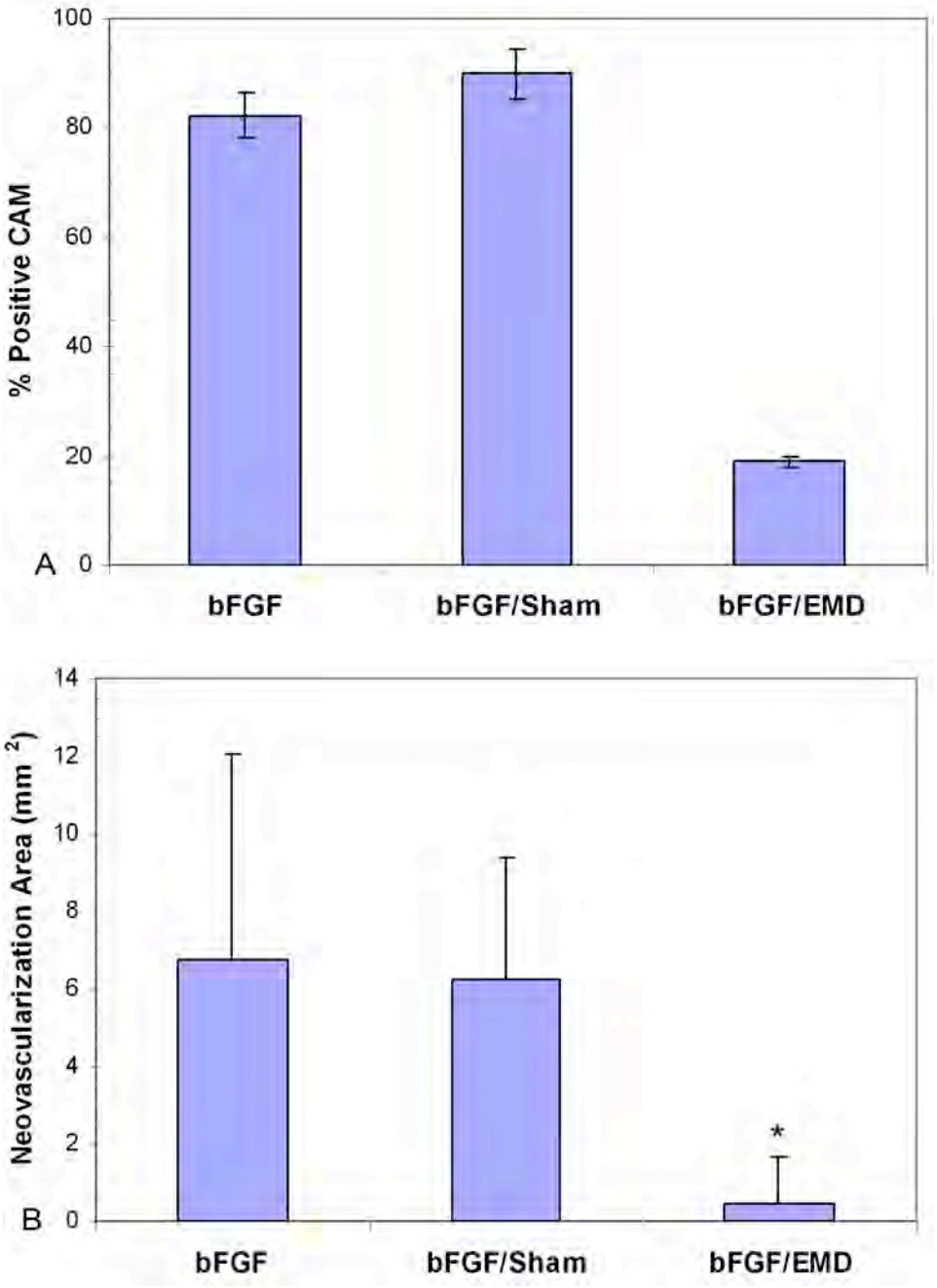

Figure 2-8. Quantitative analysis of angiogenesis response to bFGF, sham and EMD implant in the chick CAM assay in terms of percent of positive CAMs (A) and neovascularization areas (B) (* P = 0.0008 compared to bFGF treated CAMs).

Continuous treatment for 2 more days did not further affect the neovascularization area (Fig. 2-10). In addition, no apparent signs of local drug toxicity were noted and the normal CAM vasculature appeared to be unaffected. These findings suggest that sustained delivery of EMD478761 may be effective in treating angiogenesis-related diseases.

2.5 Discussion

Angiogenesis plays a vital role in normal physiological development, such as wound healing, embryogenesis, and many diseases including solid tumors and ocular neovascularizations. Previous studies demonstrated that continuous delivery of endostatin by an osmotic pump increased its potency and efficacy on tumor therapies (9). In this study, we designed sustained release implants to locally and continuously deliver EMD478761. As expected, the release rates of the implants were governed by their size, matrix concentration, and curing temperature.

Quiescent normal vessels do not express detectable levels of integrin $\alpha_v\beta_3$, however, bFGF stimulates the specific expression of the integrin $\alpha_v\beta_3$ on angiogenic blood vessels in CAM (25, 85). Since EMD478761 is an $\alpha_v\beta_3$ integrin antagonist, we first examined the inhibitory effect of EMD478761 on bFGF-induced angiogenesis in a modified CAM model. Differing from previous CAM assays where the testing compounds are often added exogenously to the angiogenesis stimuli (25, 83), we used a sustained release implant to continuously and locally deliver the drug. Sustained delivery of EMD478761 significantly suppressed bFGF-induced angiogenesis without affecting

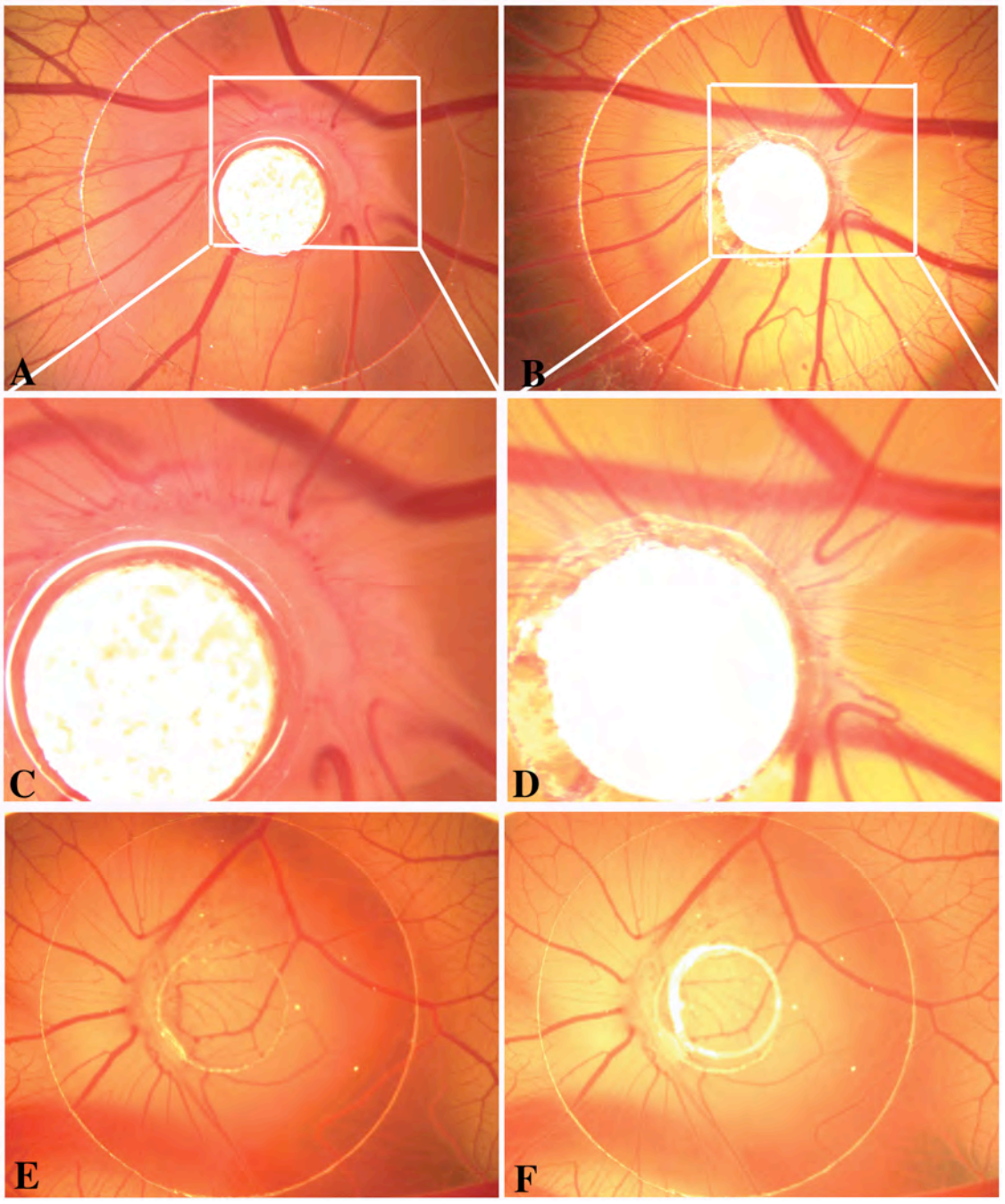

Figure 2-9. Effect of EMD implant on bFGF induced angiogenesis regression.

A). Right after implantation; B). 2 days after EMD implant treatment; C, D). Magnified neovasculature from A) and B); E, F). Before and 2 days after sham implant treatment.

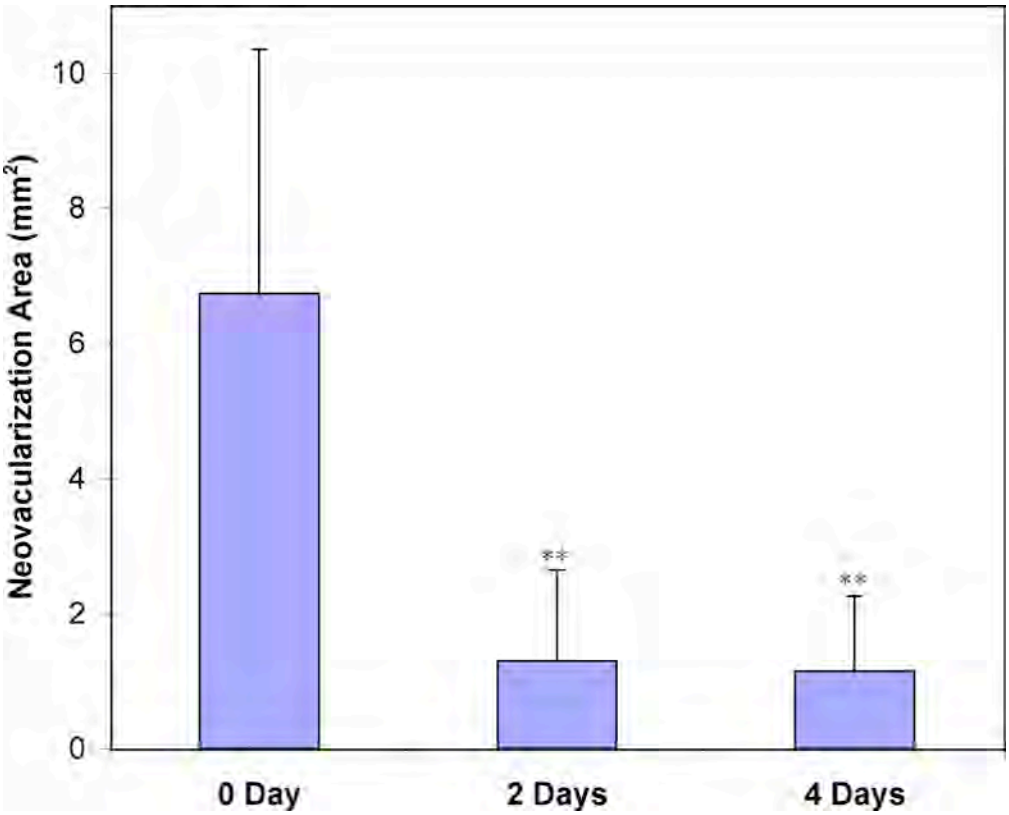

Figure 2-10. Effect of EMD478761 on bFGF-induced angiogenesis regression from the sustained release implant. Histograms show mean neovascular area ± SD after treatment with EMD478761 implant for 0, 2, and 4 days (** P< 0.001).

normal CAM vessels, suggesting that the drug acts as an angiogenic antagonist. This antagonistic effect could be the result of EMD478761 interacting and/or binding to the $\alpha_v\beta_3$ integrin expressed on cell membrane of sprouting CAM vessels. Moreover, sustained-delivery of EMD478761 dramatically reversed bFGF-induced angiogenesis in the CAM. As endothelial cells are implant players for neovascularization, regression of angiogenesis may be due to EMD478761-induced endothelial cell proliferation arrest and

subsequent programmed endothelial cell death. On the other hand, the over-expressed integrin $\alpha_v\beta_3$ on bFGF-induced neovasculature may be preferentially occupied by EMD478761, due to the high binding affinity of EMD478761 to integrin $\alpha_v\beta_3$, leading to the disruption of integrin-mediated endothelial cell survival signals. In addition, integrins are constantly produced and recycled between cell plasma and intracellular compartments. Sustained delivery of EMD478761 may continuously bind to the unoccupied integrin receptors that recycled back to the plasma, therefore constantly suppresses many cellular events involving integrin signaling. The data presented here not only showed that sustained delivery of EMD478761 has an anti-angiogenesis effect on the CAM, but also that this effect is restricted to proliferating vessels rather than mature/quiescent vasculature, indicating that EMD478761 holds a high selectivity as anti-angiogenic agent. The potent suppression of bFGF-induced angiogenesis demonstrated the activity of this integrin antagonist and its potential applications to CNV.

It should be noted that the CAM assay has its own limitations as it relates to the interpretation of the angiogenic response. The main limitation is the nonspecific inflammatory reactions that may develop as a result of implantation, addition of angiogenic stimuli, or potential contamination. The inflammatory reaction often impedes the quantification of angiogenesis responses to treatments, making vessel counting impossible. Other limitations include possible false increase of vessel density due to the rearrangement of existing vessels that follow contraction of the membrane, and time for inducing angiogenesis. Many developmental studies show that by embryonic day 10, CAM is fully developed, while its final arrangement continues until by embryonic day 18. We performed angiogenesis induction on 10-day old embryos when vasculogenesis

has already stopped. In this study, we quantified the angiogenic response by measuring the neovascularization area instead of angiogenesis index (57, 83) or vascular numbers (86)

Previous experiments using CAM and rabbit corneal models demonstrated that there are at least 2 distinct integrin-dependent angiogenesis pathways: 1) one induced by basic fibroblast growth factor (bFGF) and tissue necrosis factor α (TNF- α), and mediated by integrin $\alpha_v\beta_3$; 2) the other mediated by integrin $\alpha_v\beta_5$ and induced by vascular endothelial growth factor (VEGF), transforming growth factor α (TGF- α) or the phorbol ester phorbo 12-myristate 13-acetate (PMA) (25). The data presented in this study suggest that integrin-dependent angiogenesis pathways may be suppressed by specific integrin antagonists.

2.6 Conclusions

Sustained delivery of EMD478761 by a PVA reservoir implant significantly inhibits bFGF-induced angiogenesis in the CAM and it can also regress neovascularization. In addition, mature CAM vasculatures are not affected possibly due to the absence of integrins $\alpha_v\beta_3$ and $\alpha_v\beta_5$. These results suggest that integrin antagonists may represent a potentially powerful therapeutic approach for angiogenesis related diseases.

Chapter 3: Experimental Choroidal Neovascularization Suppression in Rats from EMD478761 Microimplant

Part of the results of this chapter was published in the following journal article:

Y. Fu, M. L. Ponce, M. Thill, P. Yuan, N.S. Wang and K.G. Csaky. 2007. Angiogenesis Inhibition and Choroidal Neovascularization Suppression by Sustained Delivery of an Integrin Antagonist EMD478761. *Invest Ophthalmol Vis Sci*. 48(11): 5184-90.

3.1 Purpose

Initial studies on the CAM assay suggest that EMD478761 can suppress cytokine-induced angiogenesis. The results from this screening experiment motivate the more relevant animal studies to investigate if EMD478761 can inhibit choroidal neovascularization in a rat model from a sustained release microimplant.

3.2 Introduction

Choroidal neovascularization is the primary cause of severe vision loss in retinal diseases. In the presence of CNV, the barrier function of Bruch's membrane is compromised. CNV can develop within the subretinal space between the RPE and the photoreceptor outer segment or under the RPE. Several therapeutic strategies have been developed to inhibit the growth of new choroid vessels (71, 72, 87-89). However,

efficient CNV suppression is not only dependent on novel therapeutic drugs, but also on the appropriate delivery method. Due to the protective barriers encountered in the eye and to the short half-lives of the majority drugs inside the vitreous, a long-release formulation of drug delivery could be more appropriate for the treatment of CNV. In this study, we have designed a sustained release microimplant and investigated its effect on CNV inhibition in rats.

The inhibitory effect of EMD478761 on experimental CNV was studied with a well validated laser trauma rat model. In this model, laser photocoagulation selectively ablates the photoreceptor outer segments, RPE, choroicapillaris, and portions of the anterior choroid. The subsequent wound response includes the in-growth of fibroblasts, RPE, and vascular endothelial cells that form a defined neovascular lesion (90). In addition, this particular animal laser model does not exhibit the rapid spontaneous regression of the neovascular process. Therefore, this is a suitable and well-accepted model to study the effect of sustained delivery of EMD478761 on angiogenesis inhibition and/or regression of CNV.

3.3 Materials and Methods

3.3.1 Microimplant Design and in vitro Release Rates

EMD containing microimplants were designed (Fig. 3-1) in a similar fashion to the circular implant using the following procedures: a polyvinyl alcohol (PVA) weight/volume (w/v) solution was formulated by placing appropriate amount of PVA

(Airvol® 125) in 30 ml of molecular biology grade water in a closed vial, and placed in a water bath at 100°C until completely dissolved. Several PVA concentrations were formulated ranging from 10% to 20%. The freshly made PVA solution was poured onto a glass plate forming a thin film. Compressed pellets, containing about 250 µg of EMD478761 were embedded within this film during its wet phase. After allowing the film to dry at room temperature, sections of the film with the drug core centered within the section were cut with a razor blade. Each section represented a reservoir microimplant measuring 1x1x2 mm. Sham implants were made in a similar fashion except that no drug was incorporated. All implants were sterilized (3×10^4 grays, gamma radiation) before use.

In vitro release rates on representative implants of each design were measured daily with an HPLC. Each implant was placed in a vial with a constant volume of phosphate buffered saline (PBS) (pH 7.4) at 37° C. The PBS was replaced every 24 hours to simulate sink conditions. HPLC detection parameters were set as previously described in chapter 2. The release rates were determined by calculating the amount of drug released in a given volume over time and recorded for each implant design in µg/day (± 1 SD). The cumulative drug released was calculated by integrating the area under the release rate curve and recorded separately for each implant design in µg ± 1 SD

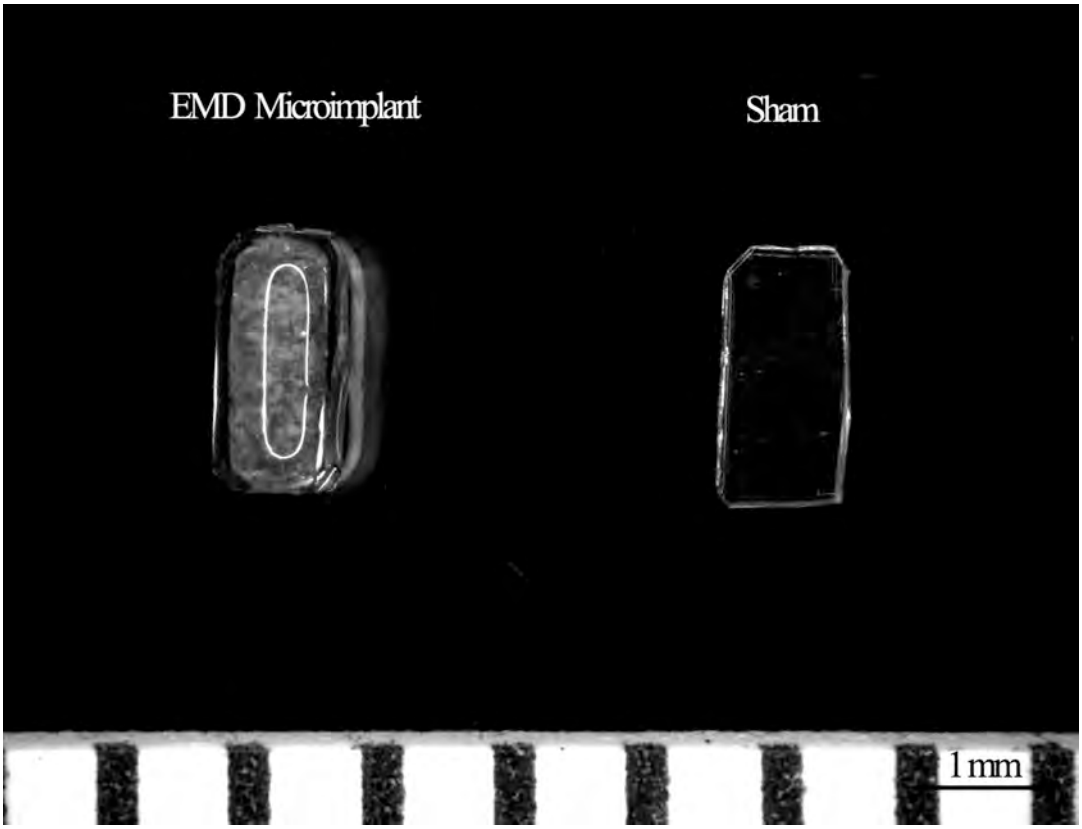

Figure 3-1. Representative image of microimplant made from 15% PVA. Sham implant contains no drug. The final dimension of the microimplant is 1 x 1 x 2 mm.

3.3.1 Animals and CNV Induction

All procedures were performed with strict adherence to guidelines for animal care and experimentation prepared by the Association for Research in Vision and Ophthalmology, and by the National Eye Institute/National Institutes of Health. Male adult (250 g) Brown-Norway rats (Charles River Laboratories, Raleigh, NC) were used to evaluate the effect of intravitreal EMD478761 microimplants versus control implants on laser-induced experimental CNV. The rats were anesthetized for all procedures with intramuscular

ketamine at 70 mg/kg and xylazine at 30 mg/kg. After receiving anesthesia, the pupils of the rats were dilated with 1% tropicamide ophthalmic solution (Mydriacyl®, Alcon, Fort Worth, TX). The fundus was visualized with a slit lamp biomicroscope (Haag-Streit, Mason, OH) using a slide coverslip as a contact lens. A diode red laser (810 nm; Iris Medical Instruments, Inc., Mountain View, CA) was used to induce CNV by rupturing the Bruch's membrane. Laser parameters were set to 75 µm spot size, 100 ms exposure, and 150 mW power. A series of four laser lesions were placed at approximately equal distance around the optic discs of both eyes of the animals. Eyes that bled or showed no bubble formation were excluded.

3.3.3 Intravitreal Injections

To examine whether bolus injection of EMD478761 is sufficient to abrogate the development of CNV, single intravitreal injection of 10 µl of 0.5 mg/ml EMD478761 was performed through a 32 gauge delivery needle (Hamilton Co., Reno, NV) under a Zeiss operating microscope (Thornwood, NY) on 5 animals immediately after laser photocoagulation. For control studies, rats with rupture of Bruch's membrane in each eye were given intravitreally 10 µl of PBS or no injection.

3.3.4 Intravitreal Implantation

In the current study, an EMD microimplant or a sham implant was placed in the vitreous cavity of the right eye, and the left eye served as laser control. The conjunctiva was

dissected and a small single incision was made with a 20 gauge needle in the superior globe, just posterior and parallel to the ora serrata, allowing the microimplant to be inserted within the vitreous. The posterior segment was evaluated immediately after insertion to confirm proper placement of the microimplant into the vitreous cavity. All eyes were treated with topical antibiotic ointment (Fougera®, E.Fourera & Co, Melville, NY).

3.3.5 CNV Quantification using FITC-dextran Perfusion

CNV was labeled by vascular perfusion with high molecular weight fluorescein isothiocyanate (FITC)-dextran (MW = 1x 10^6) by a similar method previously described (90, 91). The rats were sacrificed with 100% CO_2 2 weeks after laser photocoagulation and perfused with 5 ml of PBS, 5 ml of 4% (w/v) paraformaldehyde (PFA) and 5 ml of 10mg/ml high molecular weight FITC-dextran (Sigma, St. Louis, MO). Eyes were immediately enucleated and fixed in 4% PFA. Choroidal flatmounts were made, as previous described (90, 91), by hemisecting the eye and removing of the retina. CNV from implant treatment, intravitreal injection and laser controls was thereafter examined by a fluorescence microscope (Olympus BX50, Melville, NY). Images of the neovascular lesions were captured with a CCD color video camera (Retiga EX, Burnaby, BC, Canada) coupled to a Macintosh computer. Areas of CNV were measured with Image J (ver 1.32j, NIH, Bethesda, MD). The overall procedures are illustrated in Fig. 3-2.

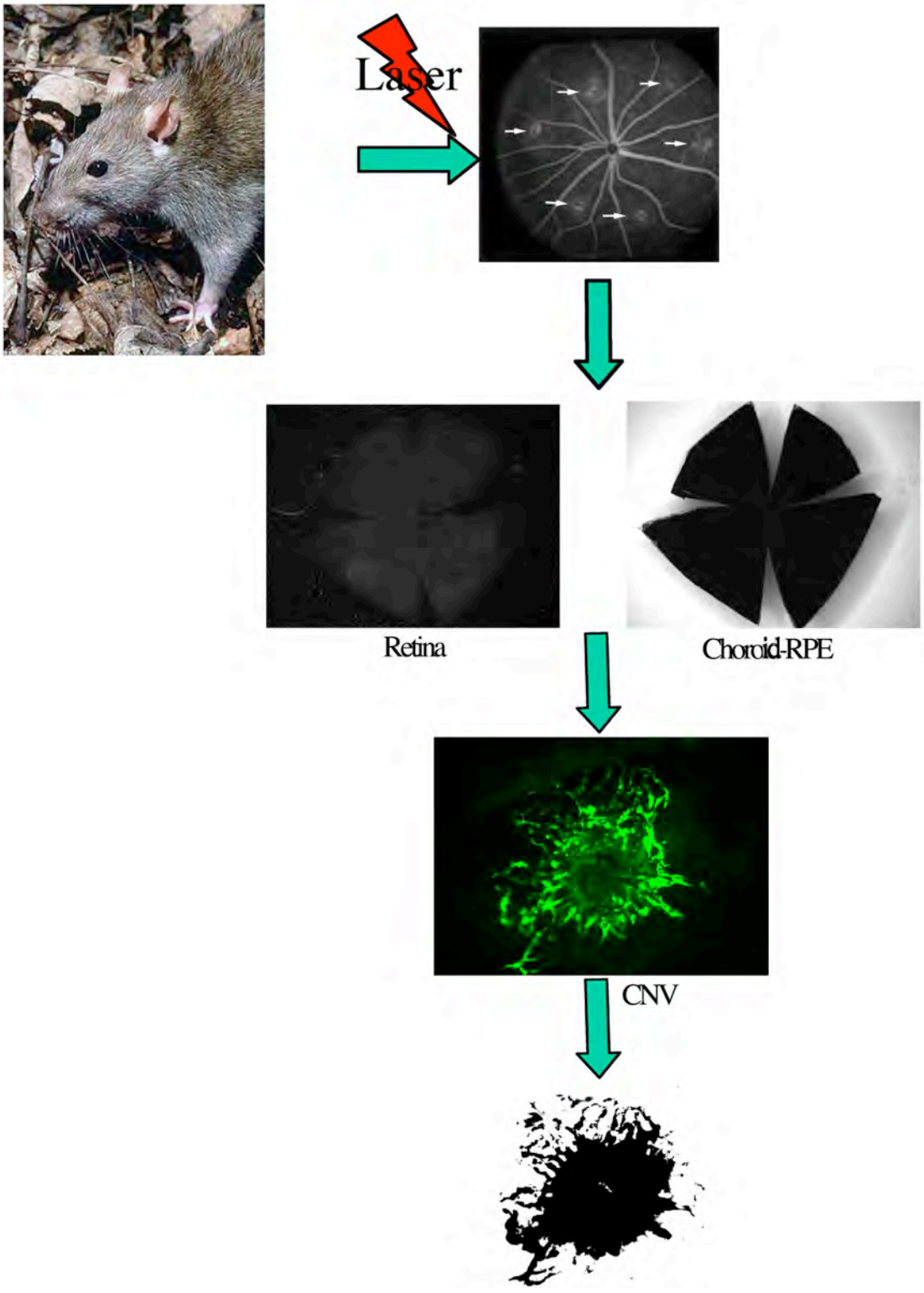

Figure 3-2. Flow chart of laser induction of CNV in rats.

3.3.6 Histopathological Studies

Five eyes from each treatment group were collected 2 weeks after laser photocoagulation for histologic studies. Treated CNV lesions were compared with the control lesions, which had been induced with the same pattern of laser injury. After euthanasia, rat eyes were immediately collected, placed in plastic molds filled with embedding medium (Tissue-Tek O.C.T. Compound, Sakura Finetek, Torrance, CA) and flash frozen on dry ice. Frozen eyes were sectioned transversely on a cryostat at -20˚C at 10-µm thick. Ocular frozen sections were air dried and fixed with freshly prepared 4% PFA in PBS at room temperature for 15 minutes and rinsed with PBS three times. The prepared sections were then stained with hematoxylin and eosin.

Further studies on CNV lesions were performed using vibrating microtome sections. After euthanized, the eyes were enucleated and fixed in 4% PFA for 4 hours and then the eyes were cleaned and hemisected to remove the anterior segment. The posterior segment of the eye was embedded in 7% (w/v) agarose type XI (Sigma, St. Louis, MO), and sectioned with a vibrating microtome (Leica, VT-S1000, Bannockburn, IL) at 100 µm thickness. The vibration frequency was set to 3 Hz. Ocular sections were blocked with 5% normal goat serum in I.C.C. buffer (0.5% bovine serum albumin, 0.2% Tween-20, 0.05% sodium azide, PBS, pH 7.3) at 4°C for 4 hours. Sections were incubated with Alexa Fluor 488-conjugated isolectin IB4 (1:50, Invitrogen, Carlsbad, CA) and 4',6-diamidino-2-phenylindole, dihydrochloride (DAPI, 1:1000, Invitrogen) in 2% normal goat serum in I.C.C buffer overnight at 4°C. Sections were then washed three times 15 minutes each with I.C.C. buffer and mounted onto slides with Gel-mount

(Biomedia Corp., Foster City, CA). Images were taken with a confocal microscope (SP2: Leica, Exton, PA).

3.3.7 Statistical Analysis

All data are presented as the mean ± SD. The data were statistically evaluated by student's t-test. $P \leq 0.05$ is considered statistically significant.

3.4 Results

3.4.1 In vitro Release Rates of the Implants

Microimplants made with different concentrations of PVA demonstrated a similar release profile: deliver an initial burst of drug on the first day, followed by a constant release rate for the next 10 days, which then gradually decreased over time (Fig. 3-3). Moreover, the release rates of the implants were inversely related to their PVA concentrations. Implants made with higher PVA concentrations showed slower release rates as expected. In addition, the steady-state mean release rates between days 2 and 11 remained constant, typical for a diffusion controlled reservoir implant (84). The steady-state release rate of the implants made with 15% PVA was 18.5 ± 3.8 µg/day. Those made with 10% and 20% PVA had steady-state release rates of 28.5 ± 9.6 µg/day and 13.4 ± 3.2 µg/day, respectively. These results indicate that the microimplants can slowly release drug for over 17 days.

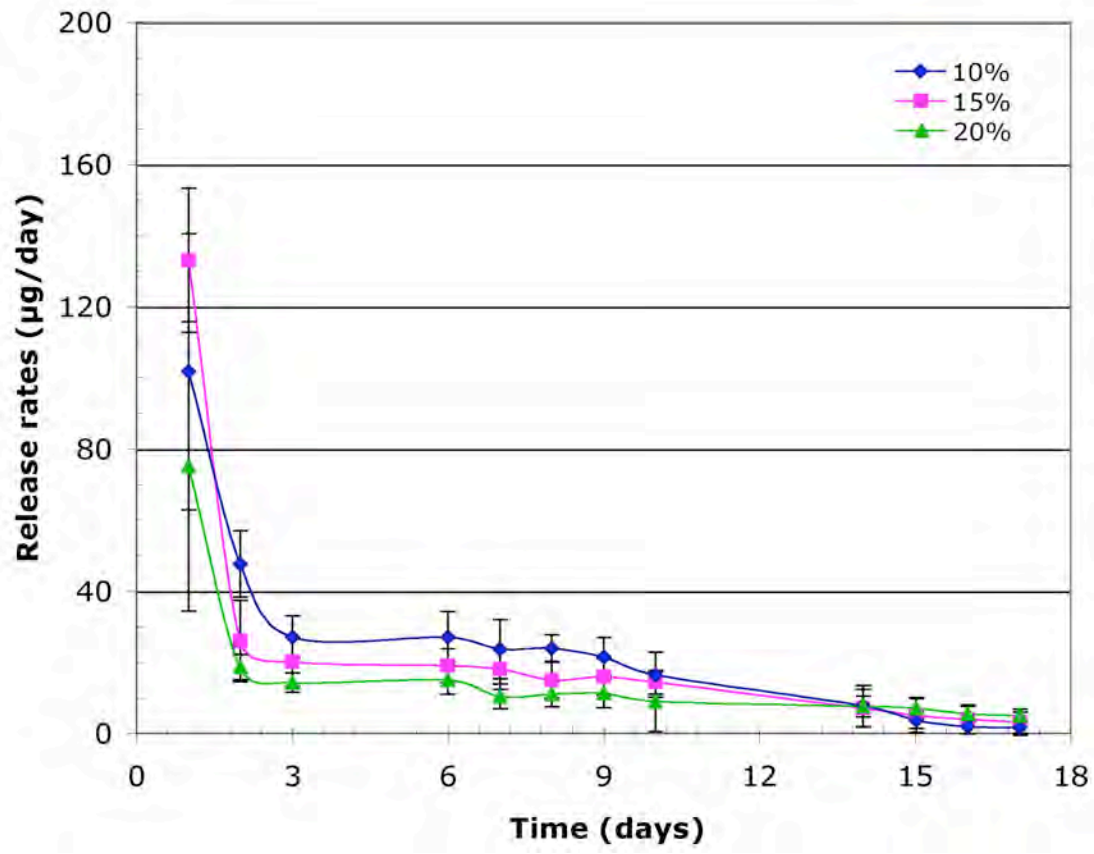

Figure 3-3. Mean release rates of the microimplants made with 10%, 15% and 20% PVA.

3.4.2 Effect of Intravitreal Injection of EMD478761 on Laser-Induced CNV

Laser photocoagulation of the RPE-choroid resulting in reproducible experimental CNV has been well validated by several groups (90, 92-94). To examine whether bolus administration of EMD478761 can lead to significant suppression of the development of laser-induced CNV, a single intravitreal injection of EMD478761 at the dose of 5 µg was performed on 5 animals immediately after laser injury. 14 days after treatment, the area of CNV was measured by image analysis. The size of the CNV lesions treated with

EMD478761 appeared to be smaller than that of PBS control (Fig. 3-4). However, the differences (12%) between them were not statistically significant (P = 0.68). This suggests that single intravitreous injection in rats at the maximal allowable soluble dose is not able to maintain levels of EMD478761 sufficient to significantly inhibit CNV.

3.4.3 Effect of EMD478761 Microimplant on Laser-Induced CNV

To explore the feasibility of local and sustained delivery of EMD478761 microimplants to inhibit laser-induced CNV in rats, we placed an EMD microimplant or sham implant into the vitreous cavity of the right eye after the laser-induction was performed. Left eyes served as laser controls. Five animals from each treatment were sacrificed 14 days after implantation. EMD microimplants inhibited CNV relative to sham implant and laser controls in a statistically significant fashion ($P < 0.05$). 14 days after laser induction, in the eyes that received EMD478761 microimplant, the mean CNV areas of the lesions decreased 65% and 63%, respectively, as compared to those of laser controls and sham implant treated eyes (Fig. 3-5, 3-6). In addition, there was no significant difference between sham implant and laser controls (Fig. 3-5, 3-6).

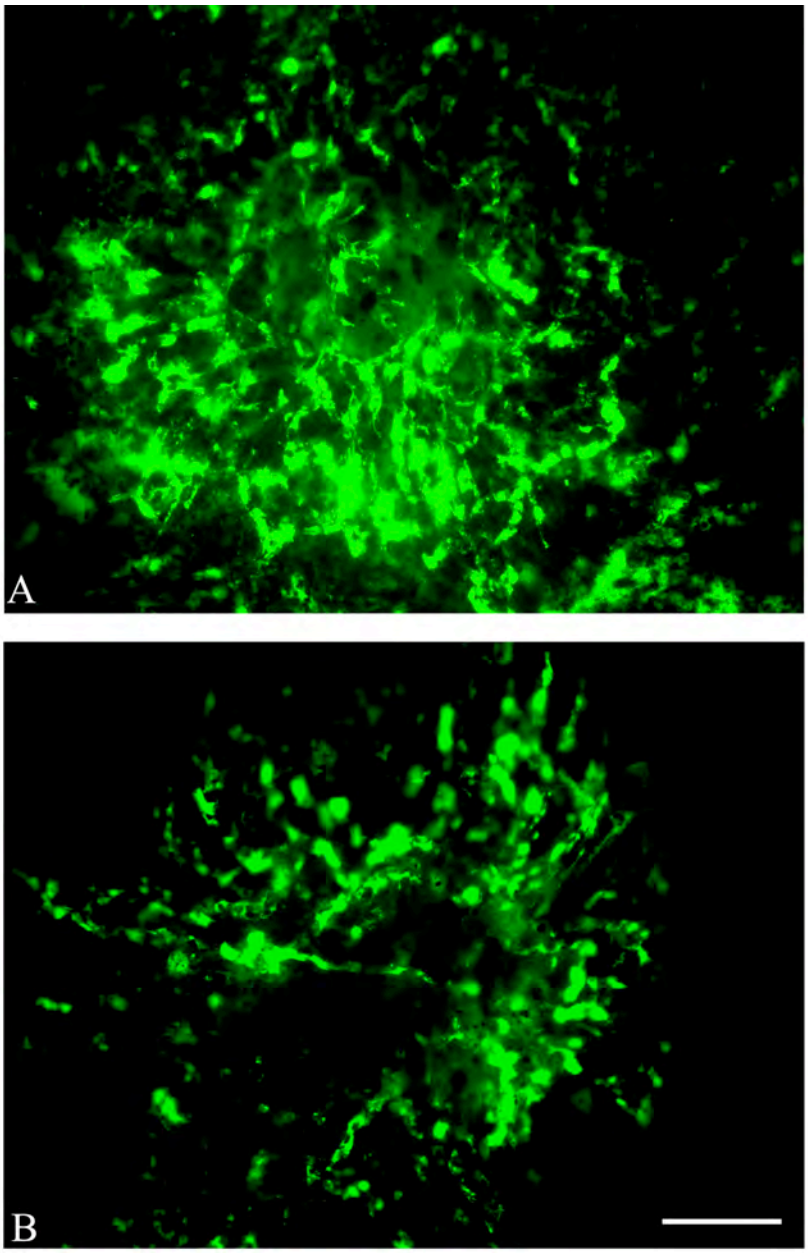

Figure 3-4. Effect of intravitreal injection of EMD48761 on laser-induced CNV. A) CNV control with intravitreal PBS injection; B) Intravitreal EMD478761 treated CNV. The vasculature was labeled with FITC-dextran 2 weeks after laser photocoagulation. Scale bar represents 100 μm.

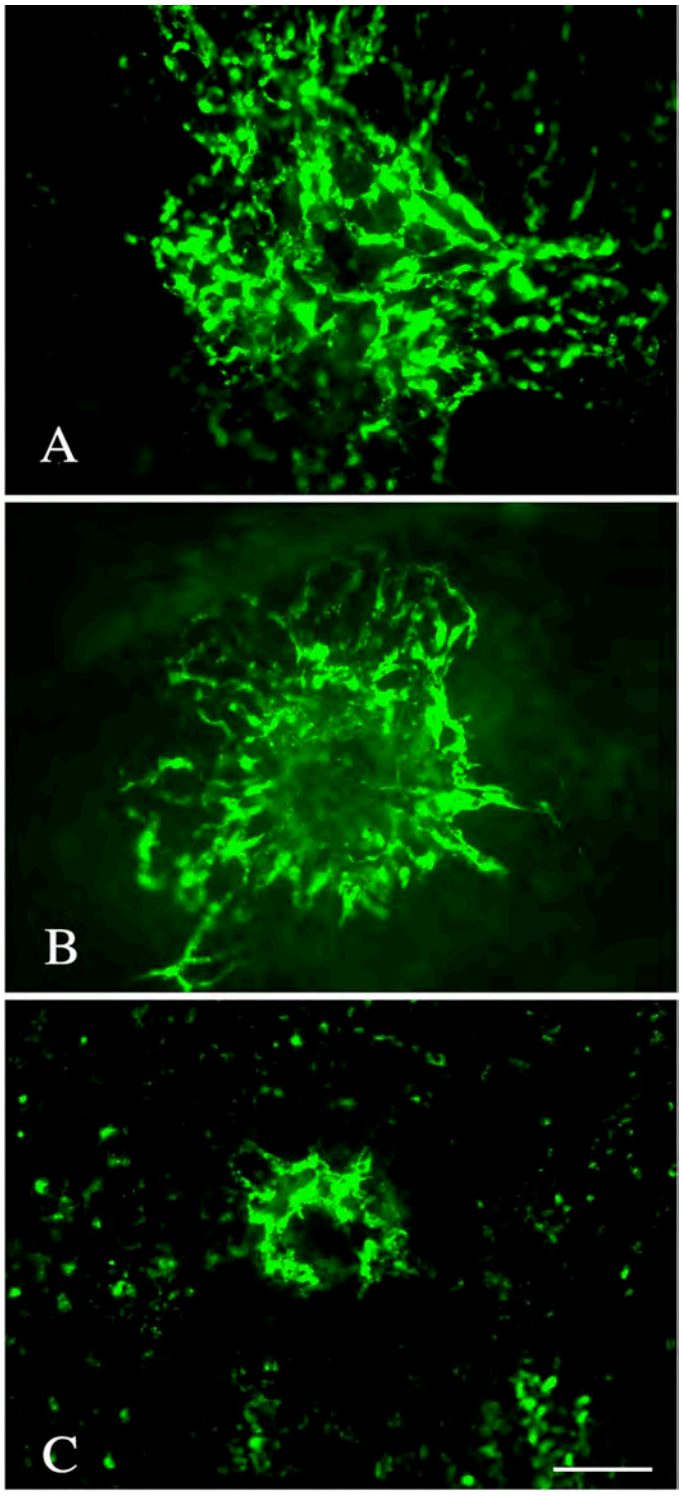

Figure 3-5. Effect of EMD478761 microimplant on laser-induced CNV. A) Laser control lesion; B) Sham implant treated CNV; C) EMD478761 microimplant treated CNV. Scale bar represents 100 μm.

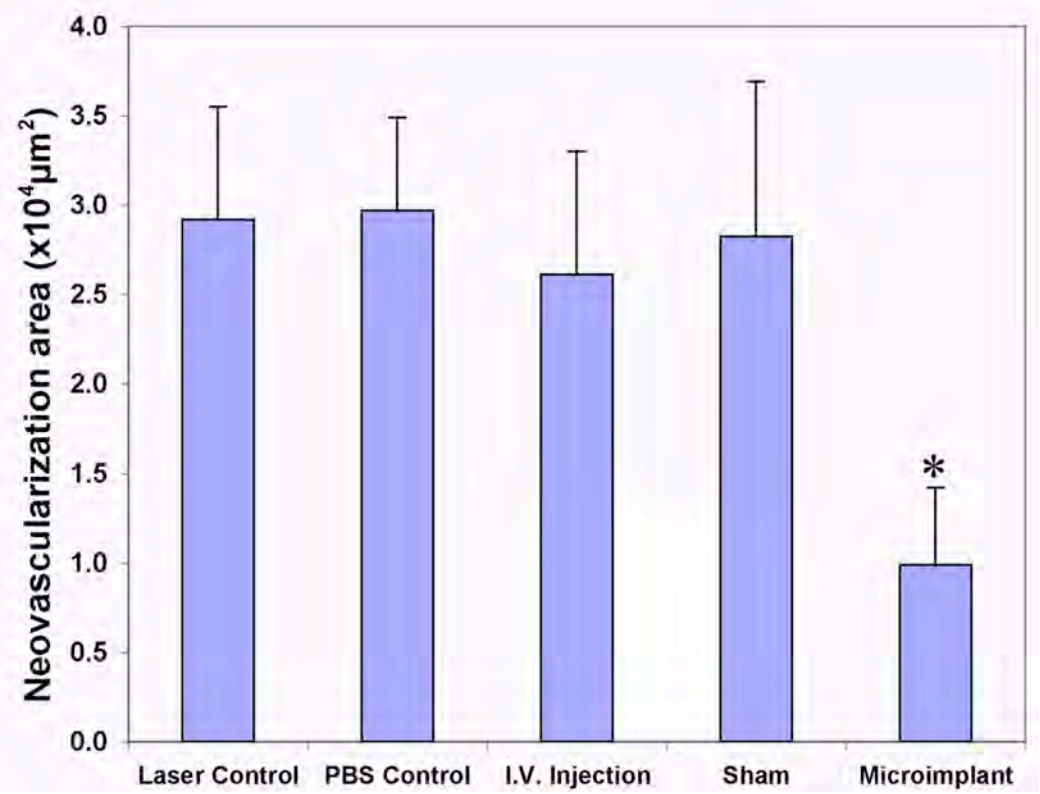

Figure 3-6. Quantitative CNV areas measured from lesions 2 weeks after laser treatment (* $P < 0.05$ compared to laser control and sham). The vasculature was labeled via cardiac perfusion 2 weeks after laser photocoagulation.

3.4.4 Histological Studies

Two weeks after CNV induction, histopathology of eyes treated with laser or PBS revealed numerous new blood vessels arising from the disrupted RPE and Bruch's membrane (Fig. 3-7A and B). Eyes treated with intravitreal bolus injection of EMD478761 demonstrated a similar response to those treated with PBS (Fig. 3-7C). In contrast, eyes with the EMD microimplant treatment showed only very thin proliferative

membranes and few new blood vessels under the retina (Fig. 3-7E). Sham implant treated eyes showed a similar response to those of laser controls (Fig. 3-7A, D), indicating that there was no inhibitory effect of the sham implant on CNV. These results are consistent with those of CNV areas calculated from choroidal flatmounts. Examination of the slides showed an absence of inflammatory cells in both EMD implants and sham implants.

Results from immunohistochemical staining with isolectin IB4 (Fig. 3-8), which selectively stains vascular cells and allows visualization of CNV, corroborates the above findings. Control eyes (Fig. 3-8A, C) demonstrated extensive new vessel formation under the retina. Intravitreal injection of EMD478761 failed to inhibit CNV, while sustained delivery of EMD478761 using a microimplant almost completely suppressed the development of CNV (Fig. 3-8 B, D).

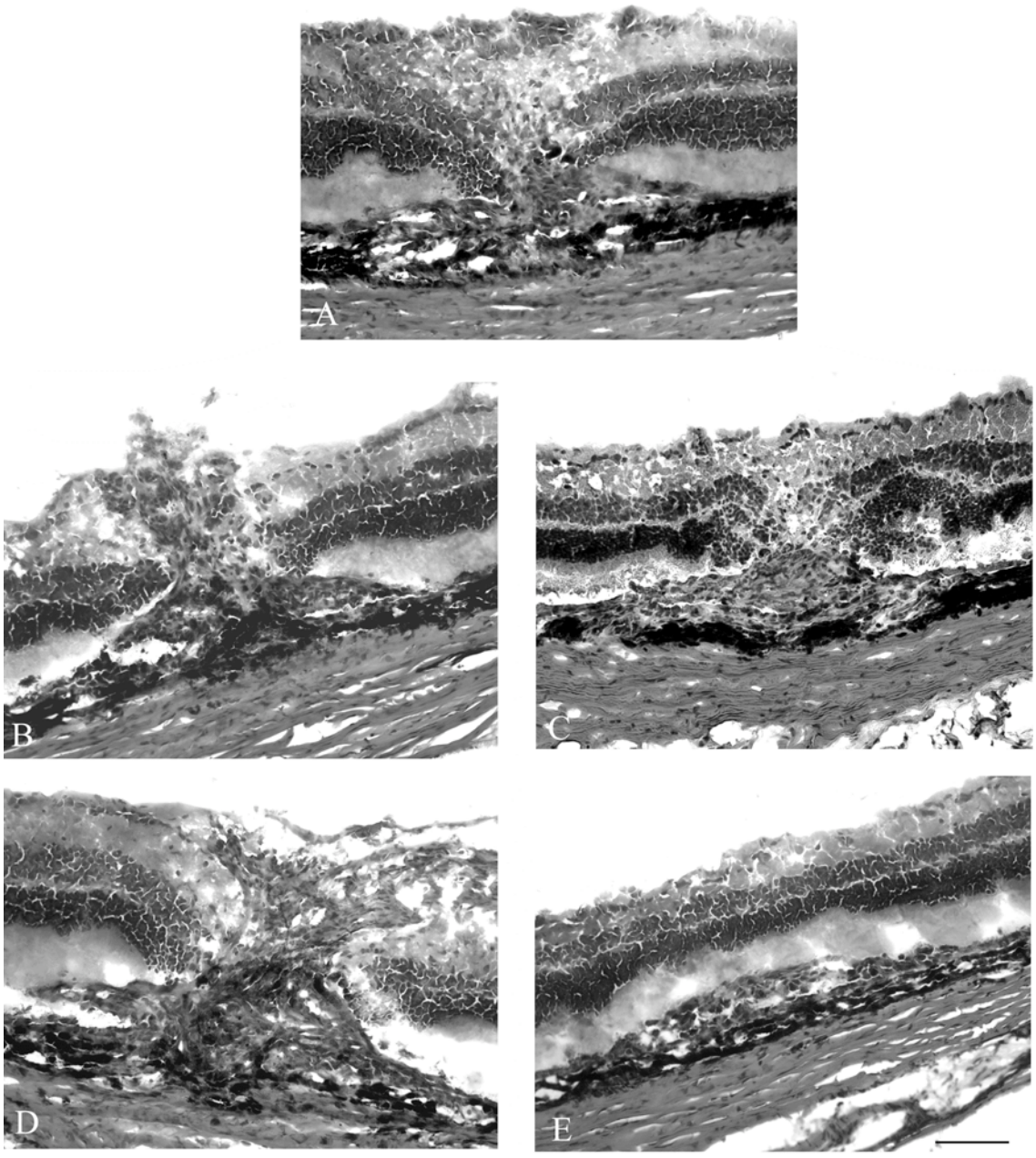

Figure 3-7. Hematoxylin-eosin stained light microscopy images of CNV 2 weeks after laser photocoagulation. Each image shows the center of CNV lesions. Minimum of 10 lesions per treatment was examined. (A-E) Histologic sections of the eye with laser control, intravitreal PBS injection, intravitreal EMD 478761 injection, sham implant And EMD478761 microimplant treatment, respectively. Scale bar represents 100 μm.

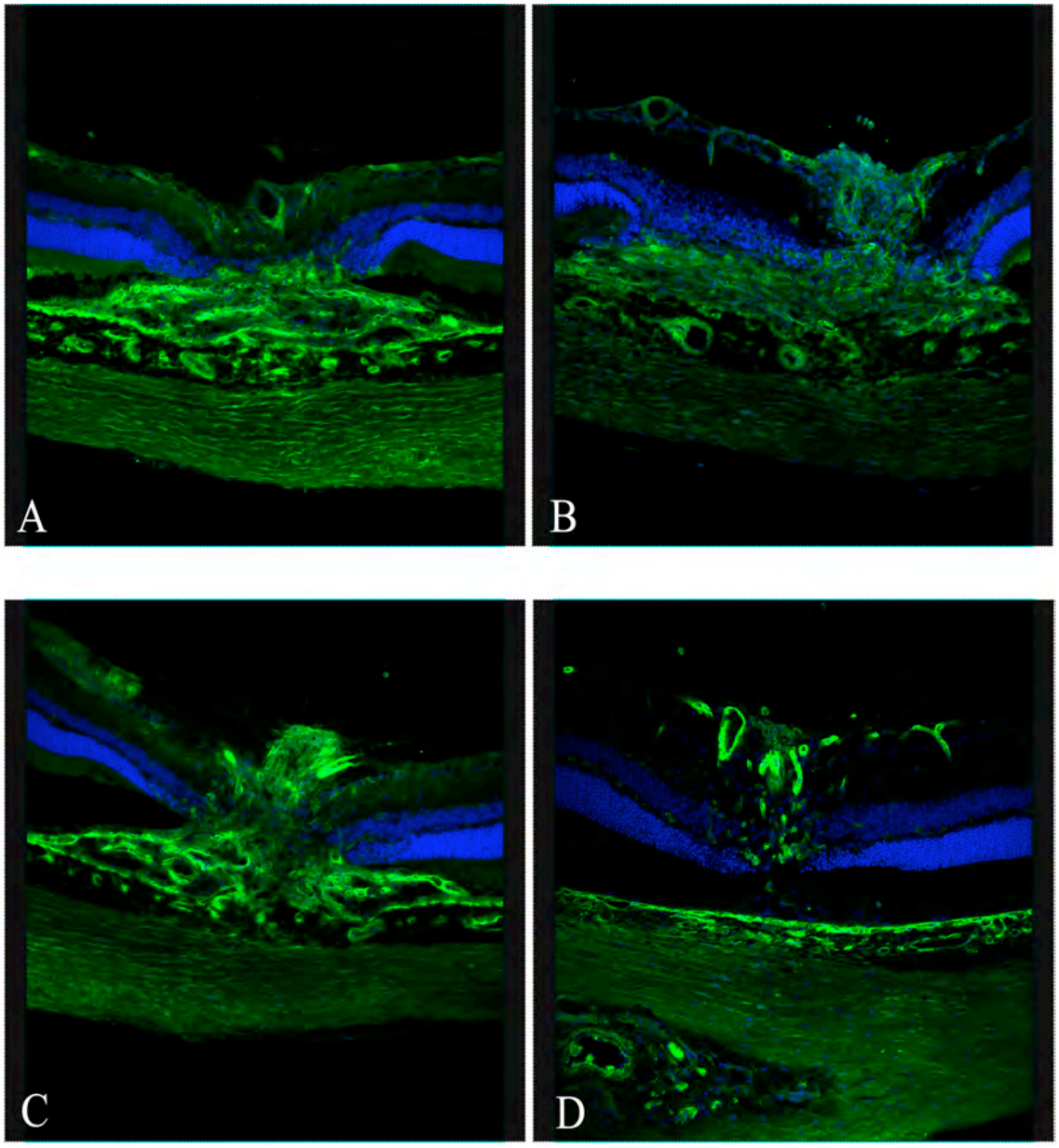

Figure 3-8. Immunohistochemical staining of CNV lesions in rats. Vibrotome sections of CNV (14d) were stained for vascular cells with isolectin IB4 (green) and nuclei were counterstained with DAPI (blue). Each image shows the center of the lesion. A) CNV cross section of control eye; B) CNV lesion from an intravitreal EMD478761 treated eye; C) Sham implant treated CNV lesion; D) CNV from an eye treated for 14 days with an EMD478761 microimplant.

3.5 Discussion

CNV posses a great vision threat to the senior population world wide. Conventional treatments have demonstrated limited success in improving or preserving the visual function of CNV affected patients. The roles of anti-angiogenic agents are important in that these agents can affect various aspects of the angiogenic cascade, including endothelial cell migration and proliferation, and neovasculature formation. Although numerous antiangiogenic compounds such as triamcinolone acetonide, TNP-470 and some monoclonal antibodies , have been used to target choroidal neovascularization (33, 58, 72, 93, 95-97), results are far from satisfactory. Currently there are only two anti-VEGF therapies, Macugen™ (pegaptanib sodium, Eyetech, Inc.) and Lucentis™ (ranibizumab, Genetech, Inc.), that have been approved by the FDA for the treatment of advanced AMD. However, the majority of these drugs are delivered via intravitreal injections (33, 93, 97, 98). Given the formidable ocular drug delivery barriers and the short half-lives of drugs inside the vitreous, maintaining therapeutically efficacious levels of drug may be achieved either by continuous or repeated injections, or by a mechanism whereby the drug is sustained released by an implanted device. Although the laser-induced model is controversial as to whether it mimics the most common form of naturally occurring CNV, in age-related macular degeneration, its essential process resembles that of CNV, including breaking of Bruch's membrane, vascular endothelial cell migration and proliferation, and tube formation. Moreover, this model does not exhibit the rapid spontaneous regression of the neovascular process which makes it useful for the evaluation of anti-angiogenic treatments. In this study, we demonstrated a sustained drug delivery approach to locally sustained deliver EMD478761, a small

molecule integrin antagonist of $\alpha_v\beta_3$ and $\alpha_v\beta_5$, to the site of neovascularization in a laser-induced rat model.

Angiogenesis is partially regulated by integrins (24, 25). The $\alpha_v\beta_3$ and $\alpha_5\beta_1$ integrins appear to be over-expressed in laser-induced CNV in rats (88) and mice (26), but not on normal choroidal vessels. The high expression and up-regulation of these integrins suggests that they may play an important role in CNV. Indeed several antagonists to these integrins have been developed, and they potently inhibit cytokine- and tumor- mediated angiogenesis in different animal models (26, 58, 99-103). Intravitreal injection of cyclic RGD, an α_v-integrin antagonist, effectively inhibited progression of laser-induced CNV in rats (93). Systemic administration of JSM6427, an integrin antagonist to $\alpha_5\beta_1$, significantly suppressed the development of CNV in mice by 33 to 40% (26). In this work, we observed that intravitreal bolus injection of EMD478761 failed to attenuate the development of CNV. The low efficacy of this delivery route was not surprising as the dosage used in this study, which was limited by its aqueous solubility (~500 µg/ml), was 20 times lower than that used for cyclic RGD peptides (93). Other possible explanations for this observation include the quick turnover of the integrin $\alpha_v\beta_3$ receptor ($t_{1/2} < 10$ minutes) (104) and rapid elimination of the drug from the vitreous (9, 10). The limited drug solubility, the small vitreous volume, which can be estimated at approximately 56 µl (105), as well as the lower levels of drug extraction efficiency from ocular tissues (less than 65%, H. Kim, 2007, unpublished data) preclude a direct, *in vivo* pharmacokinetic measurement of EMD478761 in the rat eye. However, all of these possibilities could be obviated by the use of a sustained delivery device. In addition, to our best knowledge, sustained delivery of an integrin antagonist

with an implant has not been previously studied. For these reasons, we have designed a sustained release delivery system that would provide a therapeutic dose for this compound for an extended period of time.

Sustained release microimplants have been shown to be beneficial in ocular delivery of other antiangiogenic compounds in that not only they can bypass the main ocular delivery barriers by being directly inserted into the vitreous cavity, but also prolong the half-life of the drug. For example, it has been previously shown that sustained-release 2-methoxyestradiol silicone implant was safe in normal rabbits and suppressed CNV in rats (70). In another study, Ciulla *et al*. demonstrated the potent inhibition of laser induced CNV in rats by the sustained release of triamcinolone acetonide from matrix type microimplants (71). However, both of these studies were relatively qualitative and focused on the effect of the implants on the thickness of the lesions by counterstaining the sections with hematoxylin and eosin. The present study demonstrates that EMD478761 can be delivered intraocularly using a sustained release PVA reservoir microimplant. Animals treated with the EMD478761 microimplant exhibited a 63% reduction in the CNV area 2 weeks post implantation compared with sham treated animals. Furthermore, new vessels and thicker neovascularization membranes were observed in both untreated and sham treated eyes compared to EMD478761 implant treated eyes. The increased potency seen in the sustained delivery approach may be attributed partially to the continuous presence of the drug around the neovascularization tissues. Therefore, the angiogenic integrin receptors might be constantly suppressed, leading to significant suppression of the development of CNV. Although previous studies revealed that polyvinyl alcohol tended to accumulate at the

CNV lesion site (106), the fact that there was no significant difference between sham implant treated eyes and laser controls, indicated that CNV inhibition was not an artifact of the PVA polymer, but the result of EMD478761 released from the microimplant. Histologic studies performed on those eyes treated in the same manner confirmed this finding.

The mechanism by which EMD478761 exerts its anti-angiogenic effect is likely to be similar to that by which other integrin antagonists act. A predominant characteristic of CNV is the excessive growth of new blood vessels from the pre-existing vasculature. Endothelial cells play a pivotal role as they form a tube in every blood vessel and are actively involved in vascular remodeling during CNV. Therefore, EMD478761 could exert their inhibitory effect through either anti-adhesion of endothelial cells to the extracellular matrix (93), induction of apoptosis of endothelial cells (107), or through changes in the regulation of integrin expression (108). Additional studies of the mechanisms of the drug's action mode will be investigated in the late chapters to further assess the anti-angiogenic efficacy of EMD478761 via this sustained delivery system.

3.6 Conclusions

In conclusion, sustained release EMD478761 implants suppressed laser-induced CNV in rats. These results provided new evidence that sustained release of EMD478761 may be useful in the treatment of neovascular ocular diseases.

Chapter 4: A Dual Integrin Antagonist EMD478761 Induces Endothelial Cell Apoptosis *in vitro* and Reverses Angiogenesis *in vivo*

4.1 Purpose

To investigate EMD478761's action mode on angiogenesis inhibition and on its ability to reverse angiogenesis in vivo.

4.2 Introduction

In chapter 2 and 3, we demonstrated that sustained delivery of EMD478761 inhibited bFGF-induced angiogenesis in the CAM assay and suppressed laser-induced choroidal neovascularization in rats. However, as a new compound, its anti-angiogenic mechanisms are still unknown.

Angiogenesis is a multistage complex physiological and pathological event, involving endothelial cell activation, extracellular matrix degradation, cell proliferation, migration and tube formation. Therefore, each stage of the angiogenesis cascade could be a potential therapeutic target. As vascular endothelial cells are the key players in new vessel formation and vascular remodeling, novel anti-angiogenic agents could act by

preventing endothelial cell adhesion or proliferation, or by regulating the expression of extracellular matrix receptors, or by inducing the apoptosis of endothelial cells.
In this chapter, we have investigated the action modes of this small molecule, EMD478761, both *in vitro* and *in vivo*. Particular attention was paid to the ability of this compound to inhibit endothelial cell proliferation, and to induce cell apoptosis on different substrates and in a laser-induced CNV rat model.

Apoptosis, or programmed cell death, is a highly ordered form of cell suicide. Apoptosis involves chromatin condensation, DNA fragmentation, and the formation of membrane-enclosed apoptotic bodies containing well-preserved organelles (109-112). We hypothesize that EMD478761 inhibits angiogenesis by induction of endothelial cell apoptosis. To test this hypothesis *in vitro*, we studied caspases activation and Annexin V staining in HUVECs in the presence or absence of EMD478761; *in vivo*, we examined apoptosis using terminal deoxynucleotidyl transferase (TdT)-mediated deoxyuridine triphosphate (dUTP) nick end labeling (TUNEL) on laser-induced CNV lesions.

4.3 Materials and Methods

4.3.1 Compound

EMD48761, an inner salt of a diastereomerically pure benzoxazione with dual antagonism to integrins $\alpha_v\beta_3$ and $\alpha_v\beta_5$, was obtained from Merck KGaA (Darmstadt, Germany). It was developed specifically for ophthalmic use. EMD478761 was

solubilized to a concentration of 0.5 mg/ml in PBS. Its retention time determined by HPLC was 7 minutes.

4.3.2 Endothelial Cell Culture

Early passage of human umbilical vein endothelial cells (HUVEC) were obtained from Vec Technology Inc. (New Jersey, NY). Cells were maintained in RPMI 1640 (Invitrogen, Gaithersburg, MD) supplemented with 20% bovine calf serum (BCS) (Hyclone Laboratories, Logan, UT), 200 µg/ml endothelial cell growth supplement (ECGS) (BD Biosciences, San Jose, CA), 5 units/ml heparin (Sigma, St. Louis, MO), 100 units/ml penicillin and 50 µg/ml gentamicin at 37 °C. For all experiments, cells were used between passages 3 and 7.

4.3.3 Endothelial Cell Adhesion Assay

Adhesion assay was performed on 96-well plate. Tissue culture 96-well plates were incubated either with 100 µl of 5 µg/ml of human fibronectin (Sigma, St. Louis, MO), or 3 µg/ml of recombinant human vitronectin (Invitrogen, Gaithersburg, MD) overnight at 4°C. Coated plates were blocked with 0.5% heat denatured bovine serum albumin (BSA) (Sigma) for 1 hour at 37°C and rinsed three times with PBS. Control wells were blocked with BSA without prior coating. Sub-confluent HUVECs were detached with Versene (Invitrogen) and washed with RPMI1640 without phenol red. Cells were pre-incubated with EMD478761 (0-10 µg/ml) for 30 minutes at 4°C prior to adhesion for 1 hour at

37°C on fibronectin-or vitronectin-coated plates. After incubation, unattached cells and residual buffer were removed. Cell adhesion was evaluated by fixing and staining the adherent cells with 20% methanol containing 0.2% crystal violet. The plates were extensively rinsed with deionized water and the dye was solubilized with 2% sodium dodecyl sulfate (SDS). Absorption values at 595 nm were determined for each well with an ELISA microplate reader (Tecan Safire, Durham, NC).

4.3.4 Endothelial Cell Proliferation Assay

Cell proliferation was carried out using a XTT proliferation assay kit (Roche, Indianapolis, IN). This assay is based on the cleavage of a yellow tetrazolium salt, XTT, to form an orange formazan dye by mitochondrial dehydrogenases in living cells (Fig. 4-1). Briefly, sub-confluent HUVECs were detached with trypsin/EDTA and seeded at a density of 2 x 10^4 cells/well in a 96-well plate in the presence or absence of EMD478761 (0 – 1.2 µg/ml). Some cells were treated with 2 µg/ml of C16Y, an anti-angiogenic

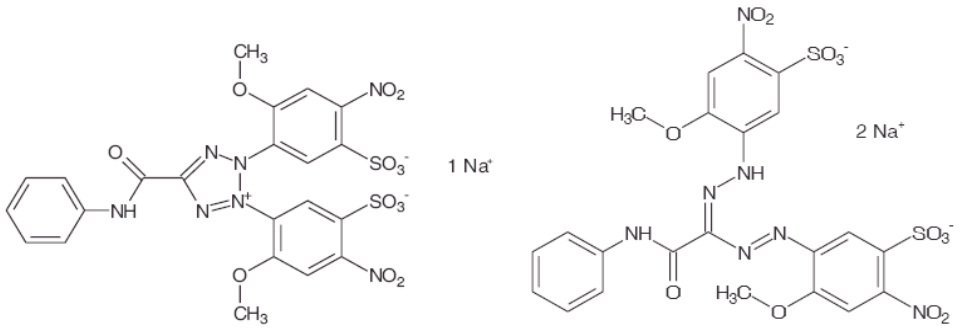

XTT Formazan

Figure 4-1. Metabolization of XTT to a water soluble formazan salt by live cells.

peptide. After 24 hours of incubation, cell proliferation was assayed according to the manufacture's instructions. Initial number of cells served as control.

The effect of EMD47876 on human endothelial cell proliferation was further investigated immohistochemically by examining bromodeoxyuridine (BrdU) incorporation, the expression of cell cycle regulatory proteins, proliferating cell nuclear antigen (PCNA) and p21. In brief, 8-well tissue culture treated glass chambers (BD Biosciences) were coated with 20% bovine calf serum (Hyclone, Logan, Utah) in RPMI 1640 medium (Invitrogen) for 1 hour at 37 °C. HUVECs were collected and plated at 3 x 10^5cells/well in pre-treated 8-chambers. After the cells reached subconfluence, the medium was replaced with endothelial cell serum free medium (Invitrogen) supplemented with 0.1% BSA. Cells were incubated with 0, 0.02, 0.2 and 0.6 µM EMD 478761 in the presence (BrdU incorporation) or absence (PCNA and p21 expression) of 10 µM BrdU (Invitrogen, Eugene, OR) for 24 hours. Cells were then fixed with 4% PFA for 15 min at room temperature and blocked with 5% normal goat serum (Sigma) in I.C.C buffer for 1 hour. Cells which were treated in the presence of BrdU, were incubated with Alexa Fluor 660-conjugated anti-BrdU antibody. For detection of PCNA and p21 expression, cells were incubated with anti-PCNA or p21Waf1/Cip1 primary antibodies (Cell Signaling Technology, Berverly, MA) for 1 hour at 1:200 dilution in I.C.C buffer. The antigens were then detected with secondary antibodies conjugated to Texas-red X (PCNA) or Alexa 488 (p21). The slides were mounted with anti-fade gel-mount medium (Biomedia Corp., Foster City, CA). Images were taken with a Leica CRT 5000 fluorescence microscope (Exton, PA).

4.3.5 Endothelial Cell Detachment

Tissue culture 6-well plates were incubated overnight at 4°C with 3ml of 5 µg/ml human fibronectin (Sigma, St. Louis, MO) or 3 µg/ml vitronectin (Invitrogen). The plates were then blocked with 0.5% bovine serum albumin (BSA) in PBS. HUVECs were seeded at a density of 2 x 10^5 cells/well in complete medium and incubated overnight. Cells were starved 30 minutes in human endothelial basal medium containing 0.1% BSA. Different amounts of EMD478761 were added to the medium, as specified. After 12 hours treatment, cells were examined and stained with Alexa® Fluor 568-conjugated phalloidin (Invitrogen) to visualize the actin fibers. Phase contrast and fluorescence images were acquired.

4.3.6 Tube Formation

Tube-forming assays were performed as previously described with slight modifications (83). HUVECs were grown until sub-confluence and treated with 0-1 µM of EMD478761 for 1 hour in serum free medium. Cells were collected and plated onto 48-well dishes containing Matrigel (100 µl/well) at 24,000 cells/well in RPMI 1640 medium containing 10% of BCS. Tube assays were performed in the presence of 0-1 µM of EMD478761 as specified. Controls included cells incubated with medium only or with 100 µg/ml C16Y, a peptide known to block tube formation. After overnight incubation, cells were fixed and stained with Diff-Quick fixative (methanol) and solution II (6.25% (w/v) each of azure A and methylene blue; Dade AG, Dudingen, Switzerland), and the

tubes were examined and photographed. EMD478761 was tested in triplicate, and the assay was repeated three times.

4.3.7 In vitro Detection of Endothelial Cell Apoptosis

The ability of EMD478761 to induce endothelial cell apoptosis was examined in vitro by using different substrates. HUVECs cultured on vitronectin- or fibronectin-coated 6-well plates to 80% of confluence were incubated with different concentrations of EMD48761 as specified, for 12 hours or 24 hours.

4.3.7.1 Quantification of apoptosis by flow cytometry

After treatment, both floating and attached HUVECs were collected and washed with PBS. The pellets were subjected to Annexin V/propidium iodide (PI) staining using an ApopNexin™ Annexin V FITC apoptosis kit according to the manufacture's instructions (Chemicon, Temecula, CA). The resulting fluorescence was measured by flow cytometry (FACSCalibur, Becton Dickinson), and the percentage of apoptotic cells was calculated with Cell Quest software (version 3.1f, Becton Dickinson). Cell staining with a combination of Annexin V and PI reveals either non-apoptotic cells (Annexin V-/PI-), early apoptotic cells (Annexin V+/PI-), late stage apoptotic cells (Annexin V+/PI+), or necrotic cells (Annexin V-/PI+).

4.3.7.2 Identification of apoptosis by Western blotting

Subconfluent HUVECs grown on vitronectin-or fibronectin-coated 6-well plates, were treated with EMD478761 for 12 hours or 24 hours as indicated. Both floating and

attached cells were collected and lysed in RIPA buffer (Pierce, Rockford, IL) containing complete protease inhibitors (Roche). Protein concentrations were determined using the BCA assay kit (Pierce). Equal amounts of total protein were separated under reducing conditions by 4-12% sodium dodecyl sulfate-polyacrylamide gel electrophoresis (SDS-PAGE). Separated proteins were then transferred onto nitrocellulose membranes (Invitrogen). Membranes were blotted with 5% non-fat milk in TBST buffer (Tris-buffered saline, 0.05% Tween-20, pH 7.3) before Western blotting with monoclonal anti-caspase 3, 8, 9 or anti- glyceraldehyde-3-phosphate dehydrogenase (GAPDH) antibodies (Cell Signaling Technology). Membranes were washed three times 5 min each with TBST and then incubated with anti-mouse or anti-rabbit peroxidase secondary antibodies for 1 hour. Immune complex on nitrocellulose membranes were detected by enhanced chemiluminescence (Pierce). GAPDH served as loading control.

4.3.8 Identification of Apoptotic Cells in vivo by TUNEL Staining

In vivo apoptosis study was performed on experimental laser-induced CNV in Norway-Brown rats. CNV induction was performed as described in Chapter 3. 2 weeks after CNV induction, 10 µl of 0.5 mg/ml EMD478761 solution was intravitreally injected to both eyes of the animal. Control animals received 10 µl of PBS. Treated eyes were enucleated 6, 12, 24 and 48 hours after the injections were performed. At each time point, 5 eyes were used to make the choroidal flatmounts and 5 eyes were embedded in agarose gel after removing their anterior segments. The posterior segments of the eyes were sectioned transversely with a vibrotome at 100 µm thickness for TUNEL staining.

Apoptosis was detected from choroidal-RPE flatmounts and vibrotome sections using an ApopTag® in situ apoptosis detection kit, a TUNEL based DNA fragmentation assay, according to the manufacture's instructions with slight modification (Chemicon). In brief, the flatmounts and vibrotome sections were post-fixed with a solution of ethanol: acetic acid (2:1) for 5 min at -20°C. Samples were washed twice with PBS. 20 µl freshly prepared TdT enzyme was applied to each sample and incubated for 3 hours at 37°C in a humidified chamber. The enzymatic labeling was stopped by a stop/wash buffer and samples were counterstained with rhodamine–conjugated anti-digoxigenin. To localize apoptotic cells within the lesions, samples were also immunohistochemically stained with Alexa® Fluor 488-isolectin IB4 (20 µg/ml, from *Griffonia simplicifolia*) and DAPI (1:1000, 5 µg/ml) overnight at 4°C. Then samples were mounted in aqueous mounting medium and images were taken with a confocal microscope (SP2, Leica, Exton, PA) equipped with a 40X (1.25 n.a.) oil immersion objective lens. The resolution of the images collected was 1024 x 1024 pixels.

4.4 Results

4.4.1 Effect of EMD478761 on Endothelial Cell Adhesion

The functional role of EMD478761 on endothelial cells was first investigated using a cell adhesion assay. ECM proteins, fibronectin and vitronectin, were used to quantify the effect of EMD478761 on HUVEC adhesion 1 hour after plating. As shown in Figure 4-2, cell adhesion on fibronectin-coated surfaces was significantly elevated in the presence of

EMD478761 at all concentrations tested as compared to those on control and vitronectin surfaces. However, HUVEC adhesion to fibronectin-coated surfaces was not significantly affected by the presence of EMD478761 (Fig 4-2). Cell adhesion to control and vitronectin surfaces was slightly decreased. Significant difference was observed for cell adhesion to vitronectin with EMD478761 at a concentration higher than 0.2 μM.

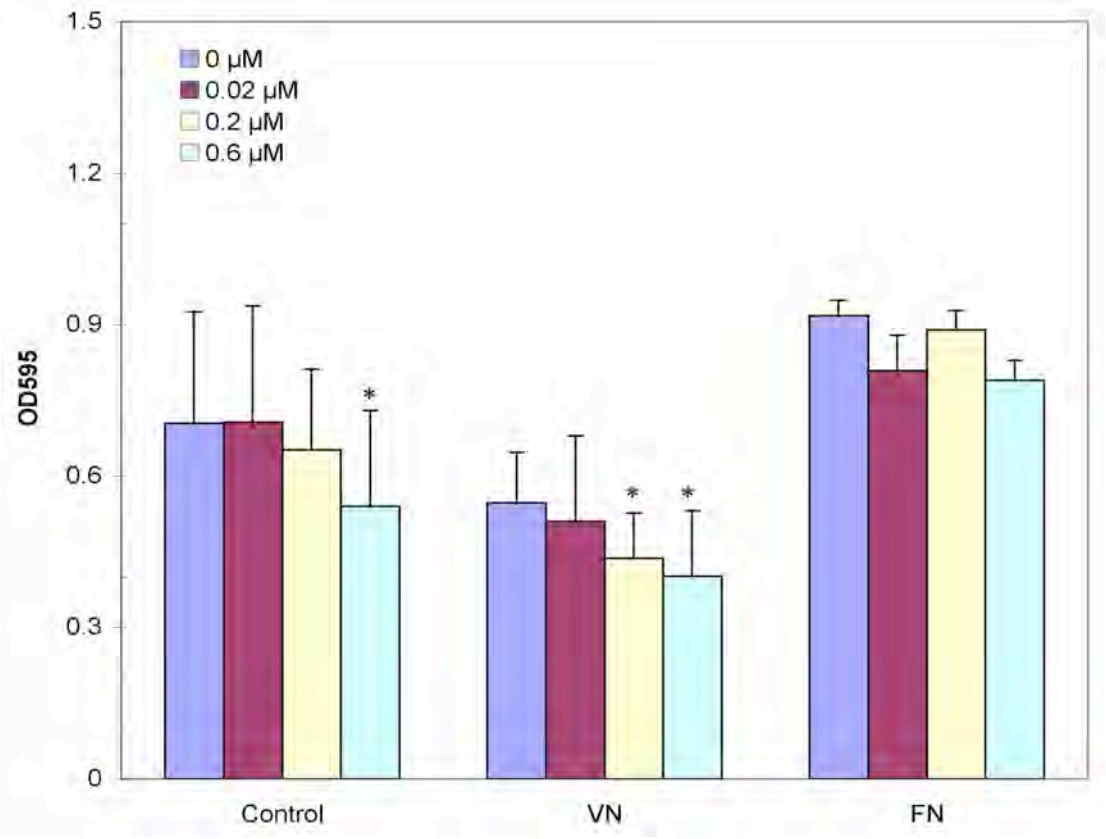

Figure 4-2. Effect of EMD478761 on HUVEC adhesion to fibronectin (FN) - and vitronectin (VN)-coated surfaces. HUVECs were plated onto ECM protein coated 96-well plates in the presence of different concentrations of EMD478761 for 1 hour. Results are mean ± SD of quadruplicates of 1 representative experiment (* $P < 0.05$ compared to control). The experiment was repeated three times.

4.4.2 Effect of EMD478761 on Endothelial Cells Proliferation

EMD478761 inhibited and reversed angiogenesis *in vivo* as demonstrated in Chapter 2 and 3, and it affected endothelial cell adhesion to vitronectin. Since endothelial cell proliferation is necessary for the formation of new vessels, we decided to examine the role of EMD478761 on endothelial cell proliferation. To this end, we performed a series of proliferation assays on cultured HUVECs using different concentrations of EMD478761. We observed that HUVEC proliferation was inhibited by the presence of EMD478761 in a dose-dependent manner as demonstrated by the XTT assay (Fig. 4-3). Inhibition followed an exponential response. Proliferation was completely inhibited at 500 ng/ml. Control C16Y anti-angiogenic peptide inhibited by 73.3% at 2000 ng/ml.

The effect of EMD478761 on endothelial cell proliferation was further investigated with immunohistochemistry studies of DNA synthesis and the expression of cell cycle regulatory proteins, PCNA and p21. Results showed that treatment of HUVECs with EMD478761 revealed a dose-dependent inhibition of BrdU incorporation, as compared to control (Fig. 4-4). These results demonstrated that EMD478761 inhibited DNA synthesis in cultured endothelial cells since the majority of cells treated with EMD478761 between 0.2 μM and 0.6 μM did not incorporate BrdU (red nuclei). In parallel, the effect of EMD478761 on PCNA, a protein that is actively expressed during the cell cycle, was also examined. The presence of EMD478761 was observed to decrease the expression of PCNA as the dose of the drug increased and its expression was not detected at concentrations higher than 0.2 μM (Fig. 4-5). These results suggest that EMD478761 inhibits the cell cycle by a mechanism that suppresses the expression of PCNA. In addition, we investigated the effect of EMD478761 on p21, a cyclin protein

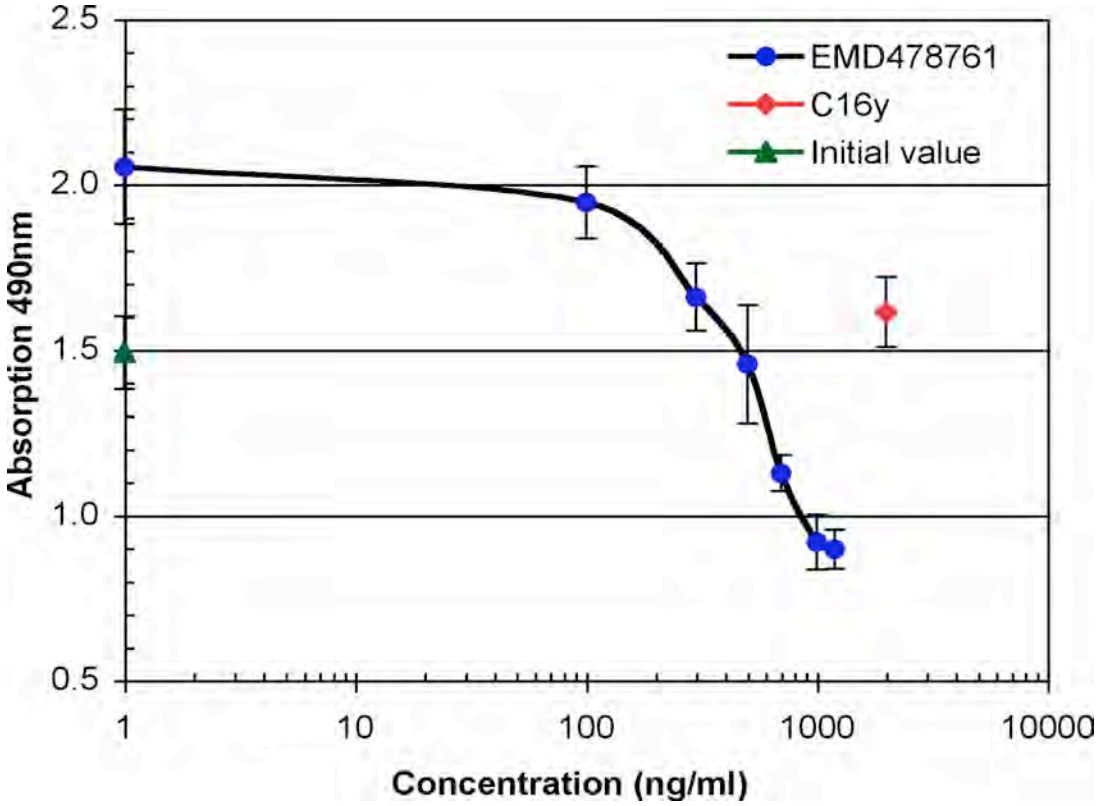

Figure 4-3. Effect of EMD478761 on endothelia cell proliferation by XTT assay. HUVEC proliferation was tested by XTT assay in 96-well plate. C16Y, a known anti-angiogenesis peptide was used as positive control at a concentration of 2 µg/ml. Solid triangle (▲) indicates the absorption value with initial number of cells. The experiment was repeated three times. Results are mean ± SD 1 representative experiment.

that regulates the cell cycle at the G1 phase and is not expressed during cell proliferation. Our results showed that p21 was not expressed in untreated proliferating cells (Fig.4-6 top middle panel). However, treatment with EMD478761 induced the expression and nuclear localization of p21 in a dose-dependent manner (Fig. 4-6 lower middle and right

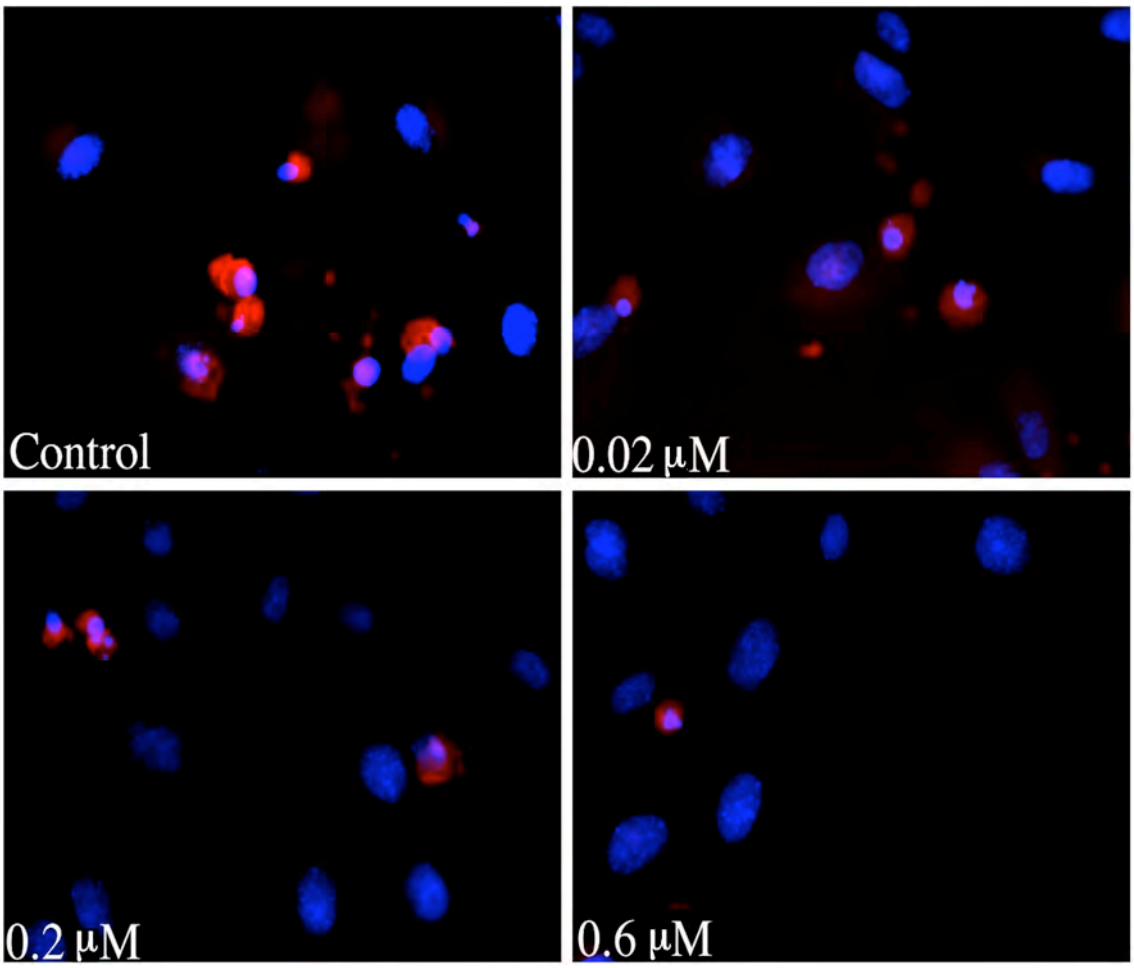

Figure 4-4. Effect of EMD478761 on endothelial cell proliferation by BrdU incorporation. HUVECs were grown in the presence of EMD478761 and BrdU. Cells were then immunostained with anti-BrdU antibody. Red: Alexa 660-stained BrdU incorporation; blue: DAPI stained nuclei.

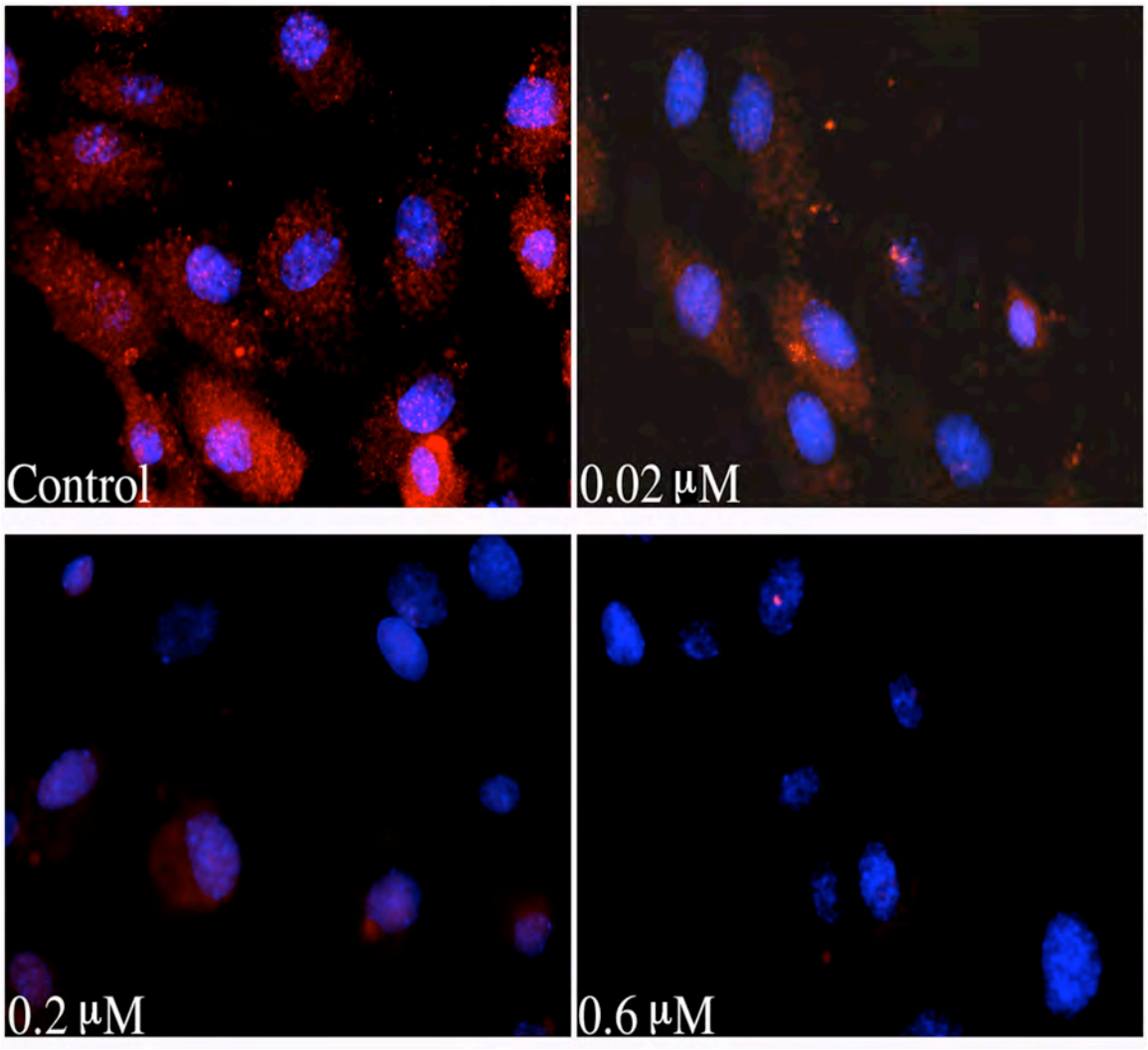

Figure 4-5. Effect of EMD478761 on PCNA expression in HUVECs. Cells were immunostained with anti-PCNA antibody and counterstained with Texas-red X-conjugated secondary antibody and DAPI. Red: Texas-red X stained PCNA; Blue: DAPI stained nuclei

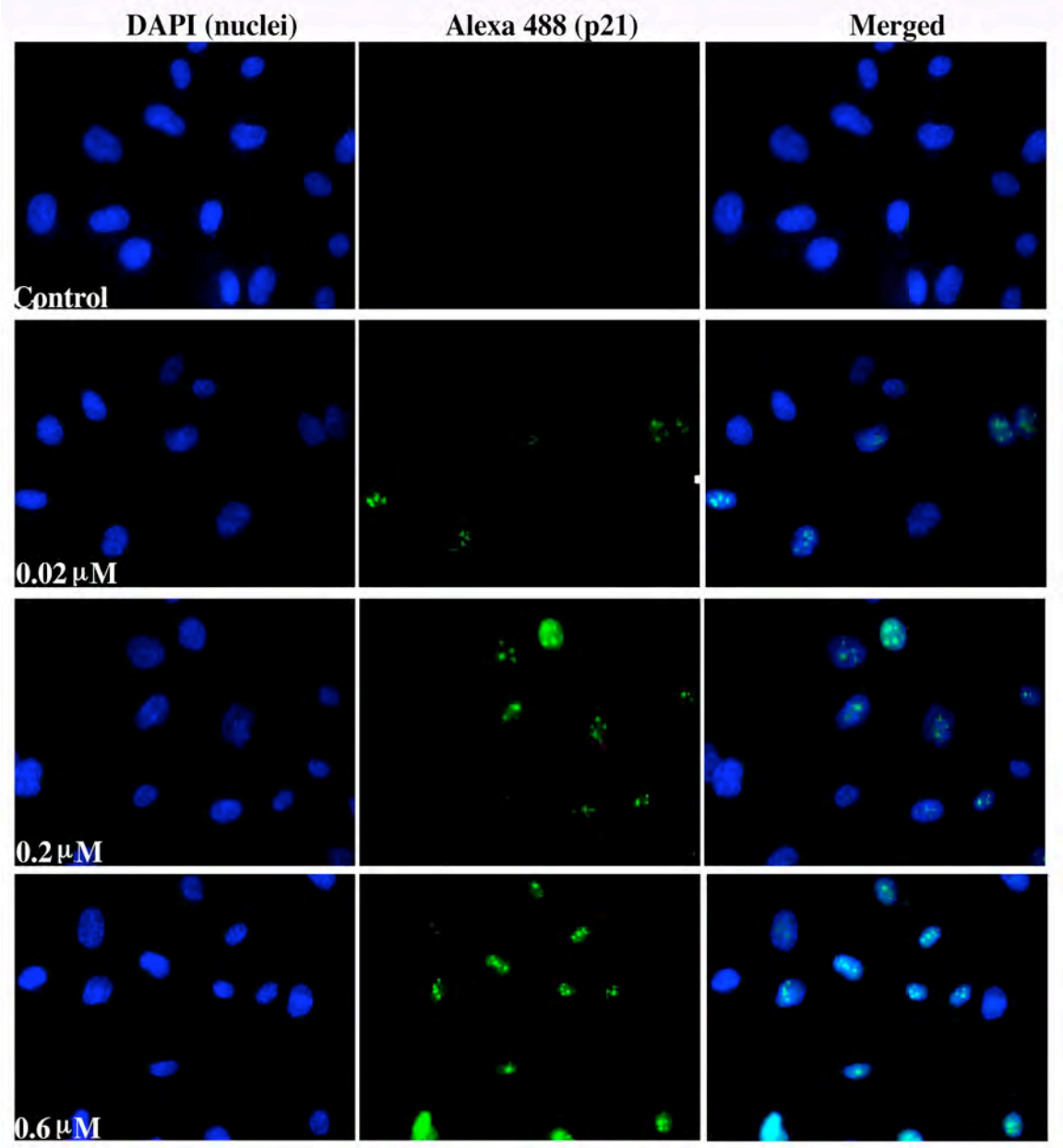

Figure 4-6. Effect of EMD478761 on regulatory cell cycle protein p21 expression in HUVECs. HUVECs were grown in serum free medium after they reached subconfluence and treated with different concentrations of EMD478761, as specified, for 24 hours. Cells were stained with primary p21 antibody at 1:100 dilution and counterstained with Alexa® Fluro 488-conjugated secondary antibody.

panel). All of these findings indicate that EMD478761 inhibits endothelial cell proliferation in a dose-dependent fashion by inducing p21 expression. The results of endothelial cell proliferation from immunohistochemistry studies were summarized in table 1.

Table 1. BrdU incorporation, PCNA and p21 expression in endothelial cells in the presence of EMD478761.

	Control	*0.02 μM*	*0.2 μM*	*0.6 μM*
BrdU incorporation	65.2 ± 2.2%	36.4 ± 13.9%	17.5 ± 5.6%	18.5 ± 12%
P value		0.089	0.0078	0.032
PCNA expression	100%	75.8 ± 1.1%	36.8 ± 13.4%	10.9 ± 0.3%
P value		0.00096	0.022	0.000005
p21 expression	0%	17.0 ± 3.2%	31.1 ± 11.6%	26.3 ± 0.1%
P value		0.0018	0.013	0.000002

Note: Data were shown in percentages of positive stained endothelial cells ± SD for 3 independent experiments. P values were calculated using Student's t test as compared to controls.

4.4.3 Effect of EMD478761 on Endothelial Cell Detachment on Vitronectin

We examined the ability of EMD478761 to detach adherent cells from their substrates. Endothelial cell adhesion to ECM protein is integrin dependent. The attachment of endothelial cells to vitronectin is dependent on the engagement of $\alpha_v\beta_3$ and $\alpha_v\beta_5$ integrins and on their localization in functional cell-matrix adhesions (113). For these experiments, HUVECs were allowed to grow to confluence on vitronectin coated 6-well plates or on 8-well chamber slides. Cells were then treated with different concentrations of EMD478761 for 24 hours. Cell morphology was monitored by phase contrast microscopy. Our results showed that EMD478761 induced morphological changes followed by the detachment of HUVECs from their substrate in a dose-dependent manner (Figure 4-7). Cells treated with 0.6 μM of EMD478761 led to the detachment of all endothelial cells, while control cells remained well spread. Since cell adhesion on ECM affects cytoskeletal dynamics (114), we examined the organization of the actin cytoskeleton of endothelial cells during the detachment process in the presence or absence of EMD478761. Immunostaining of HUVECs plated on vitronectin with Alexa® Fluro 568-conjugated phalloidin showed that EMD478761 induced rapid disruption of actin microfilaments in HUVECs followed by cell detachment from vitronectin-coated surfaces (Fig. 4-8 left panel). Control cells displayed a well ordered array of transversal actin stress fibers. In contrast, cells treated with EMD478761 were almost devoid of actin fibers.

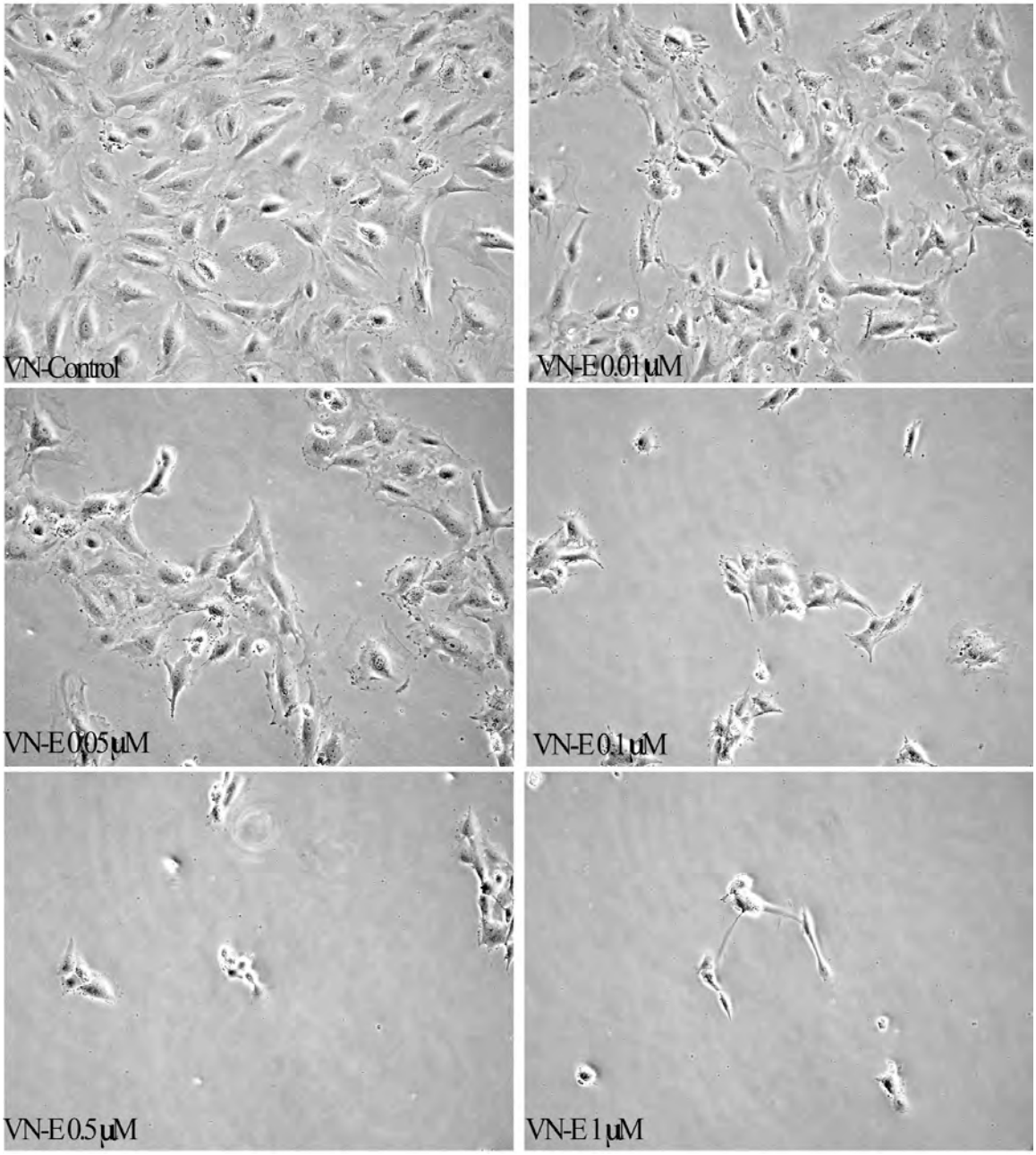

Figure 4-7. Effect of EMD478761 on HUVECs spread on vitronectin (VN)-coated surfaces. HUVECs were plated on vitronectin-coated 6-well plate. Cells were grown until confluent before EMD478761 was added. After 24 hours treatment, cells were examined with a phase contrast microscope and images or cells were taken.

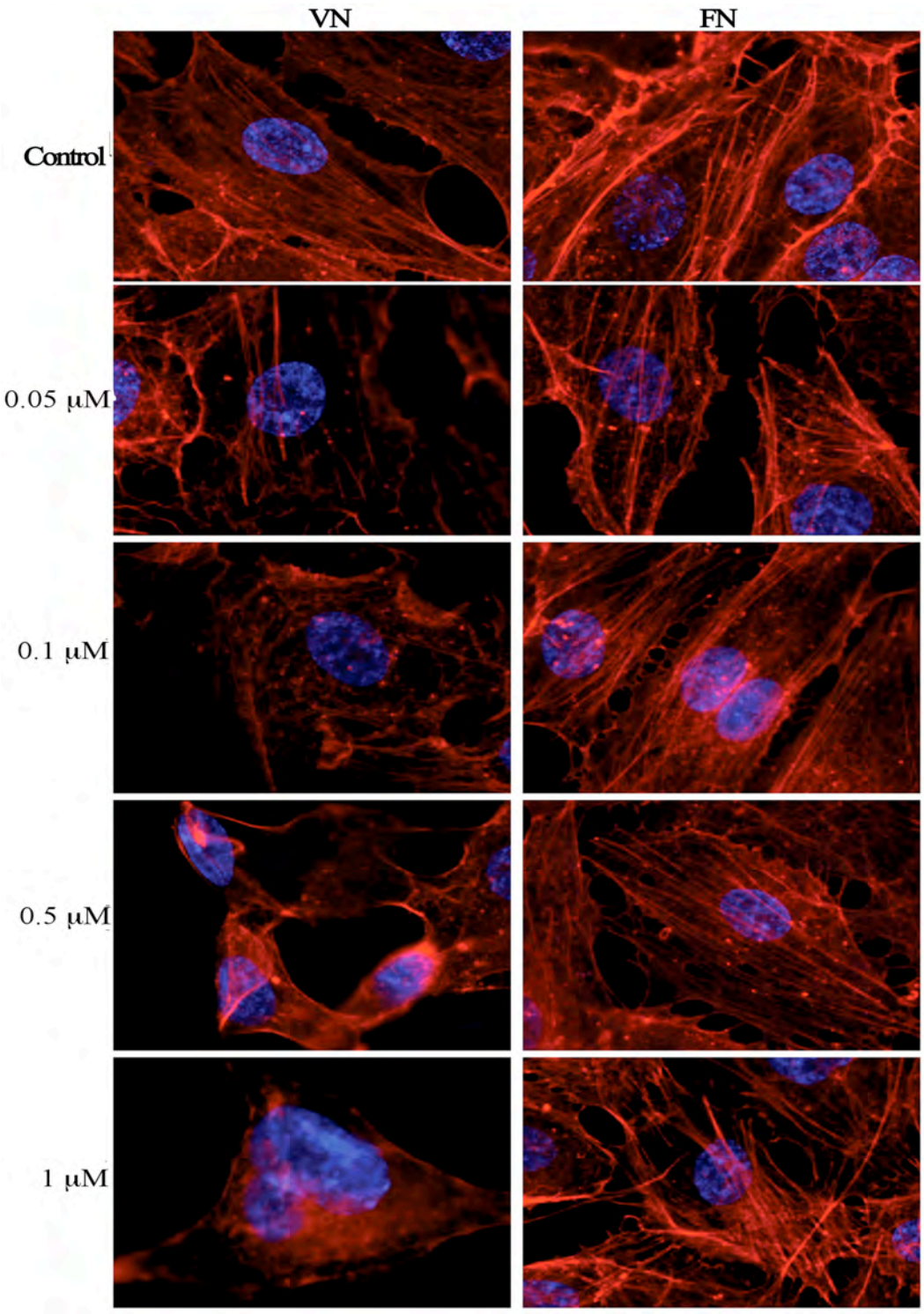

Figure 4-8. Effect of EMD478761 on actin filaments of HUVECs. Red: phalloidin stained actin filaments; Blue: DAPI stained cell nuclei. Results from one out of six independent experiments were shown.

4.4.4 Effect of EMD478761 on Endothelial Cell Detachment on Fibronectin

We tested the effect of EMD478761 on endothelial cells detachment on fibronectin, for which cell adhesion is largely mediated by $\alpha_5\beta_1$ integrin (113). HUVECs were plated on fibronectin-coated 6-well plates and 8-well chambers. In contrast to the results obtained from cells attached to vitronectin surfaces, morphologic analyses showed that EMD478761 had no significant effect on HUVECs seeded on fibronectin (Fig. 4-9). Furthermore, no apparent actin filament changes were observed (Fig 4-8, right panel). HUVECs displayed a similar organized cytoskeleton on fibronectin with EMD478761 treatment compared with control. These results suggest that the action of EMD478761 is substrate specific and may relate to endothelial cell detachment.

4.4.5 Effect of EMD478761 on Endothelial Cell Tube Formation

The ability of HUVECs to form tubes was assessed on growth factor-reduced Matrigel containing increasing concentrations of EMD478761. For this experiment, HUVECs were pre-incubated with different concentrations of EMD478761, as specified, for 30 min at 4 °C before being plated onto Matrigel overnight with EMD478761. As shown in Figure 4-10, control cells formed an organized network of endothelial tubes. In contrast, tube formation was reduced on Matrigel in the presence of 0.1 μM or higher EMD478761. The inhibitory effect of EMD478761 at 1 μM was comparable to that exerted by C16Y, a known anti-angiogenic peptide that disrupted endothelial cell tube formation, at 100 μg/ml (115).

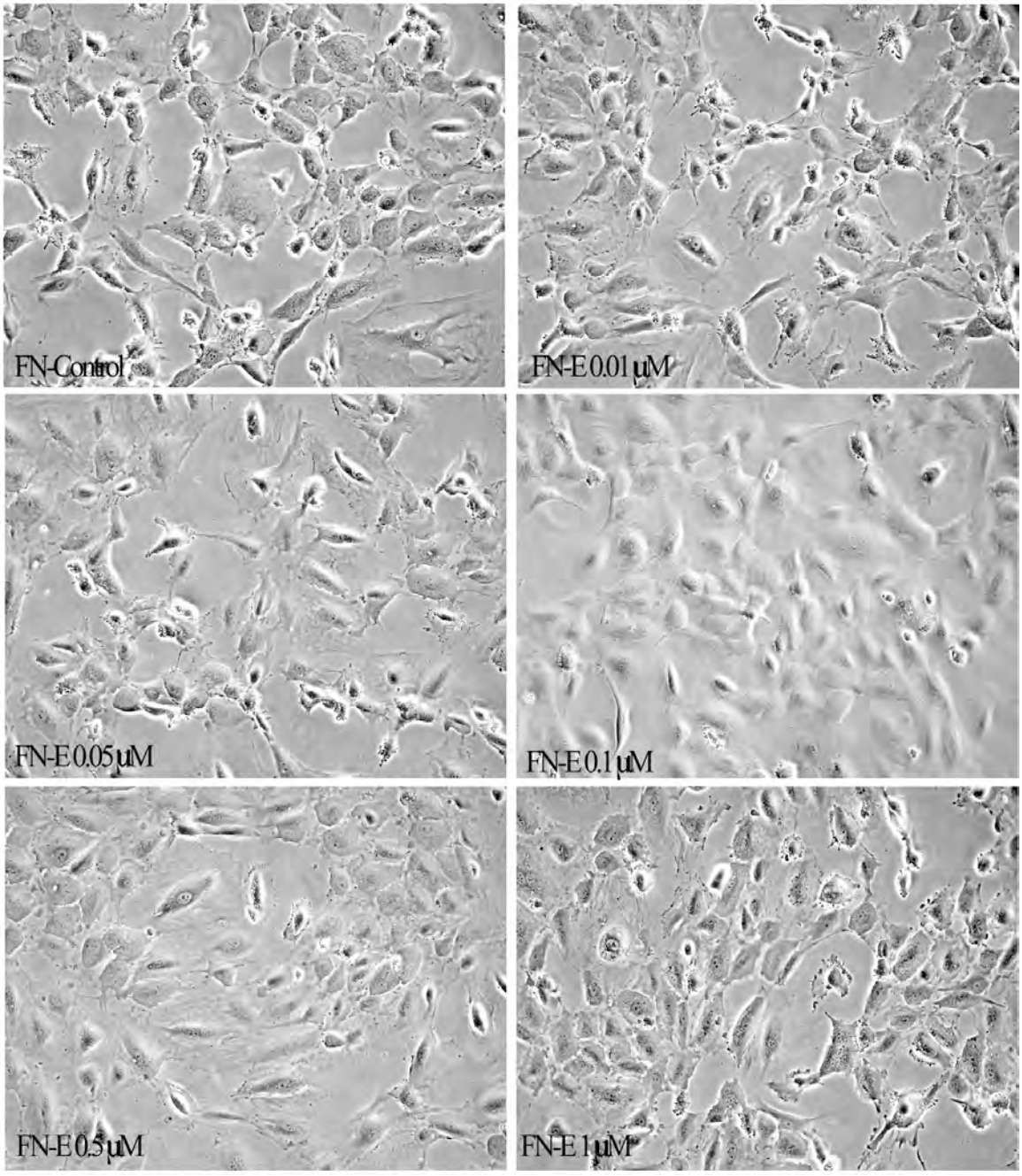

Figure 4-9. Effect of EMD478761 on HUVECs spread on fibronectin (FN)-coated surfaces. Phase contrast images were taken 48 hours after treatment. Original magnification: 20x

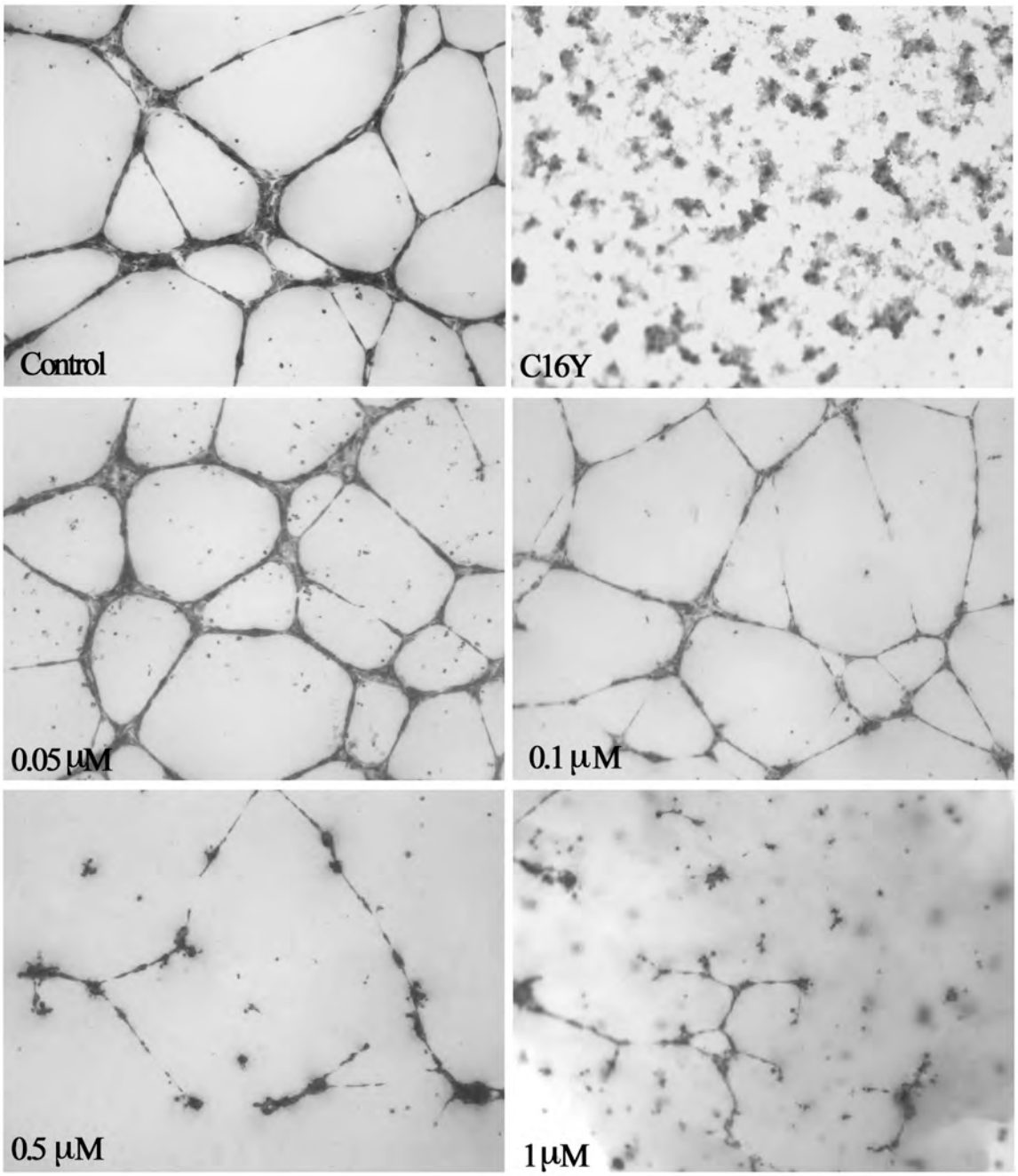

Figure 4-10. Effect of EMD478761 on HUVEC tube formation. HUVECs were pre-incubated with 0-1 µM EMD478761, as specified, for 30 min and plated onto Matrigel in the presence of different concentrations of EMD478761. HUVECs were also treated with 100 µg/ml C16Y as positive control.

4.4.6 Effect of EMD478761 on Apoptosis of Endothelial Cells in Vitro

Activation of integrins $\alpha_v\beta_3$ and $\alpha_v\beta_5$ has been shown to enhance endothelial cell survival, and lack of substrate attachment has been shown to promote anoikis (a Greek word meaning "homelessness") in endothelial cells (53, 116). Therefore, we hypothesize that antagonists to integrins $\alpha_v\beta_3$ and $\alpha_v\beta_5$ will result in endothelia cell apoptosis. To address the effect of EMD478761 treatment on HUVEC apoptosis, we first applied flow cytometry (FACS) analysis of Annexin V stained HUVECs in the presence of EMD478761 on different substrates. As shown in Figure 4-11, EMD478761 promoted a dose-dependent induction of apoptosis in vitronectin-coated surfaces, as determined by Annexin V/ propidium iodide (PI) staining 24 hours after treatment. The presence of early and late apoptotic cells in control conditions were around 21% and up to 51.4% of cells treated with a dose of 1 μM EMD478761 underwent apoptosis. In contrast, FACS analysis revealed that EMD478761 did not facilitate HUVEC apoptosis on fibronectin surfaces (Fig. 4-12). These results are consistent with those from cell detachment.

We further investigated the mechanisms by which EMD478761-induced apoptosis proceeded by examining the activation of caspases from HUVEC cell lysates prepared 12 to 24 hours after treatment by using Western blotting analysis. As shown is Figure 4-13, treatment of cells with EMD478761 on vitronectin led to a time- and dose-dependent activation of caspase-3, one of the key effector caspases, as determined by the appearance of the cleaved/active form of the enzyme and the decreased levels of the pro-caspase 3. Whereas, Western blotting revealed no evidence of caspase-3 activation for cells plated on fibronectin treated with EMD478761 in the same manner. As caspase-3 is

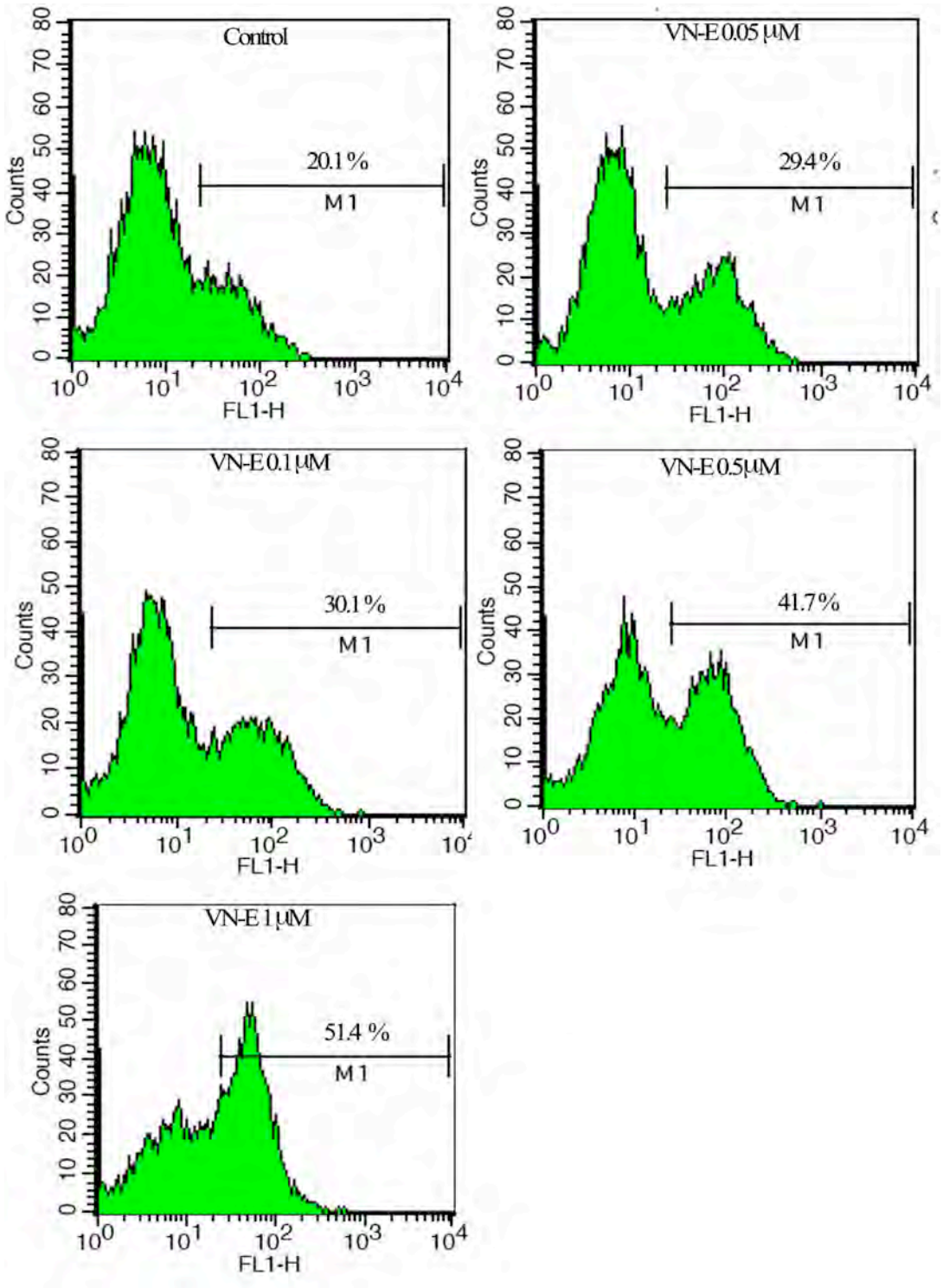

Figure 4-11. FACS analysis of HUVEC apoptosis on vitronectin surfaces. HUVECs were treated with 0-1 µM EMD478761 for 41 hours and stained with Annexin V/PI. The data are representative of three independent experiments.

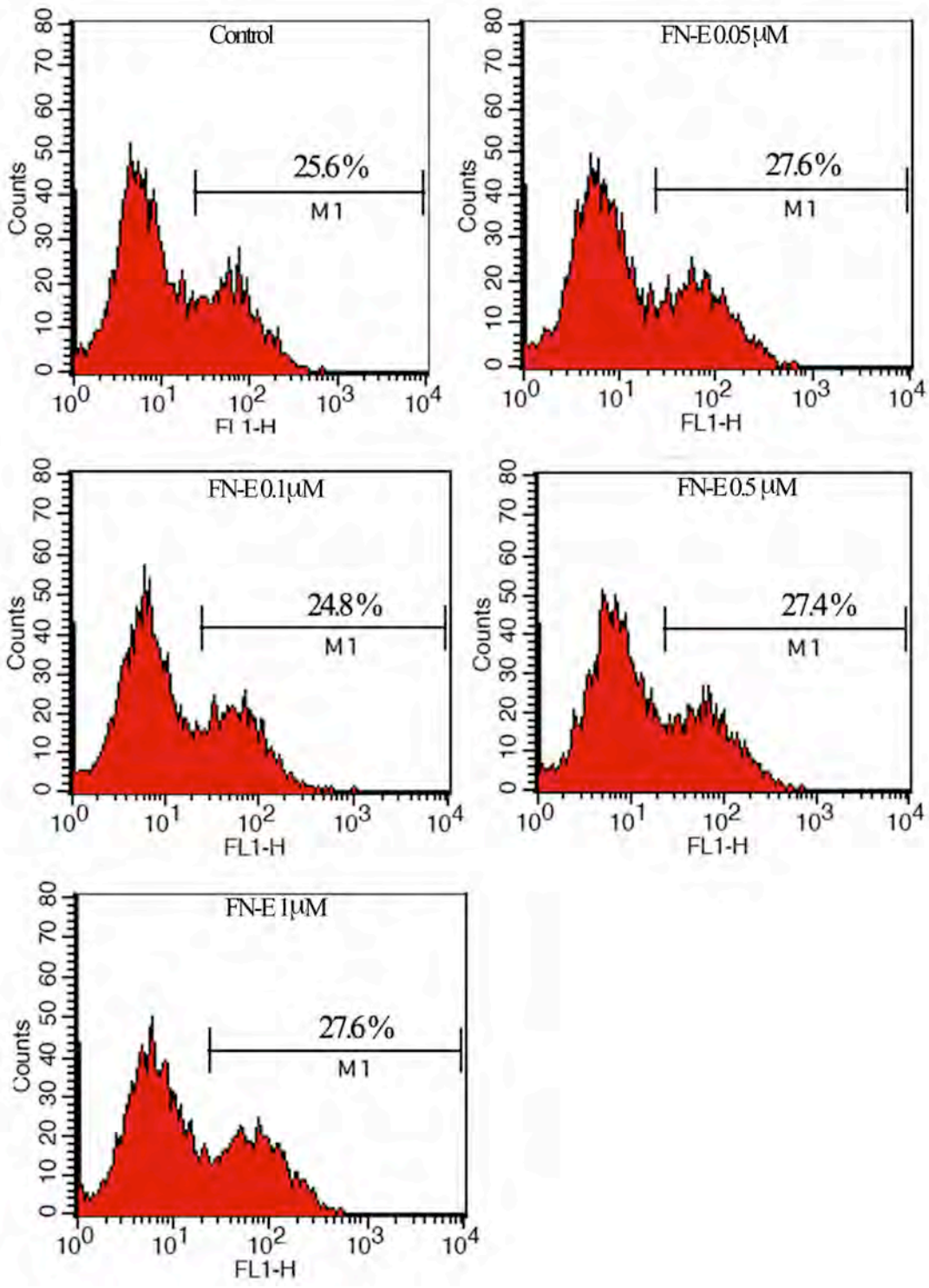

Figure 4-12. FACS analysis of HUVEC apoptosis on fibronectin surfaces. HUVECs were treated with 0-1 µM EMD478761 for 41 hours and stained with Annexin V/PI. The data are representative of three independent experiments.

a downstream apoptotic enzyme, we then examined the upstream activations of caspases, in particular caspase-8 and caspase-9. Interestingly, in our study, no caspase-8 activation was observed on cells plated on vitronectin- or fibronectin-coated surfaces, indicating that cell death did not occur by the activation of an extrinsic pathway. Treatment of cells with EMD478761on vitronectin surfaces induced an increase in the cleaved form of caspase-9 (Fig. 4-14), suggesting that cell apoptosis involved caspase-9 activation. Again, no significant effect of EMD478761 on HUVECs plated on fibronectin was found.

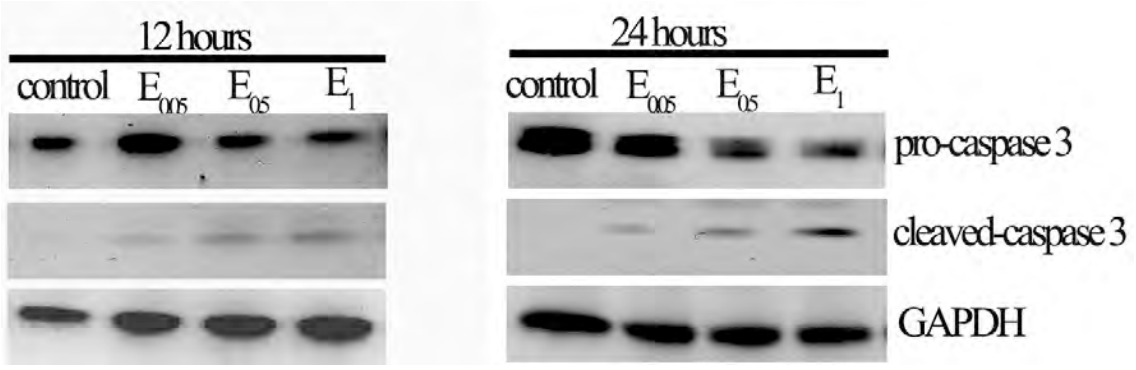

Figure 4-13. Effect of EMD478761 on the activation of caspase-3 on vitronectin surfaces. EMD478761 was added into the medium of endothelial cells plated on vitronectin after deprival of serum. After 12 or 24 hours treatment, cells were lysed in RIPA buffer containing 1x complete proteinase inhibitors. Equal amount of total proteins were separated on 4-12% SDS-PAGE and detected with anti-caspase 3 antibody. GAPDH served as loading control. The data are representative of three independent experiments.

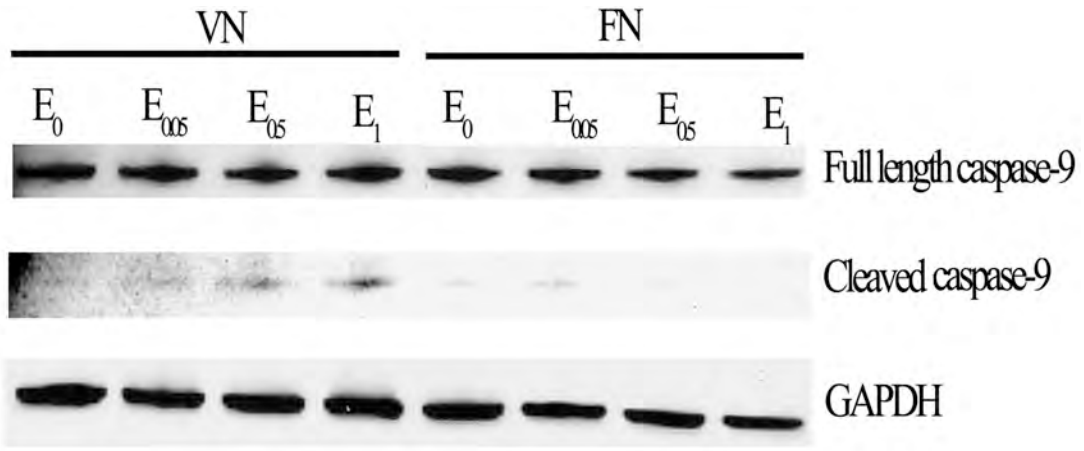

Figure 4-14. Effect of EMD478761 on endothelial cell activation of caspase-9. Endothelial cells plated on vitronectin or fibronectin were treated for 24 hours with EMD478761 at 0-1 μM, as specified. Cells lysates were fractioned and blotted with anti-caspase 9 antibody. GAPDH served as loading control. The data are representative of three independent experiments.

4.4.7 Effect of EMD478761 on Apoptosis of Vascular Endothelial Cells in Vivo

In light of the induction of endothelial cells apoptosis *in vitro*, we next examined whether EMD478761 triggers vascular endothelial cell apoptosis *in vivo* using a laser-induced CNV rat model. For these experiments, EMD478761 was given intravitreally 2 weeks after laser injury. Treated eyes were collected 0, 5, 12 and 24 hours after injection. Flatmounts were generated and stained with isolectin IB4. As shown in Figure 4-15, CNV areas with the treatment of EMD478761 appeared to be smaller than that of control by 13% to 32%, and TUNEL staining revealed that as early as 5 hours post injection,

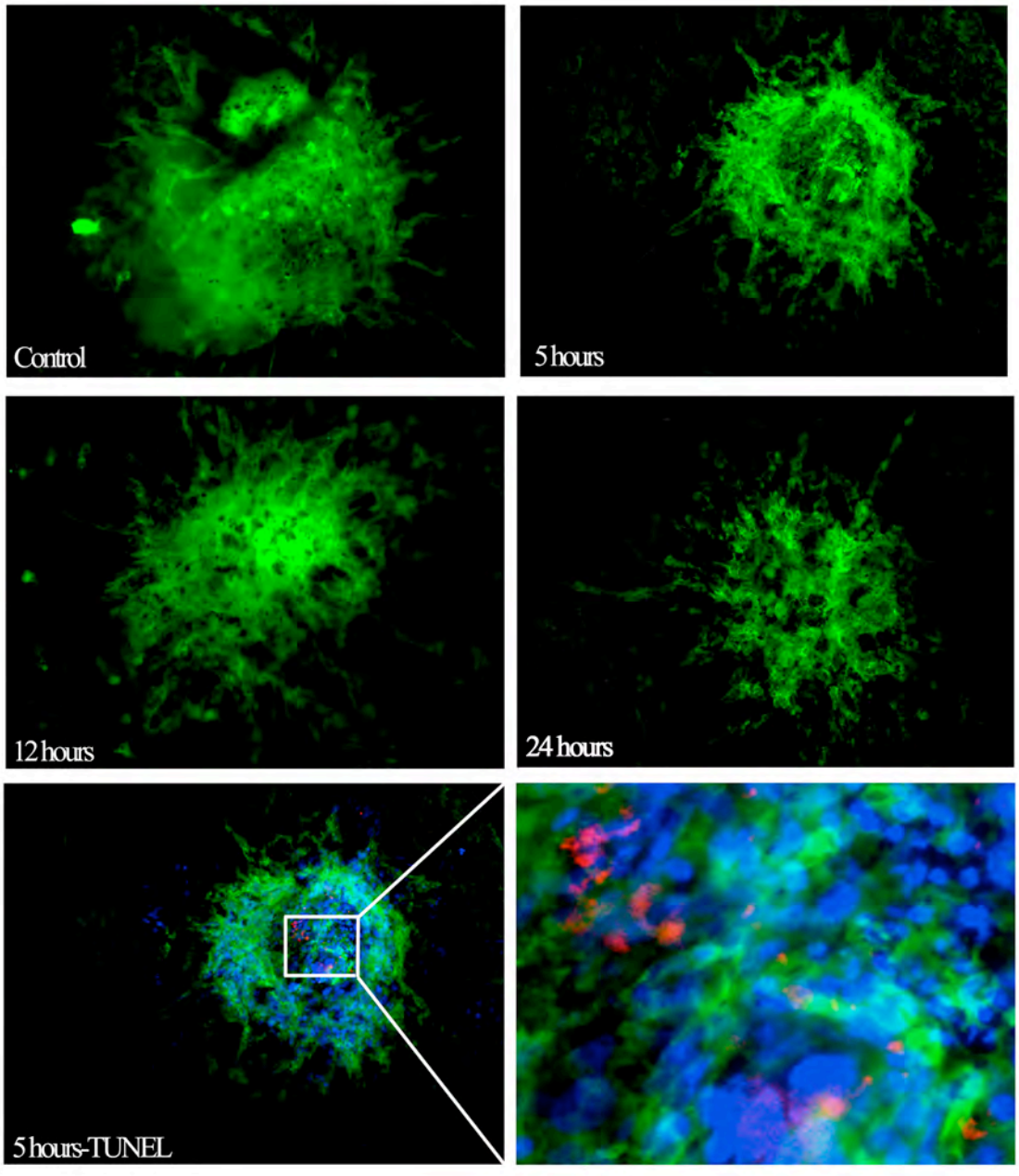

Figure 4-15. Effect of EMD478761 on laser-induced CNV regression in rats. 5 µg EMD478761 was delivered intravitreally to rat's eyes 2 weeks after laser injury. Flatmounts were generated 0, 5, 12 and 24 hours after injection and stained with isolectin IB4 (green), DAPI (blue) or TUNEL (red). The images are representative of more than 30 lesions from 2 independent experiments.

apoptosis occurred within CNV lesion. These results were further confirmed by TUNEL-stained retinal sections in which EMD478761 induced vascular endothelia cell apoptosis in the retina and within CNV (Fig. 4-16). Twenty-four hours after treatment, TUNEL labeling showed that many apoptotic cells were observed within choroidal vascular beds, suggesting that EMD478761 regressed CNV by inducing endothelial cell apoptosis. Untreated controls demonstrated highly vascularized CNV and showed minimum TUNEL labeling within the retina overlying CNV. The slightly positive TUNEL labeling of controls might be explained as a consequence of the laser photocoagulation or the presence of CNV that damaged the retina. Our results are consistent with those previously described for antagonist of $\alpha_5\beta_1$ integrin (26).

4.5 Discussion

Numerous studies have provided evidence that integrins $\alpha_v\beta_3$ and $\alpha_v\beta_5$ are highly expressed in angiogenic blood vessels in human granulation tissue, breast tumor vasculature as well as ocular neovascularization membrane(25, 58, 117). Integrin molecules $\alpha_v\beta_3$ and $\alpha_v\beta_5$ can bind to ECM proteins through an Arg-Gly-Asp (RGD)–binding site (113). Specific inhibitors, including blocking monoclonal antibodies, RGD peptide and RGD peptidomimetics have been developed and reported to inhibit tumor and ocular angiogenesis (57, 118, 119). Some of these angiogenesis inhibitors, including a humanized monoclonal anti-$\alpha_v\beta_3$ (Vitaxin; MedImmune, Gaithersburg, MD) and an $\alpha_v\beta_3$/ $\alpha_v\beta_5$–selective RGD-based cyclic peptide (cilengitide), have entered clinical trials (120, 121). Our previous studies demonstrated that EMD478761, a dual integrin

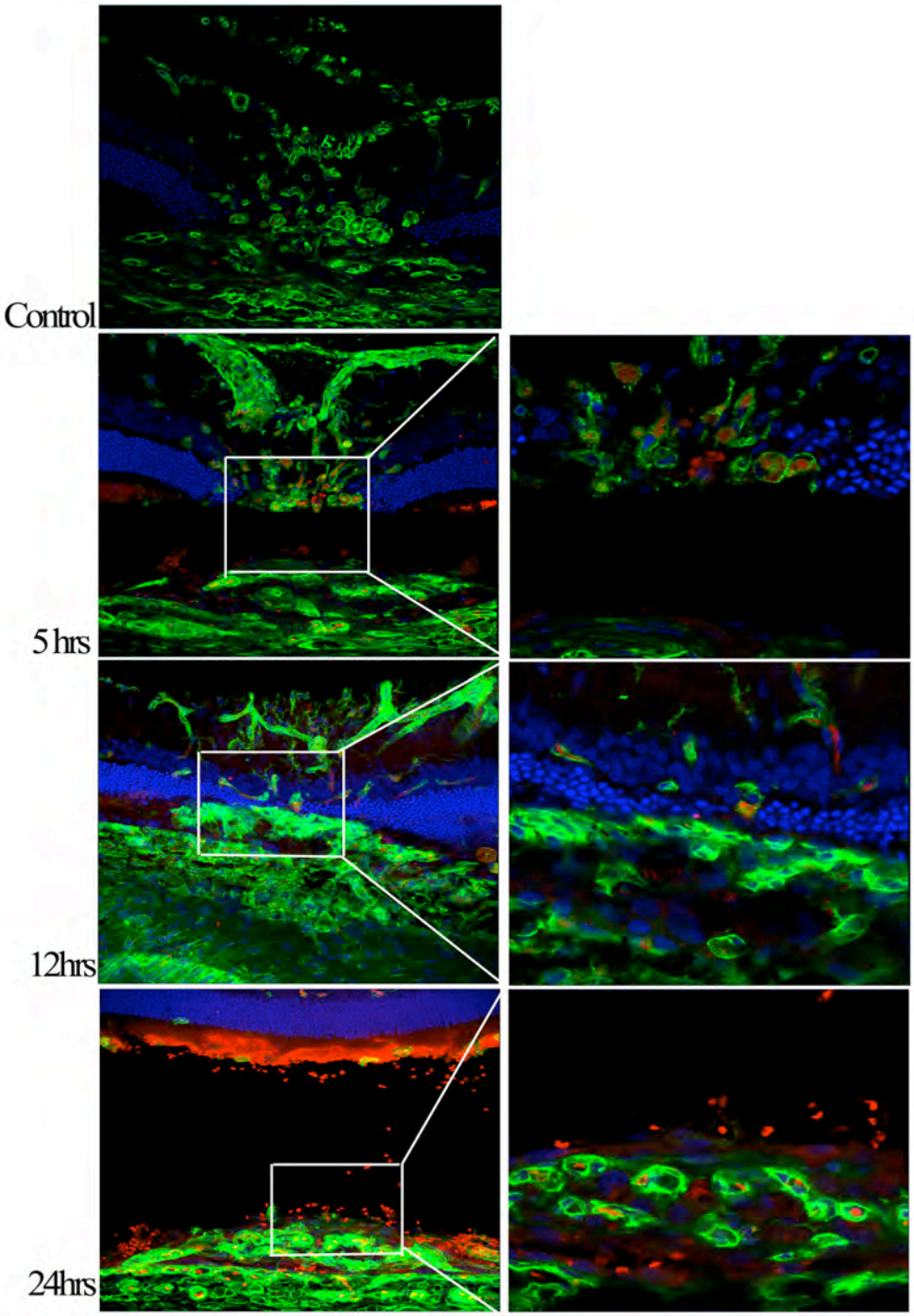

Figure 4-16. Effect of EMD478761 on vascular endothelial cell apoptosis by TUNEL assay. Red: apoptotic cells stained with TUNEL; green: vascular cells stained with isolectin IB4; blue: DAPI stained nuclei.

antagonist to $\alpha_v\beta_3$ and $\alpha_v\beta_5$, inhibits angiogenesis in response to bFGF in the CAM and prevents laser-induced choroidal neovascularization in rats. However, the drug's action mode is unknown. In this study, we have extended our previous work and investigated the antiangiogenic mechanisms of this compound. We demonstrated that EMD478761 inhibited HUVEC proliferation and tube formation, led to endothelial cell apoptosis both in vitro and in vivo. Furthermore, we found that induction of angiogenesis inhibition or regression by this compound appeared to be closely correlated with its anti-attachment effect and involved with caspase-3 dependent endothelial cell apoptosis. These results suggest a therapeutic role of EMD478761 in altering neovascularization in angiogenesis related disorders.

The mechanisms by which EMD478761 abrogates angiogenesis are complex. Previous studies have shown that bFGF-induced angiogenesis is integrin $\alpha_v\beta_3$ dependent (57), and a monoclonal antibody directed against the $\alpha_v\beta_3$ integrin diminishes angiogenesis by inducing the apoptosis of angiogenic blood vessels (24). Moreover, integrin $\alpha_v\beta_3$ provides a specific transmembrane signal that promotes angiogenic vascular cells survival *in vivo*, and antagonist to this integrin promotes the regression of human tumors (58). The $\alpha_v\beta_5$ integrin has also been shown to participate in angiogenesis, and cyclic RGDfV peptide blocks angiogenesis by inhibiting $\alpha_v\beta_5$ integrin ligation (122). We have shown in Chapter 2 that EMD478761 reverses angiogenesis by 80.6% in response to bFGF stimulation without affecting the normal CAM vasculature. A similar effect was observed in the choroidal neovascularization animal model where $\alpha_v\beta_3$ integrin is over expressed on endothelial cells of CNV membrane (25), and treatment with EMD478761, in turn, disrupted the integrity of the neovasculature and reduced the overall lesion size.

However, the extent of regression of CNV was much smaller than that of CAM. This probably reflects the inadequate dose injected or the fast clearance of this compound from the vitreous. Alternatively, the integrin $\alpha_v\beta_3$ turnover time is so short that the elapse of EMD478761 can provide the opportunity for integrin signaling. In addition, it is likely that the attenuation of the proliferative response of endothelial cells may be mediated by α_v-integrin since angiogenesis starts well before the treatment.

Previous studies indicates that cell adhesion to ECM regulates the life cycle of integrins and it is important for cellular signaling transduction (123). In our experiments, EMD478761 prevented endothelia cell adhesion to vitronectin within one hour treatment. Moreover, the induction of angiogenesis regression by EMD478761 was also found to closely correlate with its anti-proliferation and anti-tube formation effects and its ability to detach endothelial cells from specific substrates. The effects that EMD478761 showed on BrdU incorporation, PCNA and p21 expression indicated its strong anti-proliferative action on endothelial cells. Cell adhesion to vitronectin is mainly $\alpha v\beta 3$ and $\alpha_v\beta_5$ integrins mediated (113). As expected, EMD478761 led to significant endothelial cell detachment on this substrate. As a result, the actin filaments were also rapidly disrupted in a dose-dependent manner, which in turn may have led to the activation of endothelial cell apoptosis. In contrast, HUVECs attached to fibronectin-coated surfaces did not show any morphological changes or actin filament depolymerization. The disruption of endothelial cell tube formation on Matrigel by EMD478761 may be attributed partially to the alteration of an integrin signaling pathway, which could be related to cytoskeletal filaments, such as actin.

Cell detachment from ECM has been shown to promote cell death in different cell

types (93, 113). Apoptosis is controlled by multiple signaling and effector pathways that mediate active responses to external growth, survival or death factors. A hallmark of cell apoptosis is the activation of nucleases that degrade the higher order chromatin structure of the DNA into fragments of 50 to 300 kilobases and subsequently into smaller DNA pieces of about 200 base pairs in length (124, 125). These new DNA ends that are generated upon DNA fragmentation are typically localized in morphologically identifiable nuclei and apoptotic bodies and can be detected by enzymatically labeling the free 3'-OH termini with modified nucleotides. TUNEL labeling assay indicated that apoptosis occurred within CNV lesions as early as 5 hours after intravitreal injection of EMD478761.

The next possible mechanism that we investigated is that EMD478761 induced endothelial cell apoptosis through caspase-dependent pathways. Caspases, the principal biochemical effectors of apoptosis, are present in cells as inactive zymogens (pro-caspases). Once activated, upstream apoptotic signals convert these precursors into mature proteases that cleave their substrates after aspartate residues (113). Two principal caspase-dependent pathways that mediate apoptosis in endothelial cells are: the intrinsic apoptosis pathway triggered in response to mitochondrial changes, leading to caspase-9 activation, and the extrinsic pathway initiated by surface receptor mediated caspase-8 activation (126). Activation of caspase-8 and caspase-9 pathways have been described in different cell types after integrin antagonism or disruption of adhesion (127-129). Both pathways result in the down stream activation of executioner caspases, such as caspase-3. In this study, we found the activation of caspase-3 in response to EMD478761 treatment. Previous studies on a RGD mimetics, S 36578-2, showed that detachment-induced cell

death in HUVECs resulted from activation of the Fas and caspase-8 pathway (113, 127). Interestingly, in our experimental conditions, no caspase-8 activation was detected; while the cleavage of caspase-9 was observed. This suggests that the intrinsic pathway appears to dominate over the extrinsic pathway in endothelial cell apoptosis on a vitronectin surface. In contrast, EMD478761 did not exert any apoptotic effect on HUVECs plated on fibronectin surfaces as we did not observe any cleavage of caspases. Therefore, EMD478761 did not promote integrin-mediated cell death, a model where unligated or antagonized integrins directly recruit caspase-8 and trigger the apoptosis of adherent cells. Apparently, further investigations will warrant a better understanding of the antiangiogenic action mode of this compound, and guide the optimization of therapeutic interventions.

4.6 Conclusions

In summary, we provided several lines of evidence that EMD478761 might offer an effective treatment for angiogenesis associated diseases. We demonstrated that EMD478761 prevented human endothelial cell proliferation and tube formation, as well as induced endothelial cell detachment and triggers endothelial cell apoptosis on vitronectin. *In vitro*, EMD478761 induced cell cycle arrest as indicated by reduced BrdU incorporation, decreased proliferating nuclear antigen (PCNA) expression and an increased p21 protein levels in the nuclei. EMD478761 also prevented HUVEC adhesion, caused endothelial cell detachment from vitronectin, as well as activated the caspase-3 apoptotic pathway in a time- and dose-dependent manner. *In vivo*,

EMD478761 induce endothelial cell death in vascular cells within the neovascularization lesions in laser-induced CNV as determined by TUNEL staining. These results suggest that EMD478761 may have an important application to angiogenesis-related pathophysiological conditions.

Chapter 5: Integrin Regulation by EMD478761

5.1 Introduction

The interaction of cells with the extracellular matrix is mediated by integrins. Endothelial cells express many structurally distinct integrins including $\alpha_v\beta_3$, $\alpha_v\beta_5$ and $\alpha_5\beta_1$ (130). Each α β integrin combination has specific binding and signaling properties. In general, cell-substratum adhesion occurs at sites of the plasma membrane called focal contacts or adhesion plaques, where integrins and cytoskeletal proteins are concentrated (131). Adherent cells anchor via integrins to the matrix is essential to maintain the survival of the cells. Therefore, it has been suggested that cell attachment through various integrins, including $\alpha_v\beta_3$ and $\alpha_5\beta_1$, can prevent apoptosis of endothelial cells (132, 133). In addition to this structural role, integrin signaling is of vital importance to many physiological events, such as cell differentiation, migration and tube formation (134). Two types of integrin signaling exist: "outside-in" signals that originate from the matrix to the inside of the cell, promoting a variety of cellular responses, and "inside-out" signals that start at the cytoplasm and affect the adhesive properties of integrins to their matrix. It is clear that dysfunction in these processes can lead to diseases such as cancer (134). The cellular mechanisms regulating integrin function are currently the subject of considerable focus for cell biologists. One possible mechanism is integrin receptor endocytosis. The focus of this chapter is to study the effect of EMD478761 on integrin $\alpha_v\beta_3$ expression and endocytosis in human endothelial cells.

Integrin endocytosis has been shown to be connected to several phenomena, including cell migration, reorganization of extracellular matrix components and uptake of fibrinogen from plasma (135, 136). It is clear that certain integrin heterodimers are continually internalized from the plasma membrane into endosomal compartments and then recycled back to the cell surface, completing an endo-exocytic cycle (104). The integrin cycling time ranges from 10 min to 30 min depending on which of two loops the integrin recycling takes. The short loop refers to the route that integrin recycles from early endosomal compartment (EE) to the plasma membrane. The half-life of transport of $\alpha_v\beta_3$ via short-loop is approximately 3 to 5 min. However, the delivery of integrins $\alpha_v\beta_3$ and $\alpha_5\beta_1$ from the perinuclear recycling compartment (PNRC) to the plasma membrane, often refers as long-loop, has a t ½ of approximately 10 min (134). There is abundant evidence indicating that integrin traffic is Rab GTPase-and kinase-dependent (104, 137). A schematic summary of integrin turnover is shown in Figure 5-1.

Several studies have been performed to elucidate the process of integrin internalization and recycling. Among those, integrins $\alpha_v\beta_3$ and $\alpha_5\beta_1$ are mostly studied in fibroblast 3T3 cells (104), platelets (138), or calf lung endothelial cells (139). In order to track the internalized integrins and differentiate them from others, specific cell surface integrins are often labeled at 4°C with fluorescein-conjugated antibodies or tagged with membrane non-permeable biotin. At this temperature, membrane proteins can not be internalized. Labeled cells are then allowed to internalize by raising the temperature to 37°C. Surface remaining fluorescence, corresponding to non-internalized proteins, can be removed by acidic buffer wash (139) or blocked with anti-fluorescein antibodies (140). Internalized integrins are examined by fluorescence microscopy (138, 139) or

quantified by flow cytometry (139). Biotin tags are often quenched by 2-mercaptoethanesulfonate (MesNa) reduction (104). Internalized integrins are immunoprecipitated with specific anti-integrin antibodies and detected with streptavidin.

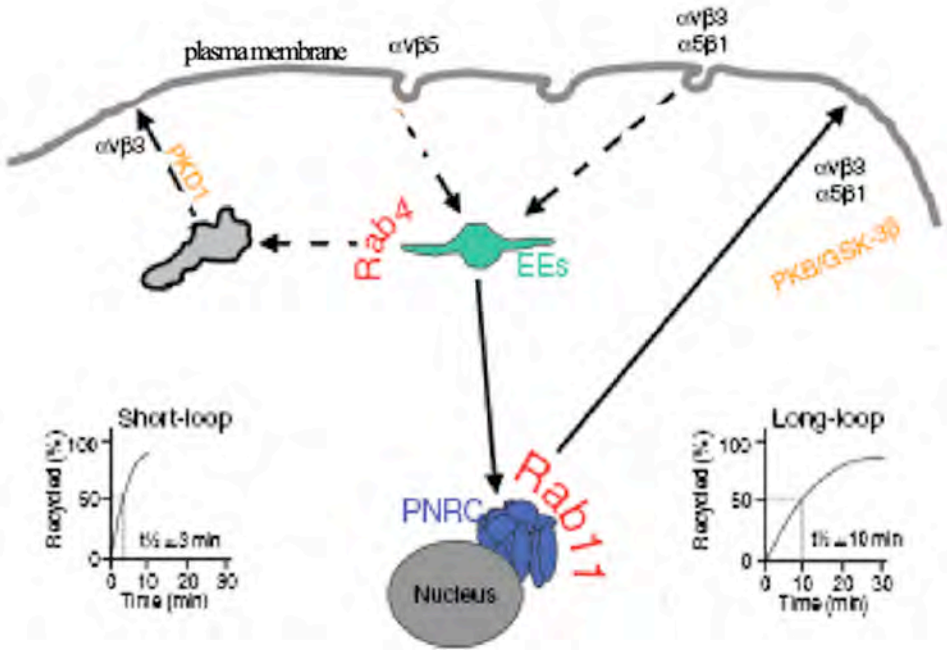

Figure 5-1. Schematic draw of integrin trafficking via short-loop (dash arrow) and long-loop (solid arrow) (Adapted from (134)). EE: early endosomal compartment; PNRC: perinuclear recycling compartment.

5.2 Materials and Methods

5.2.1 Compound and Endothelial Cell Culture

EMD 48761 was obtained from Merck KGaA (Darmstadt, Germany). It was solubilized to a concentration of 0.5 mg/ml in phosphate buffered saline (PBS). HUVECs were maintained in complete RPMI 1640 medium containing growth factors as described in Chapter 4.

5.2.2 Quantitation of Integrin Cell Surface Expression by Flow Cytometry

Cell surface $\alpha_v\beta_3$ integrins were measured by flow cytometry. For these experiments, sub-confluent HUVECs grown in 6-well plate were serum starved with human endothelial cell serum free medium (SFM) for 30 min and then cells were treated with EMD478761 at indicated concentrations (0-1μM) for 12 or 24 hours. After treatment, HUVECs were washed three times with PBS devoid of calcium and magnesium and detached from the culture dishes by incubating for 10 minute at 4°C in Versene (0.48 mM EDTA, Invitrogen). Cell surface integrins were labeled in suspension using Alexa Fluro 488-conjugated monoclonal antibodies to $\alpha_v\beta_3$ integrin (Chemicon) under non-permeabilizing conditions. The fluorescence intensity of the Alexa-488 fluorescein dye is insensitive to pH changes, which allows for the antibodies to be stripped off with low pH glycine buffer without affecting the fluorescence intensity of internalized antibodies (139). Therefore, these conditions can also be used for the following integrin

internalization studies.

5.2.3 Immunofluorescence and FACS Analysis of Integrin Internalization

To study integrin internalization, cultured HUVECs were treated with EMD478761. Cells were labeled with primary Alexa®488-conjugated antibodies against $\alpha_v\beta_3$ integrins (Chemicon) at 4°C for 1hour to prevent integrin internalization. After allowing endocytosis to proceed at 37°C for various time intervals (5, 10, 15, 20 or 30 minutes), we then detached the cells with Versene. To detect only those internalized fluorophore-labeled integrins, residual surface-bound antibodies were removed by washing the cells twice (2 minutes/wash) with an acidic antibody-stripping buffer (50 mM glycine, 150 mM NaCl, pH 2.5) at 4°C. The antibody-stripping buffer has been previously demonstrated to be able to remove cell surface bound antibodies effectively (139). After stripping, the labeled cells were either spin-coated onto a slide for immunofluorescence microscopic examination or subjected to flow cytometry analysis.

5.2.4 Quantitative analysis of integrin internalization by biotin labeling

Integrin internalization was also studied using a modified biotin-labeling technique (104). A membrane non-permeable biotin was used to label cell-surface membrane proteins and to determine integrin molecules that are internalized. The schematic representation of biotin labeling and integrin internalization detection procedures is shown in Figure 5-2.

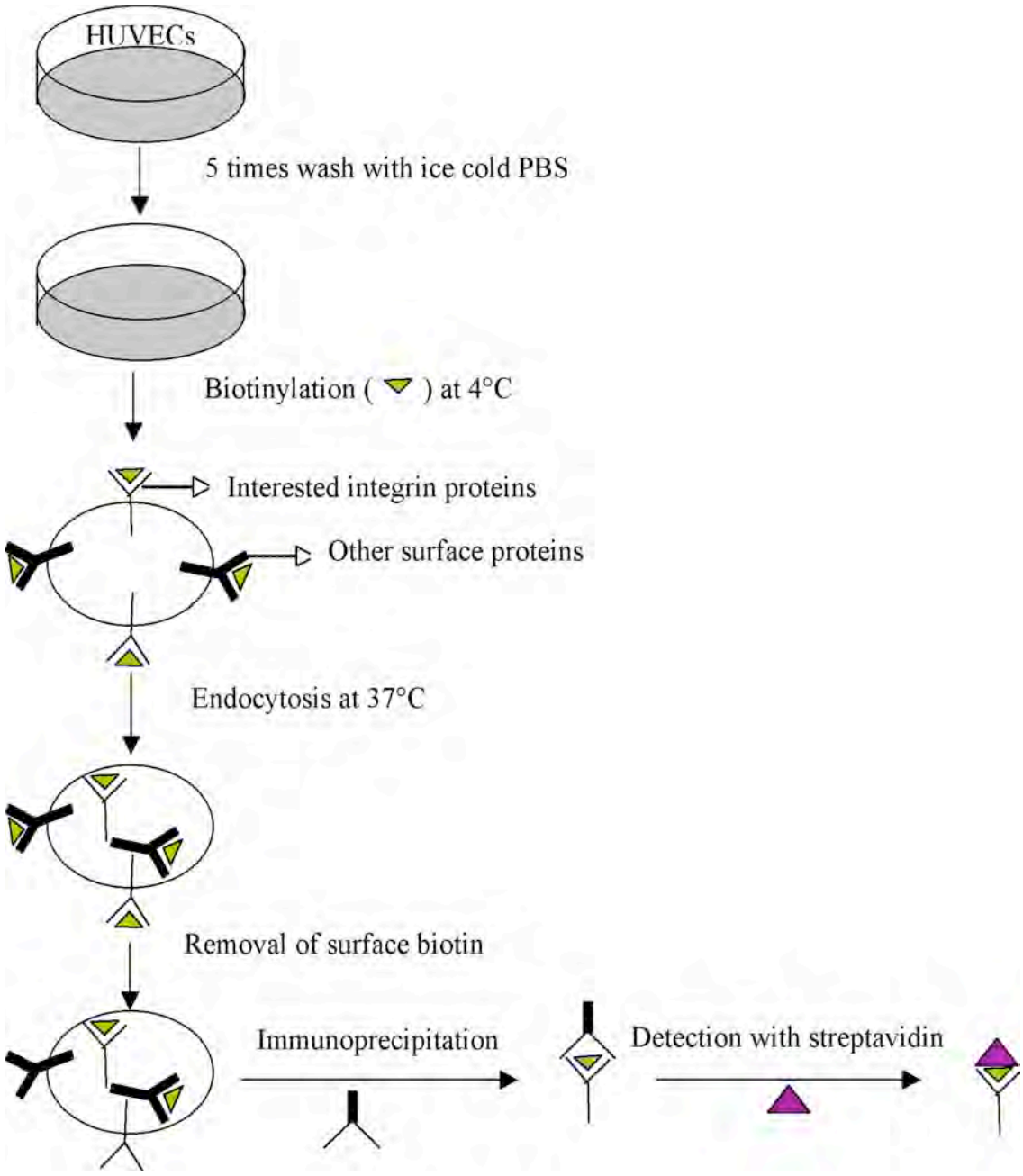

Figure 5-1. Schematic representation of integrin internalization with biotin labeling.. HUVECs were extensively washed with ice cold PBS before labeling with 1 mg/ml NHS-SS-biotin. Labeled cells were incubated at 37 °C for indicated time to allow internalization to proceed. Surface biotin was removed and internalized integrins were immunoprecipitated with specific anti-$\alpha_v\beta_3$ antibody and detected with streptavidin.

Subconfluent HUVECs were serum starved for 30 minutes and washed 5 times with ice-cold PBS to remove serum-derived proteins. Cell surface proteins (including integrins and other receptors) were biotinylated with Sulfo-NHS-SS-Biotin (Pierce; Fig. 5-3) at 1 mg/ml for 15 min at 4°C. Cells were then returned to 37°C in serum free medium in the presence or absence of 0.6 μM EMD478761 for 0, 5, 10, 20 and 30 min to allow internalization of labeled surface proteins to proceed. Cells were transferred to ice after the medium was aspirated. Biotin was removed from those non-internalized or recycled labeled proteins by incubation with a solution containing 20 mM sodium 2-mercaptoethanesulfonate (MesNa, a membrane-impermeant reducing agent; Sigma) in 50 mM Tris, pH 8.5, and 100 mM NaCl for 15 minutes at 4°C. After surface reduction, cells were washed twice with ice-cold PBS. MesNa was quenched by the addition of 20 mM iodoacetamine (IAA; Sigma) for 10 minutes and then the cells were lysed in RIPA buffer (Pierce) containing proteinase inhibitors. The protein levels were determined using the BCA protein assay kit (Pierce). Cell lysate with equal amounts of total protein was pre-cleared by incubation with protein-G beads (Millipore, Billerica MA) alone and then was immunoprecipitated with antibody $\alpha_v\beta_3$ pre-treated protein G beads. The bead-bound proteins were solubilized in boiled 1x SDS-gel sample buffer (Invitrogen) under non-reducing conditions and clarified by centrifugation. Immunoprecipitated integrins were separated with 4-12% SDS-PAGE under non-reducing conditions. Biotinylated proteins were detected with streptavidin-conjugated horseradish peroxidase (HRP) and visualized by enhanced chemiluminescence (Pierce) according to manufacture's instructions.

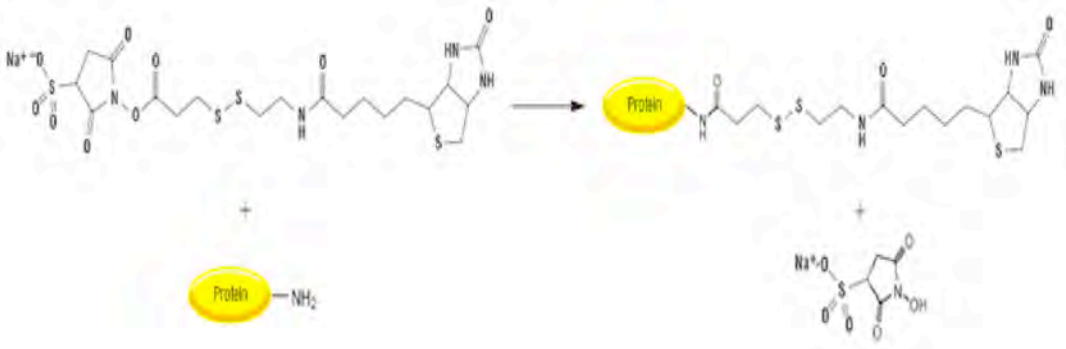

Figure 5-3. Labeling reaction of biotin with surface proteins.

5.3 Results

5.3.1 Effect of EMD478761 on Integrin $\alpha_v\beta_3$ Expression

In light of the inhibition effects of sustained delivery of EMD478761 on several *in vivo* angiogenesis assays and the involvement of integrin $\alpha_v\beta_3$ in angiogenic vessels, we first evaluated the integrin $\alpha_v\beta_3$ expression levels on endothelial cells in the presence of EMD478761. As shown in Figure 5-4, the flow cytometry analysis indicated that surface integrin $\alpha_v\beta_3$ expression levels were not significantly changed in either control or EMD478761 treated cells over the 12 hours interval. However, we observed a pronounce decrease in cell-surface integrin $\alpha_v\beta_3$ expression levels followed by cell detachment after 24 hours EMD478761 treatment.

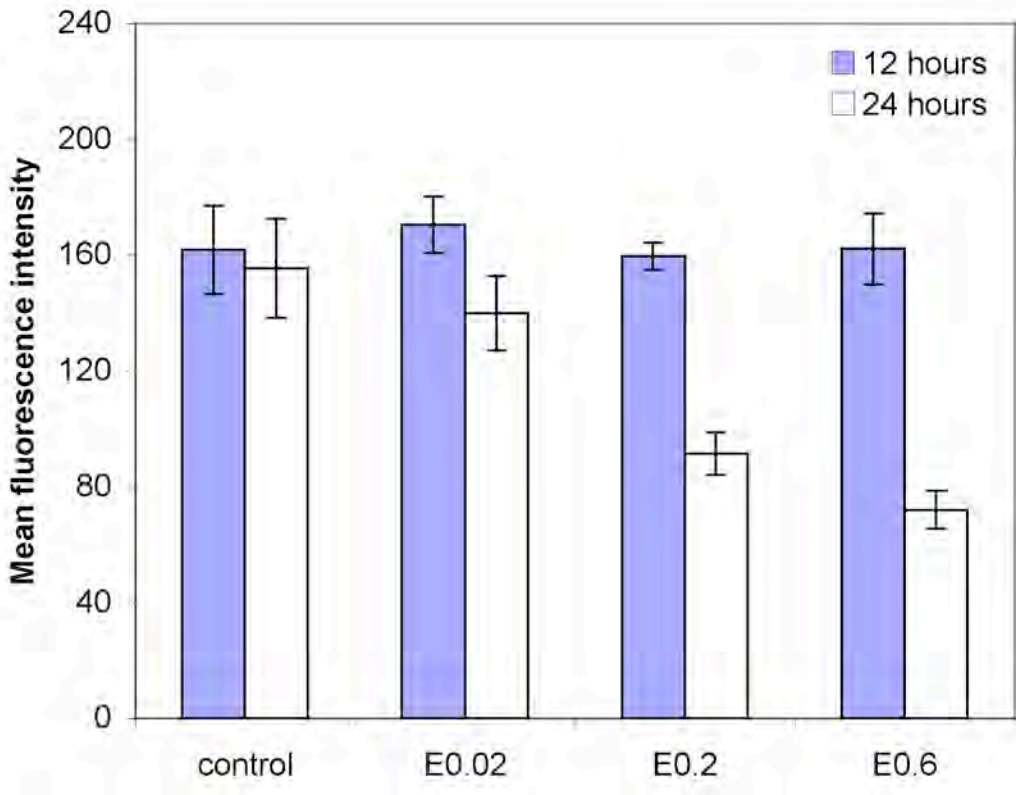

Figure 5-4. Effect of EMD478761 on endothelial cell surface integrin $\alpha_v\beta_3$ expression. HUVECs were labeled with Alexa 488-conjugated anti- $\alpha_v\beta_3$ antibodies 12 and 24 hours after EMD478761 treatment (concentration range: 0-0.6 μM). Labeled cells were subjected to flow cytometry analysis. Bar represents mean ± S.D. of 4 independent experiments.

5.3.2 Effect of EMD478761 on Integrin $\alpha_v\beta_3$ Internalization

We next examined whether EMD478761 can affect $\alpha_v\beta_3$ integrin internalization from the endothelial cell surface. For these experiments, the surface integrin of $\alpha_v\beta_3$ of HUVECs was labeled with Alexa 488-conjugated anti- $\alpha_v\beta_3$ antibody at 4 °C. The cells were

incubated either at 37°C in the presence or absence of 0.6 μM EMD478761 to allow integrin internalization to occur or at 4 °C as non-internalization control. The residual surface integrin-bound antibody was removed by an acidic glycine buffer washing. The cells were then fixed for flow cytometry analysis, or permeabilized for fluorescence microscopy examination. Our results showed a significant increase in fluorescence intensity of EMD478761-treated endothelial cells as compared to controls (Fig. 5-5), suggesting that EMD478761 affected integrin $\alpha_v\beta_3$ internalization. To confirm these observations from flow cytometry studies, cell suspensions were also subjected to fluorescence microscope visualization. As shown in Figure 5-5 insert, fluorescence microscopy of HUVECs revealed that for both control cells and EMD478761 treated cells, integrin internalization was elevated with the increasing of internalization time. However, the addition of EMD478761 markedly increased the internalization of the $\alpha_v\beta_3$ integrin as compared to control cells.

Internalization of $\alpha_v\beta_3$ integrin was detected by fluorescence microscope as early as 5 minutes after the process was allowed to proceed at 37°C, suggesting a rapid endocytosis of these surface integrins taken place in control cells and EMD478761 treated cells. Moreover, the level of increase in integrin $\alpha_v\beta_3$ internalization appeared to be more with the fluorescence microscope visualization than that of flow cytometry analysis. This might be due to the effect of the clustering and aggregation of antibody-tagged integrin $\alpha_v\beta_3$, which greatly enhanced the visualization of internalized integrins by fluorescence microscopy (139).

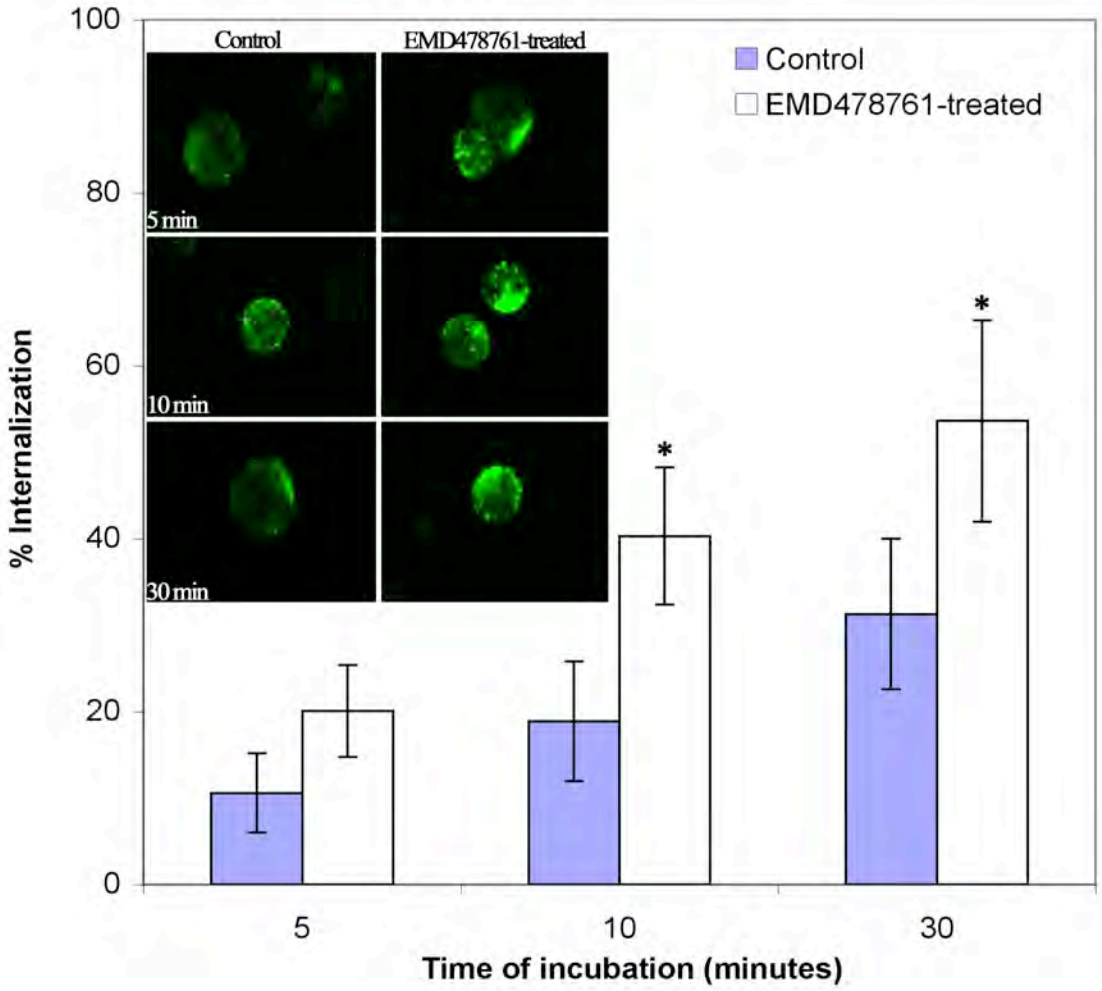

Figure 5-5. Flow cytometry analysis of integrin $\alpha_v\beta_3$ internalization in endothelial cells in the presence of 0.6 μM EMD478761. Subconfluent HUVECs were labeled with Alexa 488-conjugated anti- $\alpha_v\beta_3$ antibodies at 4°C. After incubated at 37°C for indicated time intervals, surface-bound antibodies were removed by the antibody stripping buffer. Cells were then subjected to flow cytometry analysis or fluorescence microscope visualization. Insert: fluorescence images of integrin $\alpha_v\beta_3$ internalization in the presence of 0.6 μM EMD478761. Bar represents mean ± S.D. of 3 independent experiments. ($P < 0.05$ as compared to controls)

Integrin $\alpha_v\beta_3$ internalization was further investigated by a biotin-labeling assay. Integrin $\alpha_v\beta_3$ internalization was determined by surface labeling HUVECs with Sulfo-NHS-SS-biotin at 4°C, followed by incubation at 37°C for various time intervals. Internalized integrins were assessed by immunoprecipitation, followed by Western blotting with streptavidin. The integrin $\alpha_v\beta_3$ internal pool reached a steady level by around 10 min for EMD478761 treated cells and 15 min for controls (Fig. 5-6). We also observed that the addition of EMD478761 increased the measured integrin $\alpha_v\beta_3$ internalization. These results were consistent with those of flow cytometry analysis and fluorescence microscopy observation.

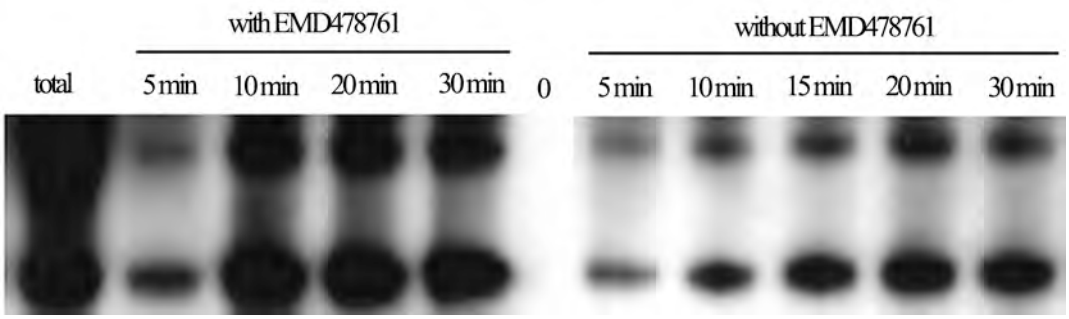

Figure 5-6. Effect of EMD478761 on integrin $\alpha_v\beta_3$ internalization by biotin labeling. HUVECs were labeled with biotin at 4°C and then they were incubated at 37°C for different time intervals, as specified. Surface remaining biotin was removed by MesNa reduction. Internalized integrin $\alpha_v\beta_3$ was immunoprecipitated and fractioned by SDS-PAGE. Biotin-labeled integrin $\alpha_v\beta_3$ was detected by streptavidin.

5.4 Discussion

Recycling of cell-surface integrins is a constitutive process in adherent cells and is believed to play a vital role in cell adhesion, remodeling of the ECM, and the migration of adherent cells (141, 142). Like other recycling events related to a variety of cell-surface receptors, the initial step of integrin recycling is integrin receptor internalization, a process believed to occur by endocytosis (141, 143). In the present study, we examined the effect of EMD478761 on the expression and internalization of the surface integrin $\alpha_v\beta_3$ in HUVECs using fluorescein and biotin labeling methods.

Our preliminary results showed that total cell-surface integrin $\alpha_v\beta_3$ expression in HUVECs was not affected by the presence of EMD478761 after 12 hours. Moreover, we observed that EMD478761 increased integrin $\alpha_v\beta_3$ internalization, which was supported by fluorescence microscopy and flow cytometry analysis, and it was further confirmed by Western blotting analysis. A possible explanation for this observation could be due to increased degradation of the endocytosed integrin $\alpha_v\beta_3$ after EMD478761 exposure, and that this degradation was compensated by increased synthesis and secretion of new integrin $\alpha_v\beta_3$, which maintained the surface levels of integrin $\alpha_v\beta_3$ despite increased of integrin internalization. However, this possibility appears to be unlikely since the observation of elevated integrin internalization was within short period of time. Increasing evidence showed that the half-life of integrin turnover in adherent cells (fibroblast and endothelial cells) is about 8-10 hours (144), while recycling of such integrins has been documented to proceed much rapidly with a half-life of about 5-10 minutes (104, 139). Therefore, the enhanced integrin internalization is more likely the

consequence of elevated integrin recycling rate rather than integrin synthesis and degradation.

Although the physiologic/pathologic significance of integrin recycling is not clearly understood, recycling of $\alpha_v\beta_3$ and other integrins has been suggested to mediate cell migration, spreading (141, 145), and modulate surface-bound ligand (138). The life cycle of integrin involves constitutive synthesis, recycling and degradation. Integrin binging to ECM was believed to prevent the degradation and internalization. Once the cells lost their contact with ECM, adhesion-dependent signals initiated by the binding of ECM to cell surface integrins was blocked. As a result, cell shape and cytoskeletal organization were changed. Therefore, the biological consequence of integrin $\alpha_v\beta_3$ internalization as seen in this experiment might be explained as a potential mechanism for limiting the extent of adhesion-dependent signaling.

Previous studies demonstrated that integrin $\alpha_v\beta_3$ recycling through long-loop or short-loop was Rab-dependent, and was regulated by platelet derived growth factor (PDGF) (104). In this investigation, we only observed that there is an increase in integrin $\alpha_v\beta_3$ internalization in the presence of EMD478761. The biological consequence of such enhanced integrin internalization may contribute to endothelial cell detachment and angiogenesis inhibition. Further studies will warrant a better understanding of the effect of EMD478761 on integrin recycling pathways.

5.5 Conclusions

In this study, we have demonstrated that endothelial cell surface integrin $\alpha_v\beta_3$ expression levels were not affected by the presence of EMD478761 for up to 12 hours. EMD478761 induced an increased internalization of this integrin.

Chapter 6: Summary and Perspectives

6.1 Summary

In summary, this study was initiated to target choroidal neovascularization by antagonizing a specific angiogenesis marker using a sustained delivery system. It was motivated by the facts that integrins $\alpha_v\beta_3$ and $\alpha_v\beta_5$ are up-regulated in the ocular angiogenic vessels while undetectable in mature/quiescent blood vessels, and anti-integrin compounds appear to potently block cytokine and tumor-induced angiogenesis in several animal models. In addition, continuous delivery of other anti-angiogenic compounds, such as endostatin, increases the efficacy and potency of anti-tumor therapies. We integrated a system that took advantages of the novel integrin antagonist, EMD478761, and a sustained delivery device, which can potentially deliver the drug at controlled release rates to the site of neovascularization, while bypassing the major ocular drug delivery barriers.

PVA reservoir type implants were designed to release the drug for a desired period of time. The parameters, which influence the release rates of the implants including PVA concentrations, implant sizes and curing temperature, were evaluated. The release rates of the implants decreased as the PVA concentrations and the curing temperatures increased, while they increased proportionally to the sizes of the implant. A circular implant was fabricated for the CAM assay, and a microimplant was designed

specifically for the laser-induced CNV rat model. Both types of implants delivered an initial burst of drug on the first day, followed by a constant release for an extended period of time, which then gradually decreased. The steady-state release kinetics followed a zero order, which is typical for diffusion controlled drug release devices.

Initial experiments were performed to investigate the angiogenic inhibitory efficacy of the EMD478761 implant using a modified CAM assay (Chapter 2). Results showed that sustained delivery of EMD478761 pronouncedly inhibited bFGF-induced angiogenesis in the CAM assay. In average, 85% and 90% of the control CAMs were positive in the presence of bFGF and bFGF with sham implant, respectively. However, only 19% of the bFGF-induced CAMs were weakly angiogenic in the presence of the EMD478761 implant. In terms of neovascularization area, bFGF alone induced an average of 6.8 ± 5.3 mm^2, and bFGF with sham implant induced a similar area of 6.3 ± 3.1 mm^2. In contrast, the presence of the EMD478761 implant dramatically decreased the neovascularization area to only 0.47 ± 1.2 mm^2. We further examined the ability of this implant to regress existing neovascularization in the CAM by adding the implant three days after the angiogenesis was induced. Interestingly, EMD478761 significantly decreased the neovascularization area by 80% after 2 days of treatment without affecting the normal CAM vasculature. These results were highly encouraging and they suggested that our sustained delivery system could be useful for the management of angiogenesis-related diseases.

A more in-depth anti-angiogenesis study was performed on a CNV animal model induced by a diode laser (Chapter 3). We compared the efficacy of intravitreal bolus injection and microimplant implantation on inhibition of CNV. EMD478761

microimplant significantly suppressed laser-induced CNV in rats by 63% to 65% 2 weeks after implantation. However, intravitreal injection of EMD478761 failed to abrogate the development of CNV. Histopathological studies corroborated the above findings. These results suggested that single intravitreous injection might not be able to deliver or maintain sufficient levels of EMD478761 to significantly inhibit CNV; therefore a sustained delivery device is necessary.

Once the anti-angiogenic properties of these implants were proved, we next examined EMD478761's action mode (Chapters 4 and 5). Endothelial cells are key player in the angiogenesis cascade as they form the lumen of every blood vessel. We found than EMD478761 inhibited endothelial cell proliferation, tube formation, and mediated endothelial cell apoptosis in a time- and dose- dependent manner. We also observed that EMD478761 induced apoptosis was substratum-dependent and involved caspase-3 activation. EMD478761 caused rapid disruption of actin microfilaments in HUVECs grown on vitronectin-coated surfaces followed by cell detachment in a dose-dependent manner, while there was no such effect was observed with cells plated on fibronectin-coated surfaces. These findings indicated that the action of EMD478761 is α_v-specific and may be mediated by inducing cell detachment.

Finally, we investigated the effect of EMD478761 on integrin receptor regulation, in particular, on integrin $\alpha_v\beta_3$ expression and internalization. Our preliminary results demonstrated that EMD478761 increased the integrin $\alpha_v\beta_3$ internalization in endothelial cells, while total surface integrin $\alpha_v\beta_3$ was not affected. This result suggests that EMD478761 increased integrin $\alpha_v\beta_3$ recycling rates. However, the biological

consequence of integrin internalization and its relationship with anti-angiogenesis abilities need to further investigated.

6.2 Perspectives

In this study, we demonstrated the anti-angiogenic potency of sustained delivery of EMD478761. However, AMD is a chronic disease, which may need months to years treatment, it will be worthwhile to design a new implant with longer release period (years) for future preclinical and clinical studies. A preliminary approach has been taken to design a composite silicone reservoir implant that can release EMD478761 at a constant rate for up to a year (Fig.6-1).

Pharmacokinetic studies will be needed to predict the drug distribution and elimination after implantation. In this study, we used rat to assess the in vivo efficacy of EMD478761, however, the vitreous volume of the rat eye is too small to perform direct pharmacokinetics studies. Moreover, the solubility of this drug in normal physiological saline is limited, conventional drug extraction methods with certain organic solvents such as acetonenitrile and methanol, are not ideal, especially when drug concentrations are extremely low. In order to obtain the experimental data, it will be better to use larger animals such rabbits. Additionally, it will also be interesting to conjugate fluorescein or contrast agents to this drug, therefore allowing direct in vivo tracking of drug distribution. Finally, it will be useful to build a mathematical model to provide a better understanding of drug movement and predict drug levels inside the eye, and offer feedback for the implant design with therapeutic levels of release rates.

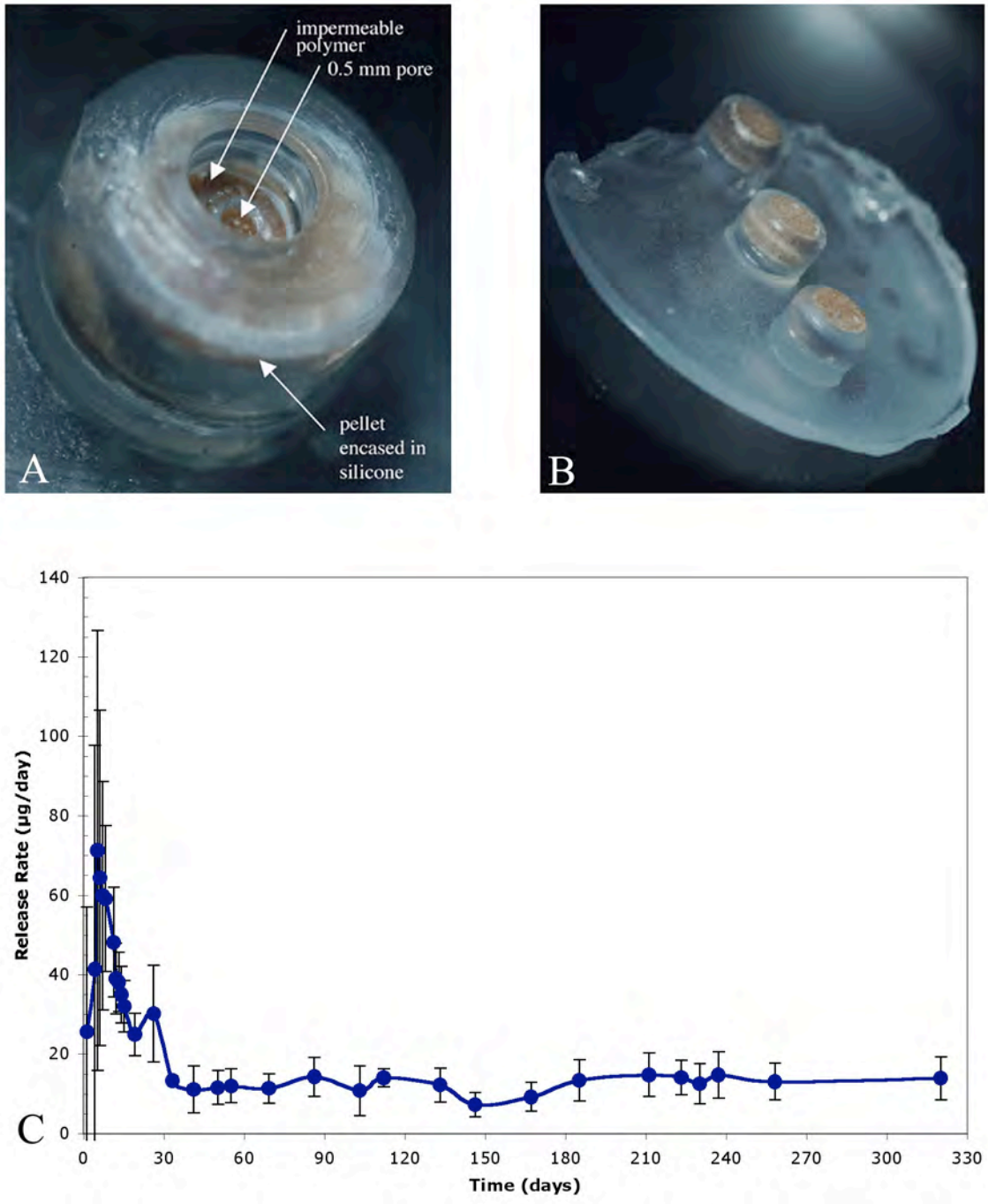

Figure 6-1. A long-term release EMD478761 implant (A, B) and its in vitro release profile (C, n = 5).

In this study, we observed that EMD478761 facilitated integrin $\alpha_v\beta_3$ internalization. However, we were not clear about its biological consequences. Future studies will warrant a better understanding regarding the connection of integrin internalization and angiogenesis suppression.

Bibliography

1. Bressler, N. M. (2004) Age-related macular degeneration is the leading cause of blindness. *Jama* **291**, 1900-1901

2. Fine, S. L., Berger, J. W., Maguire, M. G., and Ho, A. C. (2000) Age-related macular degeneration. *N Engl J Med* **342**, 483-492

3. http://www.blindness.org/publications/newsarticle.asp?x=1&NewsID=279

4. Janoria, K. J., Gunda, S., Boddu, S. H., and Mitra, A. K. (2007) Novel approaches to retinal drug delivery. *Expert Opin Drug Deliv* **4**, 371-388

5. Petermeier, K., Tatar, O., Inhoffen, W., Volker, M., Lafaut, B. A., Henke-Fahle, S., Gelisken, F., Ziemssen, F., Bopp, S., Bartz-Schmidt, K. U., and Grisanti, S. (2006) Verteporfin photodynamic therapy induced apoptosis in choroidal neovascular membranes. *Br J Ophthalmol* **90**, 1034-1039

6. Virgili, G., and Menchini, F. (2005) Laser photocoagulation for choroidal neovascularisation in pathologic myopia. *Cochrane Database Syst Rev*, CD004765

7. Suesskind, D., Voelker, M., Bartz-Schmidt, K. U., and Gelisken, F. (2007) Full macular translocation following photodynamic therapy in neovascular age-related macular degeneration. *Eye*

8. Shing, Y., Folkman, J., Sullivan, R., Butterfield, C., Murray, J., and Klagsbrun, M. (1984) Heparin affinity: purification of a tumor-derived capillary endothelial cell growth factor. *Science* **223**, 1296-1299

9. Kisker, O., Becker, C. M., Prox, D., Fannon, M., D'Amato, R., Flynn, E., Fogler, W. E., Sim, B. K., Allred, E. N., Pirie-Shepherd, S. R., and Folkman, J. (2001) Continuous administration of endostatin by intraperitoneally implanted osmotic pump improves the efficacy and potency of therapy in a mouse xenograft tumor model. *Cancer Res* **61**, 7669-7674

10. Pearson, P. A., Hainsworth, D. P., and Ashton, P. (1993) Clearance and distribution of ciprofloxacin after intravitreal injection. *Retina* **13**, 326-330

11. Heinemann, M. H. (1989) Staphylococcus epidermidis endophthalmitis complicating intravitreal antiviral therapy of cytomegalovirus retinitis. Case report. *Arch Ophthalmol* **107**, 643-644

12. Ruiz-Moreno, J. M., Montero, J. A., Bayon, A., Rueda, J., and Vidal, M. (2007) Retinal toxicity of intravitreal triamcinolone acetonide at high doses in the rabbit. *Exp Eye Res* **84**, 342-348

13. Thompson, J. T. (2006) Cataract formation and other complications of intravitreal triamcinolone for macular edema. *Am J Ophthalmol* **141**, 629-637

14. Folkman, J., and Shing, Y. (1992) Angiogenesis. *J Biol Chem* **267**, 10931-10934

15. Ferrara, N., Houck, K., Jakeman, L., and Leung, D. W. (1992) Molecular and biological properties of the vascular endothelial growth factor family of proteins. *Endocr Rev* **13**, 18-32

16. Antonelli-Orlidge, A., Saunders, K. B., Smith, S. R., and D'Amore, P. A. (1989) An activated form of transforming growth factor beta is produced by cocultures of endothelial cells and pericytes. *Proc Natl Acad Sci U S A* **86**, 4544-4548

17. Beutler, B., and Cerami, A. (1986) Cachectin and tumour necrosis factor as two sides of the same biological coin. *Nature* **320**, 584-588

18. Ishikawa, F., Miyazono, K., Hellman, U., Drexler, H., Wernstedt, C., Hagiwara, K., Usuki, K., Takaku, F., Risau, W., and Heldin, C. H. (1989) Identification of angiogenic activity and the cloning and expression of platelet-derived endothelial cell growth factor. *Nature* **338**, 557-562

19. Usuki, K., Heldin, N. E., Miyazono, K., Ishikawa, F., Takaku, F., Westermark, B., and Heldin, C. H. (1989) Production of platelet-derived endothelial cell growth factor by normal and transformed human cells in culture. *Proc Natl Acad Sci U S A* **86**, 7427-7431

20. Hynes, R. O. (1987) Integrins: a family of cell surface receptors. *Cell* **48**, 549-554

21. Miller, J. W., Adamis, A. P., Shima, D. T., D'Amore, P. A., Moulton, R. S., O'Reilly, M. S., Folkman, J., Dvorak, H. F., Brown, L. F., Berse, B., and et al. (1994) Vascular endothelial growth factor/vascular permeability factor is temporally and spatially correlated with ocular angiogenesis in a primate model. *Am J Pathol* **145**, 574-584

22. Vinores, S. A., Youssri, A. I., Luna, J. D., Chen, Y. S., Bhargave, S., Vinores, M. A., Schoenfeld, C. L., Peng, B., Chan, C. C., LaRochelle, W., Green, W. R., and Campochiaro, P. A. (1997) Upregulation of vascular endothelial growth factor in ischemic and non-ischemic human and experimental retinal disease. *Histol Histopathol* **12**, 99-109

23. Pierce, E. A., Avery, R. L., Foley, E. D., Aiello, L. P., and Smith, L. E. (1995) Vascular endothelial growth factor/vascular permeability factor expression in a mouse model of retinal neovascularization. *Proc Natl Acad Sci U S A* **92**, 905-909

24. Brooks, P. C., Clark, R. A., and Cheresh, D. A. (1994) Requirement of vascular integrin alpha v beta 3 for angiogenesis. *Science* **264**, 569-571

25. Friedlander, M., Theesfeld, C. L., Sugita, M., Fruttiger, M., Thomas, M. A., Chang, S., and Cheresh, D. A. (1996) Involvement of integrins alpha v beta 3 and alpha v beta 5 in ocular neovascular diseases. *Proc Natl Acad Sci U S A* **93**, 9764-9769

26. Umeda, N., Kachi, S., Akiyama, H., Zahn, G., Vossmeyer, D., Stragies, R., and Campochiaro, P. A. (2006) Suppression and regression of choroidal neovascularization by systemic administration of an alpha5beta1 integrin antagonist. *Mol Pharmacol* **69**, 1820-1828

27. Ikeda, Y., Yonemitsu, Y., Onimaru, M., Nakano, T., Miyazaki, M., Kohno, R. I., Nakagawa, K., Ueno, A., Sueishi, K., and Ishibashi, T. (2006) The regulation of vascular endothelial growth factors (VEGF-A, -C, and -D) expression in the retinal pigment epithelium. *Exp Eye Res*

28. Nowak, J. Z. (2006) Age-related macular degeneration (AMD): pathogenesis and therapy. *Pharmacol Rep* **58**, 353-363

29. Adamis, A. P., Shima, D. T., Tolentino, M. J., Gragoudas, E. S., Ferrara, N., Folkman, J., D'Amore, P. A., and Miller, J. W. (1996) Inhibition of vascular endothelial growth factor prevents retinal ischemia-associated iris neovascularization in a nonhuman primate. *Arch Ophthalmol* **114**, 66-71

30. Galardy, R. E., Grobelny, D., Foellmer, H. G., and Fernandez, L. A. (1994) Inhibition of angiogenesis by the matrix metalloprotease inhibitor N-[2R-2-(hydroxamidocarbonymethyl)-4-methylpentanoyl)]-L-tryptophan methylamide. *Cancer Res* **54**, 4715-4718

31. Ng, E. W., Shima, D. T., Calias, P., Cunningham, E. T., Jr., Guyer, D. R., and Adamis, A. P. (2006) Pegaptanib, a targeted anti-VEGF aptamer for ocular vascular disease. *Nat Rev Drug Discov* **5**, 123-132

32. Shen, J., Samul, R., Silva, R. L., Akiyama, H., Liu, H., Saishin, Y., Hackett, S. F., Zinnen, S., Kossen, K., Fosnaugh, K., Vargeese, C., Gomez, A., Bouhana, K., Aitchison, R., Pavco, P., and Campochiaro, P. A. (2006) Suppression of ocular neovascularization with siRNA targeting VEGF receptor 1. *Gene Ther* **13**, 225-234

33. Krzystolik, M. G., Afshari, M. A., Adamis, A. P., Gaudreault, J., Gragoudas, E. S., Michaud, N. A., Li, W., Connolly, E., O'Neill, C. A., and Miller, J. W. (2002) Prevention of experimental choroidal neovascularization with intravitreal anti-vascular endothelial growth factor antibody fragment. *Arch Ophthalmol* **120**, 338-346

34. Baka, S., Clamp, A. R., and Jayson, G. C. (2006) A review of the latest clinical compounds to inhibit VEGF in pathological angiogenesis. *Expert Opin Ther Targets* **10**, 867-876

35. Michels, S., Schmidt-Erfurth, U., and Rosenfeld, P. J. (2006) Promising new treatments for neovascular age-related macular degeneration. *Expert Opin Investig Drugs* **15**, 779-793

36. Avery, R. L., Pieramici, D. J., Rabena, M. D., Castellarin, A. A., Nasir, M. A., and Giust, M. J. (2006) Intravitreal bevacizumab (Avastin) for neovascular age-related macular degeneration. *Ophthalmology* **113**, 363-372 e365

37. Rich, R. M., Rosenfeld, P. J., Puliafito, C. A., Dubovy, S. R., Davis, J. L., Flynn, H. W., Jr., Gonzalez, S., Feuer, W. J., Lin, R. C., Lalwani, G. A., Nguyen, J. K., and Kumar, G. (2006) Short-term safety and efficacy of intravitreal bevacizumab (Avastin) for neovascular age-related macular degeneration. *Retina* **26**, 495-511

38. Spaide, R. F., Laud, K., Fine, H. F., Klancnik, J. M., Jr., Meyerle, C. B., Yannuzzi, L. A., Sorenson, J., Slakter, J., Fisher, Y. L., and Cooney, M. J. (2006) Intravitreal bevacizumab treatment of choroidal neovascularization secondary to age-related macular degeneration. *Retina* **26**, 383-390

39. Afzal, A., Shaw, L. C., Ljubimov, A. V., Boulton, M. E., Segal, M. S., and Grant, M. B. (2007) Retinal and choroidal microangiopathies: Therapeutic opportunities. *Microvasc Res*

40. Alon, T., Hemo, I., Itin, A., Pe'er, J., Stone, J., and Keshet, E. (1995) Vascular endothelial growth factor acts as a survival factor for newly formed retinal vessels and has implications for retinopathy of prematurity. *Nat Med* **1**, 1024-1028

41. Clarke, M. S. (2004) Anecortave acetate. *Ophthalmology* **111**, 2316; author reply 2316-2317

42. D'Amico, D. J., Goldberg, M. F., Hudson, H., Jerdan, J. A., Krueger, D. S., Luna, S. P., Robertson, S. M., Russell, S., Singerman, L., Slakter, J. S., Yannuzzi, L., and Zilliox, P. (2003) Anecortave acetate as monotherapy for treatment of subfoveal neovascularization in age-related macular degeneration: twelve-month clinical outcomes. *Ophthalmology* **110**, 2372-2383; discussin 2384-2375

43. D'Amico, D. J., Goldberg, M. F., Hudson, H., Jerdan, J. A., Krueger, S., Luna, S., Robertson, S. M., Russell, S., Singerman, L., Slakter, J. S., Sullivan, E. K., Yannuzzi, L., and Zilliox, P. (2003) Anecortave acetate as monotherapy for the treatment of subfoveal lesions in patients with exudative age-related macular

degeneration (AMD): interim (month 6) analysis of clinical safety and efficacy. *Retina* **23**, 14-23

44. Rasmussen, H., Chu, K. W., Campochiaro, P., Gehlbach, P. L., Haller, J. A., Handa, J. T., Nguyen, Q. D., and Sung, J. U. (2001) Clinical protocol. An open-label, phase I, single administration, dose-escalation study of ADGVPEDF.11D (ADPEDF) in neovascular age-related macular degeneration (AMD). *Hum Gene Ther* **12**, 2029-2032

45. Das, A., and McGuire, P. G. (2003) Retinal and choroidal angiogenesis: pathophysiology and strategies for inhibition. *Prog Retin Eye Res* **22**, 721-748

46. (2006) FDA labeling information. http://www.fda.gov/cder/foi/label/2006/125156lbl.pdf.

47. Narayanan, R., Kuppermann, B. D., Jones, C., and Kirkpatrick, P. (2006) Ranibizumab. *Nat Rev Drug Discov* **5**, 815-816

48. Rosenfeld, P. J., Brown, D. M., Heier, J. S., Boyer, D. S., Kaiser, P. K., Chung, C. Y., and Kim, R. Y. (2006) Ranibizumab for neovascular age-related macular degeneration. *N Engl J Med* **355**, 1419-1431

49. Rosenfeld, P. J., Rich, R. M., and Lalwani, G. A. (2006) Ranibizumab: Phase III clinical trial results. *Ophthalmol Clin North Am* **19**, 361-372

50. Ruegg, C., and Mariotti, A. (2003) Vascular integrins: pleiotropic adhesion and signaling molecules in vascular homeostasis and angiogenesis. *Cell Mol Life Sci* **60**, 1135-1157

51. Stupack, D. G., and Cheresh, D. A. (2004) A Bit-role for integrins in apoptosis. *Nat Cell Biol* **6**, 388-389

52. Ruegg, C., Dormond, O., and Mariotti, A. (2004) Endothelial cell integrins and COX-2: mediators and therapeutic targets of tumor angiogenesis. *Biochim Biophys Acta* **1654**, 51-67

53. Giancotti, F. G., and Ruoslahti, E. (1999) Integrin signaling. *Science* **285**, 1028-1032

54. Hood, J. D., and Cheresh, D. A. (2002) Role of integrins in cell invasion and migration. *Nat Rev Cancer* **2**, 91-100

55. Eliceiri, B. P., Puente, X. S., Hood, J. D., Stupack, D. G., Schlaepfer, D. D., Huang, X. Z., Sheppard, D., and Cheresh, D. A. (2002) Src-mediated coupling of focal adhesion kinase to integrin alpha(v)beta5 in vascular endothelial growth factor signaling. *J Cell Biol* **157**, 149-160

56. Pasqualini, R., Koivunen, E., and Ruoslahti, E. (1997) Alpha v integrins as receptors for tumor targeting by circulating ligands. *Nat Biotechnol* **15**, 542-546

57. Friedlander, M., Brooks, P. C., Shaffer, R. W., Kincaid, C. M., Varner, J. A., and Cheresh, D. A. (1995) Definition of two angiogenic pathways by distinct alpha v integrins. *Science* **270**, 1500-1502

58. Brooks, P. C., Montgomery, A. M., Rosenfeld, M., Reisfeld, R. A., Hu, T., Klier, G., and Cheresh, D. A. (1994) Integrin alpha v beta 3 antagonists promote tumor regression by inducing apoptosis of angiogenic blood vessels. *Cell* **79**, 1157-1164

59. Geroski, D. H., and Edelhauser, H. F. (2000) Drug delivery for posterior segment eye disease. *Invest Ophthalmol Vis Sci* **41**, 961-964

60. Galloway, N. R., Amoaku, W. M. K., Galloway, P. H., and Browning, A. C. (2006) Common eye diseases and their management. Springer-Verlag London Limited.

61. Urtti, A. (2006) Challenges and obstacles of ocular pharmacokinetics and drug delivery. *Adv Drug Deliv Rev* **58**, 1131-1135

62. Yasukawa, T., Ogura, Y., Sakurai, E., Tabata, Y., and Kimura, H. (2005) Intraocular sustained drug delivery using implantable polymeric devices. *Adv Drug Deliv Rev* **57**, 2033-2046

63. Davis, J., Gilger, B. C., and Robinson, M. R. (2004) Novel approaches to ocular drug delivery. *Curr Opin Mol Ther* **6**, 195-205

64. Moritera, T., Ogura, Y., Yoshimura, N., Honda, Y., Wada, R., Hyon, S. H., and Ikada, Y. (1992) Biodegradable microspheres containing adriamycin in the

treatment of proliferative vitreoretinopathy. *Invest Ophthalmol Vis Sci* **33**, 3125-3130

65. Sakurai, E., Ozeki, H., Kunou, N., and Ogura, Y. (2001) Effect of particle size of polymeric nanospheres on intravitreal kinetics. *Ophthalmic Res* **33**, 31-36

66. Bourges, J. L., Gautier, S. E., Delie, F., Bejjani, R. A., Jeanny, J. C., Gurny, R., BenEzra, D., and Behar-Cohen, F. F. (2003) Ocular drug delivery targeting the retina and retinal pigment epithelium using polylactide nanoparticles. *Invest Ophthalmol Vis Sci* **44**, 3562-3569

67. Barza, M., Stuart, M., and Szoka, F., Jr. (1987) Effect of size and lipid composition on the pharmacokinetics of intravitreal liposomes. *Invest Ophthalmol Vis Sci* **28**, 893-900

68. Merodio, M., Irache, J. M., Valamanesh, F., and Mirshahi, M. (2002) Ocular disposition and tolerance of ganciclovir-loaded albumin nanoparticles after intravitreal injection in rats. *Biomaterials* **23**, 1587-1594

69. Irache, J. M., Merodio, M., Arnedo, A., Camapanero, M. A., Mirshahi, M., and Espuelas, S. (2005) Albumin nanoparticles for the intravitreal delivery of anticytomegaloviral drugs. *Mini Rev Med Chem* **5**, 293-305

70. Robinson, M. R., Baffi, J., Yuan, P., Sung, C., Byrnes, G., Cox, T. A., and Csaky, K. G. (2002) Safety and pharmacokinetics of intravitreal 2-methoxyestradiol implants in normal rabbit and pharmacodynamics in a rat model of choroidal neovascularization. *Exp Eye Res* **74**, 309-317

71. Ciulla, T. A., Criswell, M. H., Danis, R. P., Fronheiser, M., Yuan, P., Cox, T. A., Csaky, K. G., and Robinson, M. R. (2003) Choroidal neovascular membrane inhibition in a laser treated rat model with intraocular sustained release triamcinolone acetonide microimplants. *Br J Ophthalmol* **87**, 1032-1037

72. Ishida, K., Yoshimura, N., Mandai, M., and Honda, Y. (1999) Inhibitory effect of TNP-470 on experimental choroidal neovascularization in a rat model. *Invest Ophthalmol Vis Sci* **40**, 1512-1519

73. Rubsamen, P. E., Davis, P. A., Hernandez, E., O'Grady, G. E., and Cousins, S. W. (1994) Prevention of experimental proliferative vitreoretinopathy with a biodegradable intravitreal implant for the sustained release of fluorouracil. *Arch Ophthalmol* **112**, 407-413

74. Martin, D. F., D.J.Parks, S.D.Melow, F.L.Ferris, R.C.Walton, N.A.Remaly, E.Y.Chew, P.Ashton, M.D.Davis, and Nussenblatt, R. B. (1994) Treatment of cytomegalovirus retinitis with an intraocular sustained-release ganciclovir implant. *Arch, Ophthalmol.* **112**, 1531-1539

75. Hashizoe, M., Ogura, Y., Takanashi, T., Kunou, N., Honda, Y., and Ikada, Y. (1995) Implantable biodegradable polymeric device in the treatment of experimental proliferative vitreoretinopathy. *Curr Eye Res* **14**, 473-477

76. Beeley, N. R., Stewart, J. M., Tano, R., Lawin, L. R., Chappa, R. A., Qiu, G., Anderson, A. B., de Juan, E., and Varner, S. E. (2006) Development, implantation, in vivo elution, and retrieval of a biocompatible, sustained release subretinal drug delivery system. *J Biomed Mater Res A* **76**, 690-698

77. Beeley, N. R., Rossi, J. V., Mello-Filho, P. A., Mahmoud, M. I., Fujii, G. Y., de Juan, E., Jr., and Varner, S. E. (2005) Fabrication, implantation, elution, and retrieval of a steroid-loaded polycaprolactone subretinal implant. *J Biomed Mater Res A* **73**, 437-444

78. Folkman, J. (2006) Angiogenesis. *Annu Rev Med* **57**, 1-18

79. Auerbach, W., and Auerbach, R. (1994) Angiogenesis inhibition: a review. *Pharmacol Ther* **63**, 265-311

80. Miller, W. J., Kayton, M. L., Patton, A., O'Connor, S., He, M., Vu, H., Baibakov, G., Lorang, D., Knezevic, V., Kohn, E., Alexander, H. R., Stirling, D., Payvandi, F., Muller, G. W., and Libutti, S. K. (2004) A novel technique for quantifying changes in vascular density, endothelial cell proliferation and protein expression in response to modulators of angiogenesis using the chick chorioallantoic membrane (CAM) assay. *J Transl Med* **2**, 4

81. Gonzalez-Iriarte, M., Carmona, R., Perez-Pomares, J. M., Macias, D., Angel Medina, M., Quesada, A. R., and Munoz-Chapuli, R. (2003) A modified chorioallantoic membrane assay allows for specific detection of endothelial apoptosis induced by antiangiogenic substances. *Angiogenesis* **6**, 251-254

82. Schlatter, P., Konig, M. F., Karlsson, L. M., and Burri, P. H. (1997) Quantitative study of intussusceptive capillary growth in the chorioallantoic membrane (CAM) of the chicken embryo. *Microvasc Res* **54**, 65-73

83. Ponce, M. L., Hibino, S., Lebioda, A. M., Mochizuki, M., Nomizu, M., and Kleinman, H. K. (2003) Identification of a potent peptide antagonist to an active laminin-1 sequence that blocks angiogenesis and tumor growth. *Cancer Res* **63**, 5060-5064

84. Baker, R. W., ed (1987) *Controlled release of biologically active agents*, John Wiley and Sons, New York

85. Clark, R. A., Tonnesen, M. G., Gailit, J., and Cheresh, D. A. (1996) Transient functional expression of alphaVbeta 3 on vascular cells during wound repair. *Am J Pathol* **148**, 1407-1421

86. Ribatti, D., Conconi, M. T., Nico, B., Baiguera, S., Corsi, P., Parnigotto, P. P., and Nussdorfer, G. G. (2003) Angiogenic response induced by acellular brain scaffolds grafted onto the chick embryo chorioallantoic membrane. *Brain Res* **989**, 9-15

87. Hikichi, T., Mori, F., Sasaki, M., Takamiya, A., Nakamura, M., Shishido, N., Takeda, M., Horikawa, Y., Matsuoka, H., and Yoshida, A. (2002) Inhibitory effect of bucillamine on laser-induced choroidal neovascularization in rats. *Curr Eye Res* **24**, 1-5

88. Kamizuru, H., Kimura, H., Yasukawa, T., Tabata, Y., Honda, Y., and Ogura, Y. (2001) Monoclonal antibody-mediated drug targeting to choroidal neovascularization in the rat. *Invest Ophthalmol Vis Sci* **42**, 2664-2672

89. Koh, H. J., Bessho, K., Cheng, L., Bartsch, D. U., Jones, T. R., Bergeron-Lynn, G., and Freeman, W. R. (2004) Inhibition of choroidal neovascularization in rats by the urokinase-derived peptide A6. *Invest Ophthalmol Vis Sci* **45**, 635-640

90. Edelman, J. L., and Castro, M. R. (2000) Quantitative image analysis of laser-induced choroidal neovascularization in rat. *Exp Eye Res* **71**, 523-533

91. Wolfe, J. D., and Csaky, K. G. (2004) Indocyanine green enhanced retinal vessel laser closure in rats: histologic and immunohistochemical observations. *Exp Eye Res* **79**, 631-638

92. Dobi, E. T., Puliafito, C. A., and Destro, M. (1989) A new model of experimental choroidal neovascularization in the rat. *Arch Ophthalmol* **107**, 264-269

93. Yasukawa, T., Hoffmann, S., Eichler, W., Friedrichs, U., Wang, Y. S., and Wiedemann, P. (2004) Inhibition of experimental choroidal neovascularization in rats by an alpha(v)-integrin antagonist. *Curr Eye Res* **28**, 359-366

94. Kato, A., Kimura, H., Okabe, K., Okabe, J., Kunou, N., Nozaki, M., and Ogura, Y. (2005) Suppression of laser-induced choroidal neovascularization by posterior sub-tenon administration of triamcinolone acetonide. *Retina* **25**, 503-509

95. Ciulla, T. A., Criswell, M. H., Danis, R. P., and Hill, T. E. (2001) Intravitreal triamcinolone acetonide inhibits choroidal neovascularization in a laser-treated rat model. *Arch Ophthalmol* **119**, 399-404

96. Morishita, T., Mii, Y., Miyauchi, Y., Miura, S., Honoki, K., Aoki, M., Kido, A., Tamai, S., Tsutsumi, M., and Konishi, Y. (1995) Efficacy of the angiogenesis inhibitor O-(chloroacetyl-carbamoyl)fumagillol (AGM-1470) on osteosarcoma growth and lung metastasis in rats. *Jpn J Clin Oncol* **25**, 25-31

97. Tolentino, M. J., Brucker, A. J., Fosnot, J., Ying, G. S., Wu, I. H., Malik, G., Wan, S., and Reich, S. J. (2004) Intravitreal injection of vascular endothelial growth factor small interfering RNA inhibits growth and leakage in a nonhuman primate, laser-induced model of choroidal neovascularization. *Retina* **24**, 132-138

98. Koh, H. J., Freeman, W. R., Azen, S. P., Flaxel, C. J., Labree, L. D., Cheng, L., Wills, M., and Jones, T. R. (2006) Effect of a novel octapeptide urokinase

fragment, A6, on experimental choroidal neovascularization in the monkey. *Retina* **26**, 202-209

99. Wilkinson-Berka, J. L., Jones, D., Taylor, G., Jaworski, K., Kelly, D. J., Ludbrook, S. B., Willette, R. N., Kumar, S., and Gilbert, R. E. (2006) SB-267268, a nonpeptidic antagonist of alpha(v)beta3 and alpha(v)beta5 integrins, reduces angiogenesis and VEGF expression in a mouse model of retinopathy of prematurity. *Invest Ophthalmol Vis Sci* **47**, 1600-1605

100. Mousa, S. A., Mohamed, S., Wexler, E. J., and Kerr, J. S. (2005) Antiangiogenesis and anticancer efficacy of TA138, a novel alphavbeta3 antagonist. *Anticancer Res* **25**, 197-206

101. Reinmuth, N., Liu, W., Ahmad, S. A., Fan, F., Stoeltzing, O., Parikh, A. A., Bucana, C. D., Gallick, G. E., Nickols, M. A., Westlin, W. F., and Ellis, L. M. (2003) Alphavbeta3 integrin antagonist S247 decreases colon cancer metastasis and angiogenesis and improves survival in mice. *Cancer Res* **63**, 2079-2087

102. Meerovitch, K., Bergeron, F., Leblond, L., Grouix, B., Poirier, C., Bubenik, M., Chan, L., Gourdeau, H., Bowlin, T., and Attardo, G. (2003) A novel RGD antagonist that targets both alphavbeta3 and alpha5beta1 induces apoptosis of angiogenic endothelial cells on type I collagen. *Vascul Pharmacol* **40**, 77-89

103. Kumar, C. C., Malkowski, M., Yin, Z., Tanghetti, E., Yaremko, B., Nechuta, T., Varner, J., Liu, M., Smith, E. M., Neustadt, B., Presta, M., and Armstrong, L. (2001) Inhibition of angiogenesis and tumor growth by SCH221153, a dual alpha(v)beta3 and alpha(v)beta5 integrin receptor antagonist. *Cancer Res* **61**, 2232-2238

104. Roberts, M., Barry, S., Woods, A., van der Sluijs, P., and Norman, J. (2001) PDGF-regulated rab4-dependent recycling of alphavbeta3 integrin from early endosomes is necessary for cell adhesion and spreading. *Curr Biol* **11**, 1392-1402

105. Hughes, A. (1979) A schematic eye for the rat. *Vision Res* **19**, 569-588

106. Kimura, H., Sakamoto, T., Hinton, D. R., Spee, C., Ogura, Y., Tabata, Y., Ikada, Y., and Ryan, S. J. (1995) A new model of subretinal neovascularization in the rabbit. *Invest Ophthalmol Vis Sci* **36**, 2110-2119

107. Lima e Silva, R., Saishin, Y., Saishin, Y., Akiyama, H., Kachi, S., Aslam, S., Rogers, B., Deering, T., Gong, Y. Y., Hackett, S. F., Lai, H., Frydman, B. J., Valasinas, A., Marton, L. J., and Campochiaro, P. A. (2005) Suppression and regression of choroidal neovascularization by polyamine analogues. *Invest Ophthalmol Vis Sci* **46**, 3323-3330

108. Yao, V. J., Ozawa, M. G., Varner, A. S., Kasman, I. M., Chanthery, Y. H., Pasqualini, R., Arap, W., and McDonald, D. M. (2006) Antiangiogenic therapy decreases integrin expression in normalized tumor blood vessels. *Cancer Res* **66**, 2639-2649

109. Traganos, F., Juan, G., and Darzynkiewicz, Z. (2001) Cell-cycle analysis of drug-treated cells. *Methods Mol Biol* **95**, 229-240

110. Darzynkiewicz, Z., Juan, G., Li, X., Gorczyca, W., Murakami, T., and Traganos, F. (1997) Cytometry in cell necrobiology: analysis of apoptosis and accidental cell death (necrosis). *Cytometry* **27**, 1-20

111. Kerr, J. F. R., and Harmon, B. V. (1991) Definition and incidence of apoptosis: An historical perspective. Apoptosis: Molecular basis of Cell Death, chapt. 1. *Cold Spring Harbor Laboratory Press*, pp. 5-29

112. Majno, G., and Joris, I. (1995) Apoptosis, oncosis, and necrosis. An overview of cell death. *Am J Pathol* **146**, 3-15

113. Maubant, S., Saint-Dizier, D., Boutillon, M., Perron-Sierra, F., Casara, P. J., Hickman, J. A., Tucker, G. C., and Van Obberghen-Schilling, E. (2006) Blockade of alpha v beta3 and alpha v beta5 integrins by RGD mimetics induces anoikis and not integrin-mediated death in human endothelial cells. *Blood* **108**, 3035-3044

114. Cazes, A., Galaup, A., Chomel, C., Bignon, M., Brechot, N., Le Jan, S., Weber, H., Corvol, P., Muller, L., Germain, S., and Monnot, C. (2006) Extracellular

matrix-bound angiopoietin-like 4 inhibits endothelial cell adhesion, migration, and sprouting and alters actin cytoskeleton. *Circ Res* **99**, 1207-1215

115. Ponce, M. L., Nomizu, M., and Kleinman, H. K. (2001) An angiogenic laminin site and its antagonist bind through the alpha(v)beta3 and alpha5beta1 integrins. *Faseb J* **15**, 1389-1397

116. Frisch, S. M., and Screaton, R. A. (2001) Anoikis mechanisms. *Curr Opin Cell Biol* **13**, 555-562

117. Brooks, P. C., Stromblad, S., Klemke, R., Visscher, D., Sarkar, F. H., and Cheresh, D. A. (1995) Antiintegrin alpha v beta 3 blocks human breast cancer growth and angiogenesis in human skin. *J Clin Invest* **96**, 1815-1822

118. Tucker, G. C. (2003) Alpha v integrin inhibitors and cancer therapy. *Curr Opin Investig Drugs* **4**, 722-731

119. Hammes, H. P., Brownlee, M., Jonczyk, A., Sutter, A., and Preissner, K. T. (1996) Subcutaneous injection of a cyclic peptide antagonist of vitronectin receptor-type integrins inhibits retinal neovascularization. *Nat Med* **2**, 529-533

120. Gutheil, J. C., Campbell, T. N., Pierce, P. R., Watkins, J. D., Huse, W. D., Bodkin, D. J., and Cheresh, D. A. (2000) Targeted antiangiogenic therapy for cancer using Vitaxin: a humanized monoclonal antibody to the integrin alphavbeta3. *Clin Cancer Res* **6**, 3056-3061

121. Holmgren, L., O'Reilly, M. S., and Folkman, J. (1995) Dormancy of micrometastases: balanced proliferation and apoptosis in the presence of angiogenesis suppression. *Nat Med* **1**, 149-153

122. Erdreich-Epstein, A., Tran, L. B., Cox, O. T., Huang, E. Y., Laug, W. E., Shimada, H., and Millard, M. (2005) Endothelial apoptosis induced by inhibition of integrins alphavbeta3 and alphavbeta5 involves ceramide metabolic pathways. *Blood* **105**, 4353-4361

123. Dalton, S. L., Scharf, E., Briesewitz, R., Marcantonio, E. E., and Assoian, R. K. (1995) Cell adhesion to extracellular matrix regulates the life cycle of integrins. *Mol Biol Cell* **6**, 1781-1791

124. Arends, M. J., Morris, R. G., and Wyllie, A. H. (1990) Apoptosis. The role of the endonuclease. *Am J Pathol* **136**, 593-608

125. Gerschenson, L. E., and Rotello, R. J. (1992) Apoptosis: a different type of cell death. *Faseb J* **6**, 2450-2455

126. Stupack, D. G., and Cheresh, D. A. (2003) Apoptotic cues from the extracellular matrix: regulators of angiogenesis. *Oncogene* **22**, 9022-9029

127. Aoudjit, F., and Vuori, K. (2001) Matrix attachment regulates Fas-induced apoptosis in endothelial cells: a role for c-flip and implications for anoikis. *J Cell Biol* **152**, 633-643

128. Frisch, S. M. (1999) Evidence for a function of death-receptor-related, death-domain-containing proteins in anoikis. *Curr Biol* **9**, 1047-1049

129. Rytomaa, M., Martins, L. M., and Downward, J. (1999) Involvement of FADD and caspase-8 signalling in detachment-induced apoptosis. *Curr Biol* **9**, 1043-1046

130. Luscinskas, F. W., and Lawler, J. (1994) Integrins as dynamic regulators of vascular function. *Faseb J* **8**, 929-938

131. Vignoud, L., Usson, Y., Balzac, F., Tarone, G., and Block, M. R. (1994) Internalization of the alpha 5 beta 1 integrin does not depend on "NPXY" signals. *Biochem Biophys Res Commun* **199**, 603-611

132. Zhang, Z., Vuori, K., Reed, J. C., and Ruoslahti, E. (1995) The alpha 5 beta 1 integrin supports survival of cells on fibronectin and up-regulates Bcl-2 expression. *Proc Natl Acad Sci U S A* **92**, 6161-6165

133. Stromblad, S., Becker, J. C., Yebra, M., Brooks, P. C., and Cheresh, D. A. (1996) Suppression of p53 activity and p21WAF1/CIP1 expression by vascular cell integrin alphaVbeta3 during angiogenesis. *J Clin Invest* **98**, 426-433

134. Caswell, P. T., and Norman, J. C. (2006) Integrin trafficking and the control of cell migration. *Traffic* **7**, 14-21

135. Coller, B. S., Seligsohn, U., West, S. M., Scudder, L. E., and Norton, K. J. (1991) Platelet fibrinogen and vitronectin in Glanzmann thrombasthenia: evidence consistent with specific roles for glycoprotein IIb/IIIA and alpha v beta 3 integrins in platelet protein trafficking. *Blood* **78**, 2603-2610

136. Gaietta, G., Redelmeier, T. E., Jackson, M. R., Tamura, R. N., and Quaranta, V. (1994) Quantitative measurement of alpha 6 beta 1 and alpha 6 beta 4 integrin internalization under cross-linking conditions: a possible role for alpha 6 cytoplasmic domains. *J Cell Sci* **107 (Pt 12)**, 3339-3349

137. Pellinen, T., and Ivaska, J. (2006) Integrin traffic. *J Cell Sci* **119**, 3723-3731

138. Wencel-Drake, J. D., Boudignon-Proudhon, C., Dieter, M. G., Criss, A. B., and Parise, L. V. (1996) Internalization of bound fibrinogen modulates platelet aggregation. *Blood* **87**, 602-612

139. Gao, B., Curtis, T. M., Blumenstock, F. A., Minnear, F. L., and Saba, T. M. (2000) Increased recycling of (alpha)5(beta)1 integrins by lung endothelial cells in response to tumor necrosis factor. *J Cell Sci* **113 Pt 2**, 247-257

140. Schober, J. M., Lam, S. C., and Wencel-Drake, J. D. (2003) Effect of cellular and receptor activation on the extent of integrin alphaIIbbeta3 internalization. *J Thromb Haemost* **1**, 2404-2410

141. Bretscher, M. S. (1989) Endocytosis and recycling of the fibronectin receptor in CHO cells. *Embo J* **8**, 1341-1348

142. Bretscher, M. S. (1992) Circulating integrins: alpha 5 beta 1, alpha 6 beta 4 and Mac-1, but not alpha 3 beta 1, alpha 4 beta 1 or LFA-1. *Embo J* **11**, 405-410

143. Varner, J. A., and Cheresh, D. A. (1996) Tumor angiogenesis and the role of vascular cell integrin alphavbeta3. *Important Adv Oncol*, 69-87

144. Dalton, S. L., Marcantonio, E. E., and Assoian, R. K. (1992) Cell attachment controls fibronectin and alpha 5 beta 1 integrin levels in fibroblasts. Implications for anchorage-dependent and -independent growth. *J Biol Chem* **267**, 8186-8191

145. Sczekan, M. M., and Juliano, R. L. (1990) Internalization of the fibronectin receptor is a constitutive process. *J Cell Physiol* **142**, 574-580